Spectral Modelling for Transformation and Separation of Audio Signals

Thomas Arvanitidis

MSc by research

University of York

Electronics

December 2014

Abstract

The Short-Time Fourier Transform is still one of the most prominent time-frequency analysis techniques in many fields, due to its intuitive nature and computationally-optimised basis functions. Nevertheless, it is far from being the ultimate solution as it is plagued with a variety of assumptions and user-specific design choices, which result in a number of compromises. Numerous attempts have been made to circumvent its inevitable internal deficiencies, which include fixed time-frequency resolutions, static sample points, and highly biased outputs. However, its most important assumption, stationarity, is yet to be dealt with effectively. A new concept is proposed, which attempts to improve the credibility of the STFT results by allowing a certain degree of deviation from stationarity to be incorporated into the analysis. This novel approach utilises an ensemble of estimates instead of a single estimation in order to investigate the short-time phase behaviour of every frequency bin. The outcome is the definition of a quality measure, *phase stability*, that discriminates the "structured" from the "artefact" frequency components. This quality measure is then used in the framework of source separation as a single application example where it is possible to investigate its potential on the performance of the algorithm. Specifically, it was used in the spectral peak picking step of a numerical model-based source separation algorithm. It was found that the phase stability quality measure acts as an effective data reduction tool, which qualifies it as a more appropriate thresholding technique than the conventional methods. Based on this example, it is anticipated that this new method has great potential. Its ability to discriminate between "structured" and "noise" or edge effect/"artefacts" qualifies it as a promising new tool that can be added in the arsenal of the STFT modifications and used in the development of a hybrid super-STFT.

Contents

List of Figures

List of Tables

Acknowledgements

I would like to express my deepest appreciation to all those who provided me the possibility to complete this report. A special gratitude I give to my supervisor, John, whose contribution in stimulating suggestions and encouragement helped me to coordinate my project.

Author's Declarations

I declare that this thesis is a presentation of original work and I am the sole author. This work has not previously been presented for an award at this, or any other, University. All sources are acknowledged as References.

Chapter 1

Introduction

The inspection of the frequency content of a signal is often required in order, for instance, to learn more about the frequency behaviour of the system from which the signal has come. Furthermore, the direct application of processing routines, such as filtering, on the frequency content of a signal may be preferred due to greater intuitiveness. It is, therefore, necessary to be able to transform the signal from its temporal representation into a spectral representation to enable such opportunities. This is achieved with the utilisation of spectral analysis techniques.

There are several techniques that accomplish the transformation of a signal from the time to frequency domain, and vice versa, with one of the most prominent being the family of Fourier approaches. Fourier techniques continue to be some of the dominant spectral analysis tools due to their intuitive nature and computationally-optimised basis functions. They, in particular in the form of the Short-Time Fourier Transform (STFT), can be found implemented in fields as diverse as physics [1], astronomy [2], chemistry [3], medical engineering [4] and geophysics [5].

Fourier approaches are plagued, however, with numerous assumptions and user-specific design choices, which result in a variety of compromises. One of the most important assumptions is stationarity. This may be disadvantageous because the frequency content of the signal may vary with respect to time, which may result in misleading data. In terms of user-specific design choices, the choice to focus on the amplitude information of the analysed data and ignore the phase

information results in incomplete analysis.

Over the years, researchers have developed adaptations of the STFT in order to compensate for its deficiencies but the assumption of stationarity is yet to be tackled effectively. Moreover, the majority of the approaches solely focus on the improvement of the credibility of the amplitude information without the consideration of the phase information. It is, then, proposed in this project a novel approach that involves the inspection of the short-time phase behaviour of the signal with the construction of an ensemble of estimates, which allows the incorporation of a certain degree of deviation from stationarity into the analysis process. This method is based on the hypothesis that the phase behaviour of the sampled frequency components that arise due to partials manifest structured patterns, whereas the phase behaviour of the sampled frequency components that arise due to statistical noise or Fourier related artefacts exhibit randomness. This is then exploited in order to produce a quality measure that aids in the discrimination of the "structured" from the "artefact" frequency components.

The attainment of a series of objectives is required for the implementation of this novel concept, which include the thorough investigation of the phase behaviour of a set of elementary synthetic example signals as calculated at their generation and obtained from the STFT in order to gain an insight and efficiently exploit it in the analysis stage, and the development of the processing tool that calculates the quality measure. The potential of this quality measure is then investigated with its incorporation in the framework of source separation as an application example.

The work conducted in this project is documented in the following chapters, starting with the essential theoretical background of the concepts utilised. The main research on the phase behaviour of simple synthetic signals, the calculation of the quality measure, the documentation of the modifications applied on the STFT algorithm in order to construct the ensemble of estimates, and the function that calculates the phase stability are then detailed. Finally, the incorporation of the phase stability quality measure in a numerical model-based source separation algorithm is explained.

1.1 Report Overview

Chapter 1 - An introduction to this project is provided in order to inform the reader about the topics on which this thesis elaborates and the scope of the research.

Chapter 2 - This chapter provides the historical and theoretical background of the main concepts and tools that are utilised in this project.

Chapter 3 - The main research conducted in this project is documented in this chapter. An overview of the assumptions and user-specific design choices of the STFT linked to their compromises is provided, followed by the motivation for this project, the investigation of the phase behaviour of a set of elementary synthetic signals with regards to the proposed method, and a few examples of the behaviour of the phase stability of both synthetic and real signals.

Chapter 4 - The documentation of the two main functions developed for the calculation of the phase stability is included in this chapter.

Chapter 5 - The work carried out on source separation is described in this chapter. It initially provides a brief historical and theoretical background on source separation with a focus on the type of the source separation algorithm implemented in this project, the motivation and reasoning for the consideration of source separation as an application example, the documentation of the algorithm, and the result analysis.

Chapter 6 - The findings and conclusions drawn for this projects are summarised in this chapter.

Chapter 7 - An agenda is compiled with a set of objectives to be attained for further validation and performance improvement of the proposed method.

Chapter 2

Background

This chapter provides the theoretical and historical background of the topics on which this project elaborates. More specifically, it reviews the background of the simplest structure found in a signal as considered by the source separation algorithm in chapter 5, describes the model that was utilised for the generation of the test signals that were used for the establishment of the principles of the phase stability quality measure in chapter 3, and provides a thorough review of the main spectral analysis method on which this research is conducted.

2.1 Note Structure: ADSR, Partials and Harmonics

The ADSR (acronym for Attack-Sustain-Decay-Release) is a temporal representation of the different stages that a note goes through, starting from the moment it is played until it ceases to exist. This model can be used for both real and synthetic sounds[1]. Each stage manifests different properties, and varies for every instrument. The following figure (fig. 2.1) portrays the generic structure of a note as described by the ADSR model. It is not clear when it was first introduced but according to Pinch [6] this model was suggested to Robert Moog from Vladimir Ussachevsky, and first appeared in this form on the ARP Odyssey synthesiser in 1972 [7]. Moorer also uses this model for the production of digital signals in his paper on computer music [8] but refers to it as 'control function'. The following

[1] Often used in the amplification stage of synthesisers.

paragraphs detail the characteristics of each phase of the ADSR model.

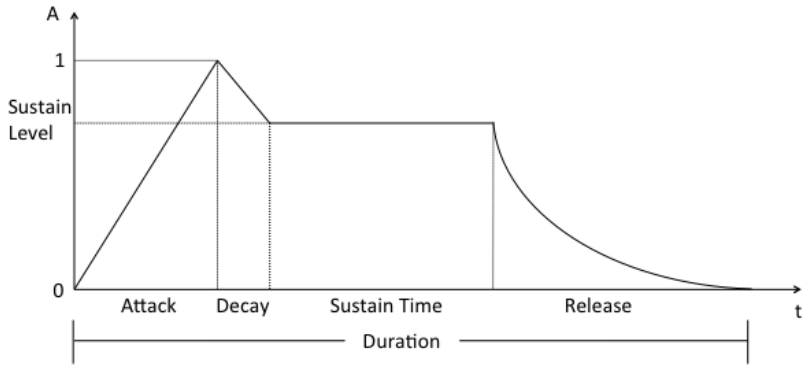

Figure 2.1: ADSR model

The attack phase, which indicates the beginning of a note, is the first stage. It is the phase where energy is first injected to the instrument. It may occur in various ways depending on the type of instrument, i.e. pluck for stringed instruments, blow for wind instruments, struck for percussive instruments. The length of this phase is usually very short. It is also complex, in the sense that it is not easily emulated with simple models, i.e. sinusoidal (detailed in section 2.2). In terms of spectral behaviour, this stage is chaotic and wideband because the energy has just been introduced to the vibrating medium and has not completely spread across it in order to form standing waves or modes, depending on the type of instrument.

Following the attack comes the decay phase, which is also relatively short in time. This stage is the transition between the chaotic behaviour of the instrument due to the travelling waves and the settling of the energy with the formation of standing waves. It is usually very subtle in real instruments, but can have dramatic effects in sounds generated by synthesisers.

The sustain is the next phase. It is usually the longest phase of a note. At this stage the standing waves or modes have been formed and the chaotic wideband spectral behaviour has become narrower and better defined. This stage may also be prolonged due to the continuous input of energy, i.e. blowing a flute steadily. The harmonic part (described in the following paragraphs) of the sound is more dominant at this stage.

The last stage is the release, which indicates the beginning of the end of a note. This is the stage where the amplitude of the note gradually tapers to zero. It may be long as well as short, depending on the physical attributes of the instrument, i.e. the sound of a bell and the sound of a snare.

All aforementioned stages differ for every instrument but also with respect to performance styles. A hard struck on the tom of a drum kit may result in a significantly long release, whereas a gentle strike might result in short release.

The spectral structure of a note describes its content in terms of partials, P [9]. Partials are the frequency components that constitute the sound. They are usually better defined in the sustain part of a note, where the standing waves and modes have been formed. The following figure illustrates the spectral structure of a guitar pluck.

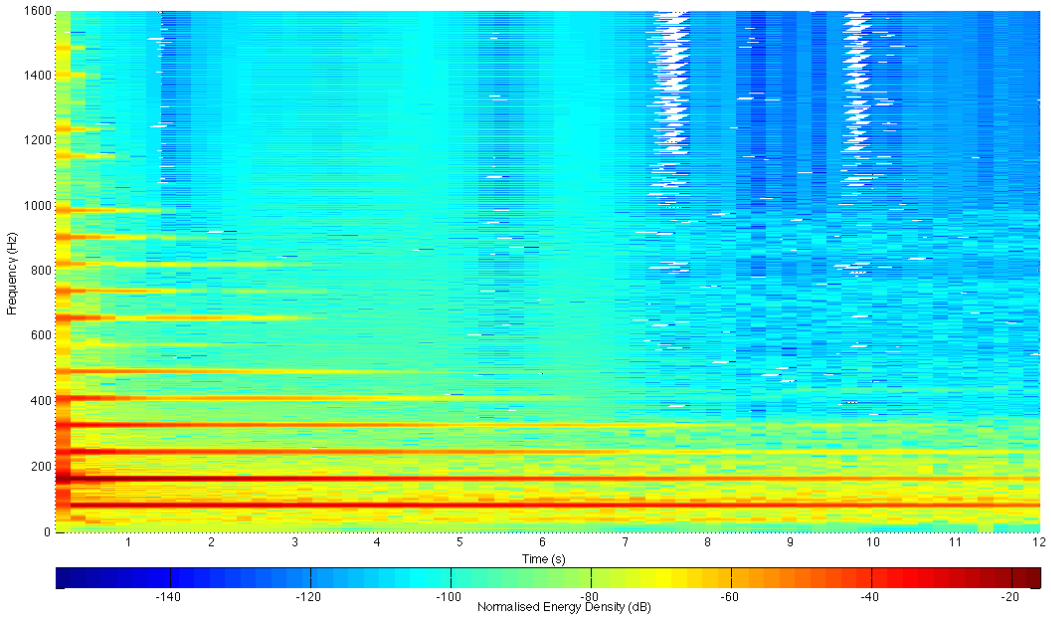

Figure 2.2: The spectral structure of a guitar pluck (frame length = 8192, overlap = 98.4375% , zpf = 2) (The white spots are artefacts due to screen resolution)

Harmonics are the partials of a sound that are an integer multiple of the fundamental partial [9]. A pleasant sound usually manifests a high degree of harmonicity, i.e. a violin note. It is important to stress that the first harmonic partial of a sound is the fundamental frequency. The expression that describes

the d^{th} harmonic is:

$$f_d = d \cdot f_0, \quad d = 1, 2, \ldots \tag{2.1}$$

In the previous example (figure 2.2), there are 18 harmonics present in total. Also it is worth noting the difference in length between the lower and higher harmonics. High harmonics tend to decay faster than the lower harmonics for real instruments.

2.2 Sinusoidal Model

The typical sinusoidal model is defined as the summation of numerous sinusoidal components with different frequencies [8]. Each sinusoidal function is considered to be a partial, p, with static amplitude, A, angular frequency, ω, and initial phase angle, $\phi(0)$. This model is described by the following equation.

$$x(t) \triangleq \sum_{p=1}^{P} A_p \sin(\omega_p t + \phi_p(0)), \quad t \in \mathbb{R} \tag{2.2}$$

A more realistic and complex version of this model, which is also the one that is used in this project, considers the argument of the sinusoidal function as its phase, and allows the amplitude and angular frequency of each component to vary with respect to time.

$$x(t) \triangleq \sum_{p=1}^{P} A_p(t) \sin(\varphi_p(t)), \quad t \in \mathbb{R} \tag{2.3}$$

where the following expressions hold:

$$\omega_p(t) = \frac{\mathrm{d}\varphi_p}{\mathrm{d}t}(t) = 2\pi f_p(t), \quad p = 1, 2, \ldots, P \tag{2.4}$$

$$\varphi_p(t) = 2\pi \int_0^t f_p(u)du + \phi_p(0), \quad p = 1, 2, \ldots, P \tag{2.5}$$

The functions $\omega_p(t)$ and $f_p(t)$ represent the angular frequency of the p^{th} partial in radians and hertz respectively, and the scalar $\phi_p(0)$ is the initial phase angle of the p^{th} partial.

The sinusoidal model allows the generation of sounds by manipulating their spectral characteristics. It is very simple and achieves the faithful reproduction of the sounds generated by many real instruments, such as flute and violin. Moreover, it achieves the generation of interesting synthetic soundscapes. The complex version of the sinusoidal model (eq. 2.3) is preferred here because it allows the production of non-stationary sound examples.

2.3 Spectral Analysis

Spectral analysis achieves the expression of the contents of a signal in terms of amplitude and phase variations with respect to frequency. The observation of the signal's contents from this point of view is often beneficial because it unveils patterns about its frequency contents that are not visible in the temporal form. Also, certain processing routines become more intuitive and simpler, such as filtering, since it provides direct access to the frequency components of the signal.

There are numerous analysis techniques that achieve the transformation of a signal into the frequency domain. However, there is not a single one that is appropriate for all signals. This project concentrates on the Short-Time Fourier Transform (STFT), and implicitly Discrete Fourier Transform (DFT), because of its wide use in signal processing, and particularly on music signals.

The Discrete Fourier Transform transfers the whole signal from time to frequency domain by describing it in terms of its basis. This basis is a set of narrowband spectral components (sinusoids) that are described in terms of frequency. When the transformation is finished, the entire signal is averaged into a

single spectrum, which describes the amount and initial phase of each sinusoid that is present in the signal. Figure 2.3 illustrates the functionality of DFT. This figure depicts a rectangular waveform in its temporal and spectral form, but also portrays the relationship between the two different representations.

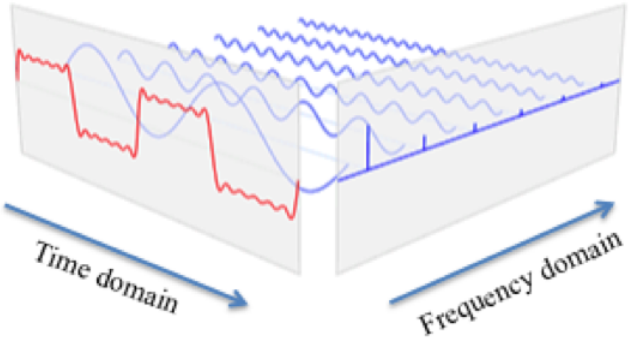

Figure 2.3: The relationship between the temporal and spectral representations of a rectangular function [10].

It is often required, however, to observe the time-varying frequency behaviour of the signal, since sound evolves with respect to time. The Short-Time Fourier Transform is one of the predominant transforms among the family of time-frequency analysis methods that allows the user to select the time and frequency resolutions. This method provides an insight to the signal's frequency behaviour at frequent time intervals by sliding a window across it and obtaining the spectra of every windowed signal.

The STFT, which is an adaptation of the DFT, is frequently preferred over other time-frequency analysis methods because its basis is orthogonal and normalised. This attribute of STFT results in faster computation of the analysis, and along with the intuitive nature of its basis functions makes it popular in many fields other than audio signal processing. It is also used in the fields of physics [1], astronomy [2], chemistry [3], medical engineering [4] and geophysics [5].

The following sections provide a review of the DFT and STFT analysis methods. This review elaborates on the functionality, assumptions and deficiencies of the aforementioned functions. Additionally, modifications of the STFT that

attempt to overcome particular limitations are examined. Finally, a list of comments is consolidated regarding to the aspects that were not considered.

2.3.1 Discrete Fourier Transform

The Discrete Fourier Transform is the digital implementation of the Fourier series [11]. The difference between the DFT and the rest of the Fourier transforms is that its input and output signals are both discrete and finite. It also assumes that the signal under analysis is periodic. The DFT transforms the signal, $x[n]$ of N samples, to the discrete frequency domain by sequentially projecting it on a set of sinusoid functions, $s_k[n]$ of period N samples, which constitute the basis of the Fourier dimension. The following material and equations can be found in [11], unless otherwise stated. Different notation was used where necessary for consistency purposes.

$$s_k[n] \triangleq \cos(\varphi_k[n]) + j\sin(\varphi_k[n]) \equiv e^{j\varphi_k[n]}, \quad n = 0, 1, \ldots, N-1 \tag{2.6}$$

$$X[k] \triangleq \sum_{n=0}^{N-1} x[n]e^{-j\varphi_k[n]}, \quad k = 0, 1, \ldots, N-1 \tag{2.7}$$

where

$$\varphi_k[n] = 2\pi f_k n + \phi_k[0], \quad n = 0, 1, \ldots, N-1 \tag{2.8}$$

$$f_k = \frac{k}{N}, \quad k = 0, 1, \ldots, N-1 \tag{2.9}$$

An alternative notation of the DFT uses the inner product operator. This is more compact and intuitive because the projection of the signal, $x[n]$, on the Fourier basis, $s_k[n]$, is more apparent.

$$X[k] \triangleq \langle x[n], s_k[n] \rangle \tag{2.10}$$

The transformation of the signal $x[n]$ of N samples results in N complex frequency coefficients, $X[k]$. These coefficients express the degree of correlation of the signal, $x[n]$, with the Fourier basis, $s_k[n]$. In practice, they describe the amplitude, $A[k]$, and initial phase angle, $\phi[k]$, of each sinusoid. This set of complex frequency coefficients, $X[k]$, comprises the signal's spectrum. Moreover, the power spectral density (PSD) of a signal is often of interest, which is merely the amplitude of every frequency component squared. According to Parseval's theorem, the total energy of the signal in time domain is equal to the total energy of its normalised frequency coefficients.

$$A[k] \equiv |X[k]| \triangleq \sqrt{X_R[k]^2 + X_I[k]^2} \tag{2.11}$$

$$\phi[k] \equiv \angle X[k] \triangleq atan2\frac{X_I[k]}{X_R[k]} \tag{2.12}$$

$$E[k] = |X[k]|^2 \tag{2.13}$$

$$E_{Total} \equiv \sum_{n=0}^{N-1} |x[n]|^2 = \frac{1}{N} \sum_{k=0}^{N-1} |X[k]|^2 \tag{2.14}$$

The spectra of a real valued signal, $x[n] \in R$, are Hermitian, which means they exhibit conjugate symmetry. Therefore:

- $Re\{X\}$ is even,
- and $Im\{X\}$ is odd.

The DFT is fully reversible and the transformation from and to the frequency domain is theoretically perfect without any loss or degradation of information[1]. The transform that achieves the reversal of the DFT is the inverse Discrete Fourier Transform (IDFT).

$$x[n] = \frac{1}{N} \sum_{k=0}^{N-1} X[k] e^{j\varphi_k[n]}, \quad n = 0, 1, \ldots, N-1 \tag{2.15}$$

where

$$\varphi_k[n] = 2\pi f_k n + \phi[0], \quad n = 0, 1, \ldots, N-1 \tag{2.16}$$

$$f_k = \frac{k}{N}, \quad k = 0, 1, \ldots, N-1 \tag{2.17}$$

The calculation of the DFT is computationally very expensive. The projection of the signal $x[n]$ of length N on one out of the N sinusoidal components $s_k[n]$, whose length is equal to the length of the subject signal, requires $N \times N$ operations. Cooley and Tukey [12] developed an optimised modification that requires $O(Nlog_{10}(N))$. This modification exploits the periodicity of $e^{j\vartheta}$, and significantly reduces the amount of operations as the length of the signal increases. The algorithm that implements this approach is called the Fast Fourier Transform (FFT), and is commonly used instead of the DFT. This optimisation allows the processing of longer signals, which is often the requirement, or the application of DFT in near real-time with the use of buffers. The only prerequisite is the length of the signal under investigation, which must be equal to the powers of two, $N = 2^b, b \in \mathbb{Z}$.

The consideration of signals of finite length has important implications on the signal's spectrum. This can be thought as windowing in mathematical and engineering terms. In particular, the rectangular window function is thought to be applied, since it is perceived as a switch that allows information to pass only

[1] In practice there is a minuscule error due to machine limitations.

between the $[0, N-1]$ interval.

$$rect[n] \equiv \Pi[n] \triangleq \begin{cases} 1, & 0 \leq n \leq N-1 \\ 0, & n \geq N \end{cases}, \quad n \in \mathbb{Z} \tag{2.18}$$

and since N is the signal's length,

$$x[n] = x[n] \times \Pi[n] \tag{2.19}$$

The windowing of a signal with the rectangular window function may result in discontinuities. It also means that the signal's spectrum is convolved with the spectrum of the window function. These are two very important deficiencies of DFT, and are described further in the following paragraphs.

Discontinuities may occur due to the arbitrary selection of the signal's length. The DFT attempts to replicate the periodic version of the windowed signal, which means it also attempts to reproduce the abnormal sudden change (fig 2.4). The decomposition of a signal with such discontinuity requires several frequency components, since the DFT basis is comprised of sinusoids that exhibit complete periods in the interval $[0, N-1]$. This phenomena is called spectral leakage, and is defined as the introduction of sidebands in frequency domain due to discontinuities in time domain.

The convolution of the signal's and window function's spectra is unavoidable. However, there is one case where the effects of this convolution are concealed in the amplitude spectrum. This is when there are no discontinuities, which may occur by chance or careful selection of the signal's starting and ending points. In this case, the sidebands in the amplitude spectrum of the signal are just not visible because their sampled frequency values happen to coincide with the nulls of the sidebands of the amplitude spectrum of the rectangular window (fig. 2.5). In practice, the basis of the DFT happens to contain the correct frequency components to map the total energy of the signal. This phenomenon is being portrayed in figure 2.6, where the sidebands are delineated with the aid of zero padding. Zero padding is a technique used to interpolate the sampled frequency values. A

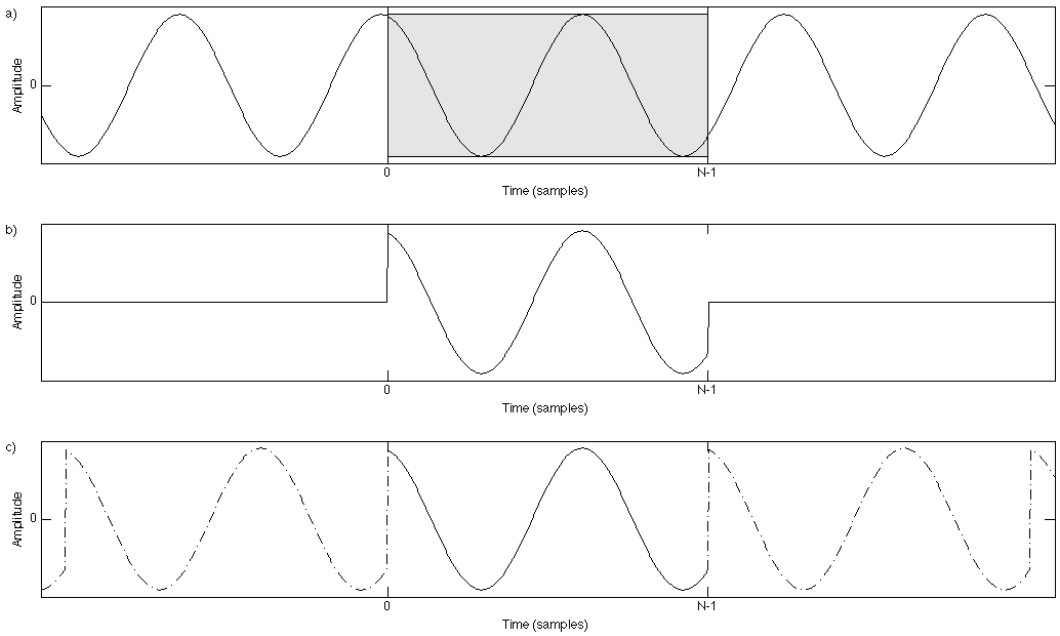

Figure 2.4: Arbitrary selection of a portion of an infinite signal and its periodic finite form as considered by DFT

more elaborate description of this functionality is included in section 2.3.1.1.

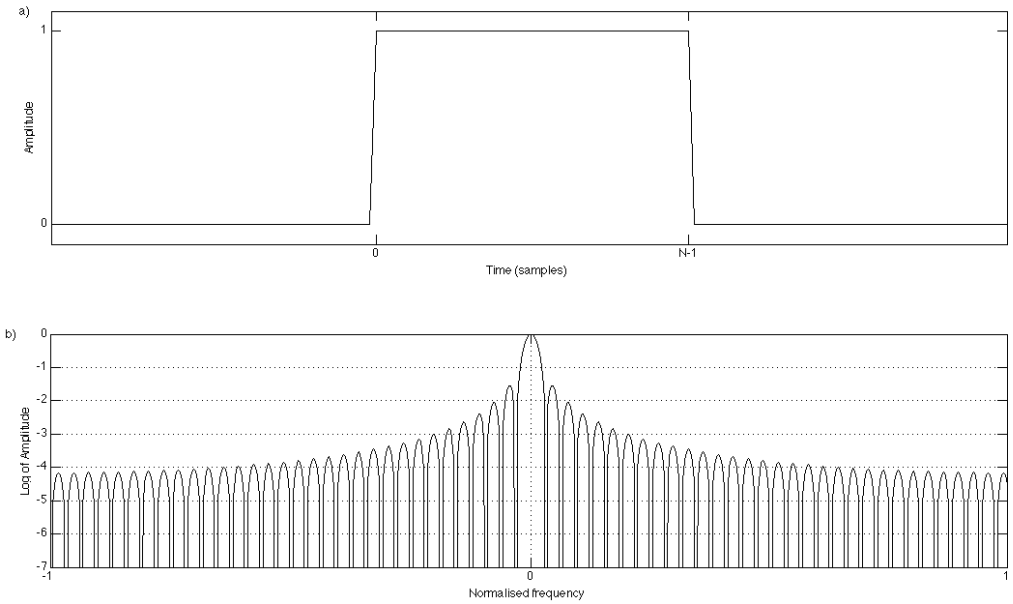

Figure 2.5: The rectangular window and its spectrum

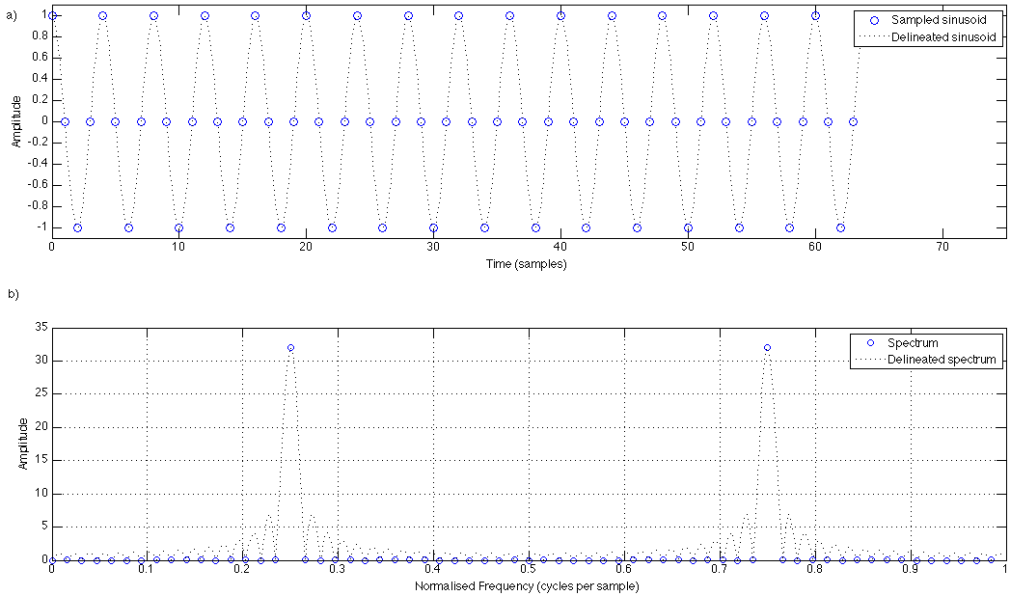

Figure 2.6: Illustration of the case where the amplitude spectral components of a signal coincide with the nulls of the sidebands of the amplitude spectrum of the rectangular window function. The amplitude spectrum of the window function has been delineated with the help of zero padding

2.3.1.1 Windowing

It was described in the previous paragraph that the windowing of a signal and the spectral convolution of the window's spectrum with the signal's spectrum are unavoidable. It was also discussed that the manifestation of spectral leakage can be avoided with appropriate selection of the starting and ending points of the signal in order to diminish discontinuities. Additional window functions were developed to compromise with discontinuities. These window functions have weighted sample values that taper towards zero at the sides of the frame. Subsequently, they force potential discontinuities towards zero.

The deficiency of these windowing functions, however, lies in the resolution of their spectral lobes. The width of their spectral lobes is bigger than the width of the spectral lobes of the rectangular windowing function, which results in less accurate estimations of the frequency components that are responsible for the height of the peak. Specifically, the spread of the main lobe is often of interest, because it is the one that has the biggest contribution to the signal's spectrum.

Two of the main topics that come with windowing were introduced so far; spectral leakage and frequency resolution. The latter is a quality value that is often considered in window picking. It is important to stress that there is no 'best' window function. Another quality measure that is usually considered is the amplitude difference between the main and the first side-lobe. It is generally true that the greater difference means less 'blurring' in the frequency domain.

Having introduced the main factors considered in the assessment of the suitability of a window function, a few popular window functions along with their parameters are listed for comparison in table 2.1. More window functions are described in greater detail in Harris' and Nuttall's papers [13, 14].

The application of any window function other than the rectangular incurs energy loss, since part of the signal's amplitude is decreased. This results in loss of information and data degradation. However, this is often exploited in STFT depending on the application for which it is used. This is described in greater detail in the following sub-section.

Window Function	Main-to-sidelobe amplitude difference (dB)	Main lobe width (sampled frequency components)
Rectangular	-13	2
Hamming	-31	4
Hann	-41	4
Blackman	-57	6

Table 2.1: Specification of a few popular window functions

2.3.2 Short-Time Fourier Transform

The Short-Time Fourier Transform provides an insight on the frequency behaviour of a signal at certain points in time. This analysis method represents the amplitude of the spectral components as a function of both frequency and time. It achieves this by sliding a window along the signal and obtaining the segment's spectra. Every part of the signal that contributes one spectrum is called frame m and it is of length L. The interval between successive frames is determined by the step variable, H. The introduction of this variable allows the overlap between successive frames. The total number of frames, M, obtained from STFT depends on three factors; (1) the signal's length N, (2) the frame length L, and (3) the step size H. It is important to stress the discard of the last frame in case it is incomplete.

$$X_m[k] \triangleq \sum_{n=0}^{L-1} x[n]w[n-(m-1)H]e^{-j\varphi_k[n]}, \qquad \begin{matrix} k = 0, 1, \ldots, L-1 \\ m = 1, 2, \ldots, M \end{matrix} \tag{2.20}$$

where

$$\varphi_k[n] = 2\pi f_k n + \phi[0], \quad n = 0, 1, \ldots, L-1 \tag{2.21}$$

$$f_k = \frac{k}{N}, \quad k = 0, 1, \ldots, L-1 \tag{2.22}$$

$$M = rounddown(\frac{N-(L-H)}{L-H}) \tag{2.23}$$

The output of the STFT is the spectrogram, which is a 3D plot. A typical representation includes the frames on the abscissa, the sampled frequencies on the ordinate (or vice versa), and the spectral density as height. The spectrogram is usually viewed from top as a 2D plot, where the time and frequency lie on the x and y axis respectively. The energy density representation is achieved through its mapping on a range of colours. An example spectrogram of a linear chirp is portrayed in figure 2.7.

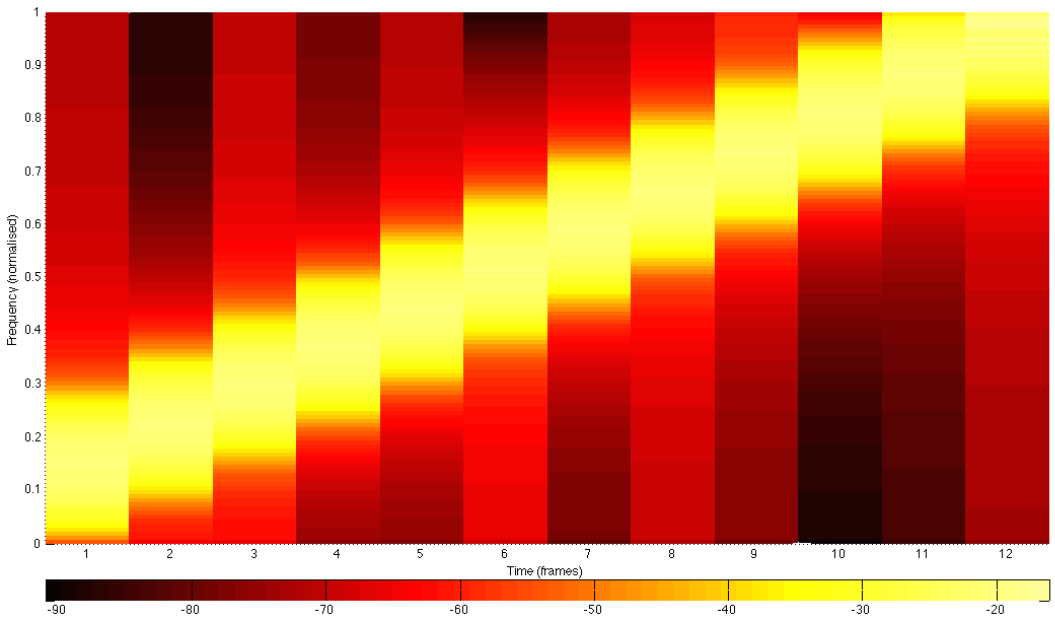

Figure 2.7: Spectrogram of a linear chirp sampled at 1024 Hz and total length 1024 samples that starts at DC at sample 1 and crosses 0.5859 at sample 512. STFT parameters: frame length = 256, overlap = 75%, zpf = 0, window function = Hamming

The step variable, H, is responsible for the amount of overlap exhibited between successive frames. Setting the step size equal to the frame length, L, gives 0% overlap. Whereas, setting the step size to a quarter of the frame length equals to 75% overlap. The following equation expresses the overlap in percentage with

respect to the frame length, L, and step size, H. In practice, percentages of overlap greater than 0 result in time interpolation for analysis with rectangular windowing function. This generates no new information, as it merely creates more data points between the spectral values that would have been obtained in the case of 0% overlap.

$$overlap(\%) = \frac{L - H}{L} \times 100 \tag{2.24}$$

It is also possible to improve the resolution portrayed across the frequency axis. This is achieved with zero padding[1], which is a simple time-domain technique that has the effect of broadband time interpolation in frequency domain. Zero padding is the introduction of a string of zeros at the end of every frame. The size of this string is usually an integer multiple of the frame length, and is calculated with the aid of the zero padding factor variable, zpf. The zpf indicates the number of points introduced between the successive values that would have been obtained with no zero padding. The introduction of zero padding increases the number of samples considered within the FFT, and the total amount of samples is determined by the following expression:

$$nfft = zpf \cdot L, \quad zpf = 1, 2, 3, \ldots \tag{2.25}$$

The STFT officially has no inverse function, although it can be defined for particular cases. One of them is the case were 50% overlap and a window function that tapers towards zero at the edges and reduces the energy of each frame to 50% have been employed during the analysis stage. The reconstruction of the original signal in time domain is achieved with the use of the overlap-add algorithm [15], in order to preserve the energy. A couple examples of window functions that taper towards zero at their edges and capture only 50% of the signals energy are the Hamming and Hann.

[1]There are also alternative ways, such as interpolating directly the frequency values.

2.3.3 Discussion

2.3.3.1 DFT versus FFT

The development of an optimisation of the DFT function was discussed in 2.3.1, the FFT. Its only prerequisite is the length of the signal under analysis to be equal to a power of 2. This is not an issue in the context of this project, as there are no constrains about the length of the signals considered. Thus, the FFT algorithm is used in order to achieve lower computational expense.

2.3.3.2 Single-estimate versus Multiple-estimate Averaged Spectrograms

The obtainment of a spectrum of lower variance, higher data credibility and reduced resolution has been suggested from Bartlett and Welch [16, 17, 18]. Both Bartlett's and Welch's approaches involve the sectioning of the subject signal in many frames, obtaining their spectra, and averaging their values. The difference between the Bartlett's and Welch's spectra lies in the step size between the consecutive frames. Bartlett's approach utilises 0% overlap, whereas Welch allows 50% overlap to be applied between the successive frames. These two approaches, however, are not appropriate for the data with which this project deals, because the averaging of the spectra deteriorates the resolution of the spectral peaks. The frequency content of audio signals varies rapidly, and therefore, it is important to not deteriorate the resolution. Thus, the single-estimate approach was utilised.

2.3.3.3 STFT parameter setting

There are many factors that require consideration prior to the analysis of a signal. Every step and variable in the STFT algorithm introduces yet another layer of complexity. It is important to carefully assess the available options in order to optimise the output of this analysis method. As it has been thoroughly explained in 2.3.1, the selection of the length of the signal alone may result in distorted output information. It is, then, obvious that the inconsiderate setting of the STFT parameters may incur significant inaccuracies on the signal's spectra.

One of the most important matters for consideration is the time-frequency resolution, which is fixed. This resolution is determined by the frame length, L,

and the sampling frequency of the signal, f_s. So far this report has used normalised examples, which means the sampling frequency was set to 1. In practice, however, it is much greater than 1. For instance, the typical sampling frequency used in most audio files is 44.100 Hz[1]. The expression that calculates the frequency resolution of the sampled spectral components, which also happens to be the lowest range of frequencies detected (f_{bin}), is:

$$f_{bin} = \frac{f_s}{L} \tag{2.26}$$

This indicates the range of frequencies that every sampled spectral component represents (bandwidth). The frequency and time resolutions are associated to the uncertainty principle, which was first observed by Heizenberg in quantum physics. For STFT it means that longer frames result in better frequency resolution, whereas shorter frames result in better temporal resolution. This effect is depicted in figure 2.8. Furthermore, the product of the standard deviations of the frequency and time elements of the spectrogram plane is always the same constant.

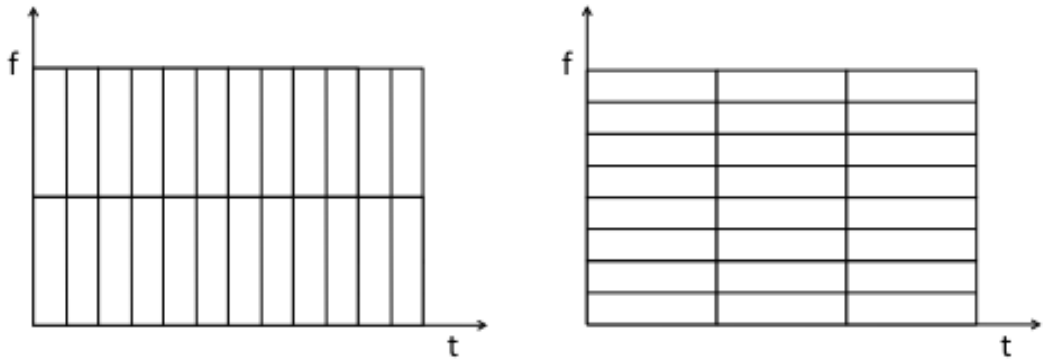

Figure 2.8: Various time-frequency resolutions

[1]According to sampling theorem, this sampling frequency allows the representation of all audible frequencies, having considered the necessary filtering applied at the high-end of the spectra, by the auditory system.

$$\Delta t \Delta f = \frac{1}{4\pi} \tag{2.27}$$

It is important to consider the frame length prior to the analysis of a signal for an additional reason. In his paper on the extraction of spectral peak parameters, Depalle [19] states that components that exhibit less than 4 periods within the frame result in considerable inaccuracies. The following table (2.2) translates what this statement means in terms of frame length and lowest frequency component detected for $f_s = 44.100$ Hz.

Frame length L (samples)	**Lowest accurately detectable frequency (Hz)**
512	344.6
1024	172.3
2048	86.2
4096	43.1
8192	21.6
16384	10.8

Table 2.2: Lowest accurately estimated frequency with respect to different frame lengths (based on [19])

Improving the time and frequency resolution with interpolation is also a matter of consideration. Although it is usually preferable to have more points because of the aesthetically nicer portray, zero padding and high percentages of overlap are not always an option. These functionalities are computationally expensive, which might be undesired due to the already computationally expensive implementation of an algorithm. Therefore, careful thought must be given on the advantages and disadvantages of these techniques prior to their employment.

2.3.3.4 Practical implementation of the STFT

Although the STFT description in 2.3.2 considers its functionality as a sliding window along the signal, its practical implementation is different. In reality, the STFT is calculated by sequentially considering a segmented portion of the signal (frame m) of length L, and analysing it with the FFT. The rest of the parameters

remain the same. In terms of its equation, the only difference is the change of the signal's and window's arguments. An example of the practical implementation of the STFT is illustrated in figure 2.9, where the framed first quarter of the signal analysed is included along with its spectrogram.

$$X_m[k] \triangleq \sum_{n=0}^{L-1} x[n + (m-1)H]w[n]e^{-j\varphi_k[n]}, \qquad \begin{matrix} k = 0, 1, \ldots, L-1 \\ m = 1, 2, \ldots, M \end{matrix} \tag{2.28}$$

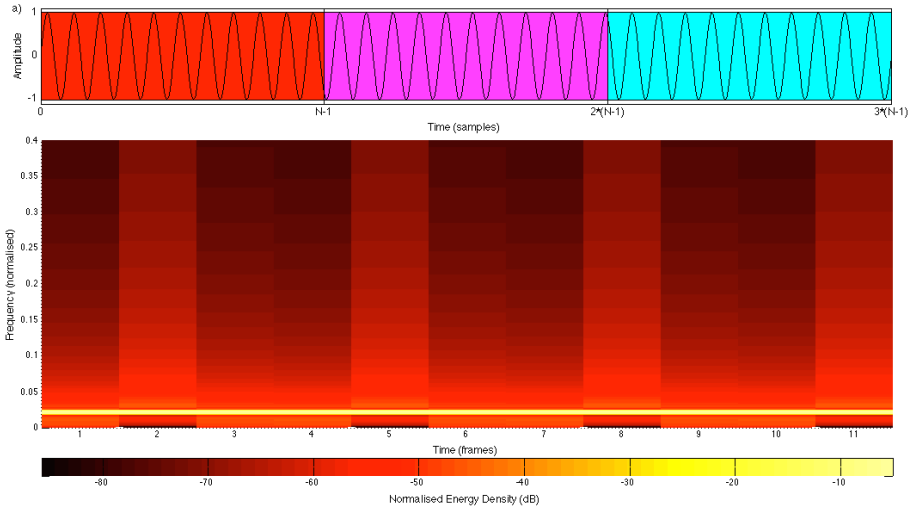

Figure 2.9: Illustration of the obtainment of a spectrogram with the practical implementation of STFT. The first quarter of the signal is depicted in a), which is analysed with a Hamming window function (due to *spectrogram* function in MATLAB). $N = 12288$, $L = 1024$, $H = 1024$, $zpf = 0$

2.3.3.5 ISTFT

The ISTFT algorithm is defined here, since it is a vital part of the source separation algorithm implemented by this project (see chapter 5). The overlap-add method [15] is implemented in order to reconstruct the original signal in its temporal form.

In the case of 0% overlap, the algorithm is straightforward. It merely transforms each frame with IFFT and places it on the correct position. It is important to stress that in the case where zero padding has been applied, only the first L samples are kept.

$$x[(m-1)L+1:(m-1)L+L] \triangleq \sum_{k=0}^{nfft-1} X_m[k]e^{-j\varphi_k[n]} \\ n=0,1,\ldots,nfft-1, \quad m=1,2,\ldots,M \tag{2.29}$$

In the case where 50% overlap has been applied, the algorithm is slightly different. The calculation of the starting and ending points of the position of each transformed frame are determined by the step variable, H. Again, if zero padding has been applied, only the first L samples are kept.

$$x[(m-1)H+1:(m-1)H+L] \triangleq \sum_{k=0}^{nfft-1} X_m[k]e^{-j\varphi_k[n]} \\ n=0,1,\ldots,nfft-1 \quad m=1,2,\ldots,M \tag{2.30}$$

2.3.4 STFT Modifications

The main limitation of the STFT, which is defined as soon as the analysis parameters are set, is the fixed time-frequency resolution. This limitation is directly connected to the STFT's (and implicitly the DFT's) implementation, and is unavoidable. However, this is not the only issue. An additional matter that requires attention is the lack of additional observations (estimations) in order to decrease the variance and bias of the obtained results. This issue is also always present but is much less considered in comparison to the limitations of the fixed grid.

These issues have been observed since very long ago (1970s), and various approaches have been developed that attempt to tackle them. The three main categories under which all STFT modifications can be catalogued are (1) multiresolution (which encompasses Adaptive STFT), (2) frequency reassignment, and (3) multitapers. Although these have often been named differently, it will be shown that despite the naming variations they share the same principles.

2.3.4.1 Multiresolution

Multiresolution for STFT-based algorithms is the calculation of the spectrum of a signal with varying window sizes (frame length). This results in a grid with unequally spaced tiles as it is portrayed in figure 2.10. The advantage of this approach is the increased frequency resolution at certain bandwidths, while maintaining the temporal resolution at other bandwidths. The main disadvantages, excluding the computational expense, is the lack of an inverse function, which precludes spectral processing.

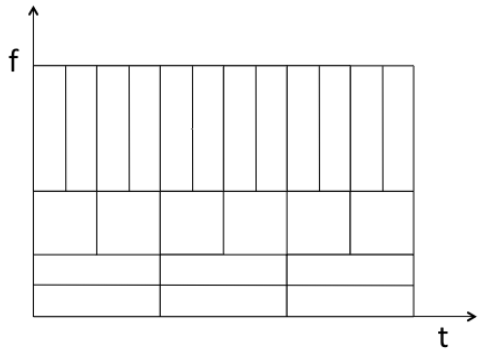

Figure 2.10: Grid representation of a multiresolution approach

The concept of the computation of the spectra with unequal resolution was first introduced by Oppenheim in 1971 [20]. In his paper, he mentioned that the unequally spaced samples (tiles) correspond to a constant Q instead of being linearly related, and attempted to establish the fundamental principles that allowed the implementation of this idea with the means they had available (non-recursive and recursive filter banks). The term constant Q refers to the ratio of the centre frequencies with the desired resolution, which is equal for all bins. In terms of music analysis, the most popular constant Q modification was Brown's [21]. Her approach was embraced by music researchers better than other approaches that she mentions in her paper, because of the intuitive resolution her algorithm utilises. This resolution maintains a good balance between musical and perceptual viewpoints.

2.3.4.2 Adaptive STFT

The adaptive STFT (ASTFT) shares many principles with the multiresolution techniques. Thus, it can be considered as a branch of the multiresolution time-frequency analysis family. Similar to multiresolution techniques, ASTFT attempts to circumvent the fixed time-frequency resolution. However, it follows a slightly different approach. ASTFT analyses the data multiple times with different frame lengths, and intelligently chooses the spectral coefficients that exhibit the best signal representation, both temporally and spectrally. Unlike multiresolution, it uses the homogenous axis of the highest resolution , but plots a combination of the analysis coefficients of all analysis. A visual illustration of the eventual result of this procedure is depicted in figure 2.11.

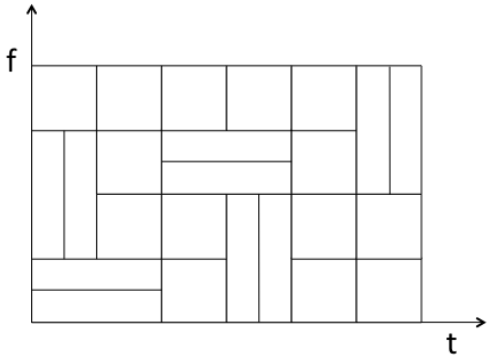

Figure 2.11: Grid representation of an ASTFT approach

The spectral coefficient combination can be achieved due to two constrains set on the parameters of each analysis; (1) zero padding of the frames of all analysis up to the frame length of the analysis with the biggest number of points considered, and (2) overlapping at certain points in time, which are determined by the overlap of the analysis with the smallest frame length. This results in the obtainment of equal number of spectral coefficients that are accurately aligned in time.

The ASTFT aims to decrease time and frequency smearing. Short frames result in undistinguishable bass harmonics from the bass drum, while they maintain the temporal characteristics of the signal, whereas long frames result in time

smearing of drums and other percussions, while they illustrate stationary partials clearlier. Therefore, the ASTFT algorithms identify transients and intelligently select small to average frame lengths for representation of this particular area (illustrated in figure 2.12), while it may select the spectral coefficients of longer windows for the representation of stationary parts.

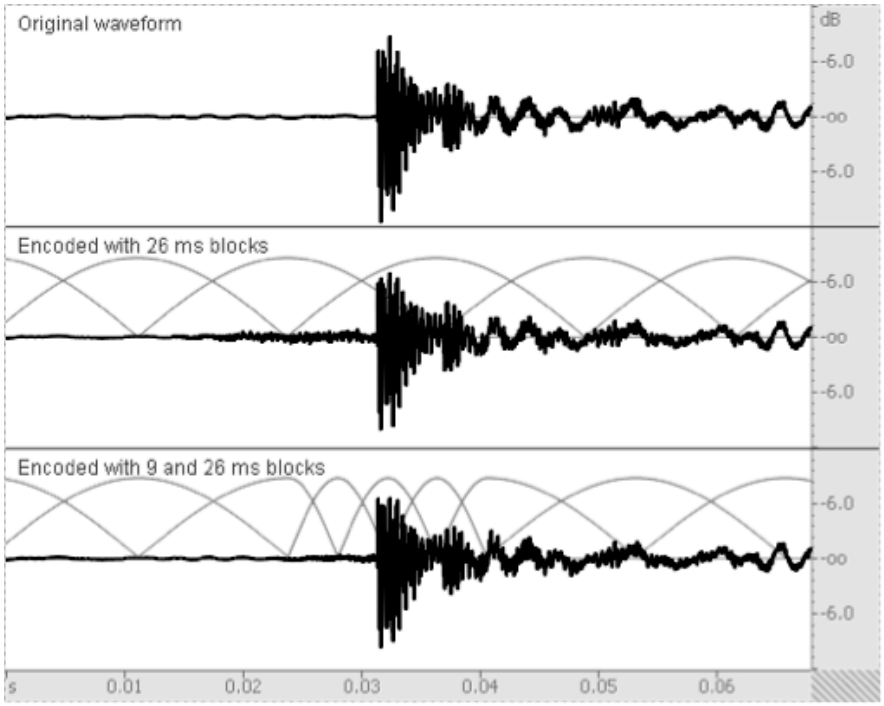

Figure 2.12: ASTFT: Illustrating the use of variable block size with respect to content, which results in smaller amounts of time smearing [22]

It is apparent that the ASTFT approaches extend the fundamental principles of multiresolution. This data-adaptive time-frequency technique was first mentioned by Jones [23]. Unlike constant Q, an inverse function is available, since the same amount of data is obtained from every analysis, and they are correctly aligned in terms of timing. An example of an inverse algorithm for ASTFT is described by Rudoy et al. [24].

2.3.4.3 Frequency Reassignment

Frequency reassignment is a technique applied on the spectra after the STFT analysis has been obtained, which attempts to provide more meaningful coordinates for the spectral components [25]. Once the STFT has been obtained with a fixed grid, the channelised instantaneous frequency (CIF) and local group delay (LGD) parameters are calculated, which are the first derivatives of the complex spectra with respect to time and frequency respectively. Then, the spectral components are plotted at the points described by the estimated CIF and LGD, which results in the reassigned spectrum of the signal.

This technique was first introduced by Kodera et al. [26] according to Fulop and Fitz [25]. In their paper, Fulop and Fitz attempt to gather all the necessary information about time-corrected instantaneous frequency (TCIF) analysis to establish a unified framework, and make information more accessible. They also provide a few examples on the application of frequency reassignment. Additionally, they provide more examples on speech and musical analysis in [27], where they also include an explicit description of the algorithm.

Despite the greater localisation of the frequency components, both in time and frequency, frequency reassigned spectra are very noisy. Meaningful results are obtained around the neighbourhood of a component, while it might incur random output at areas that contain no significant frequency components. A de-noising method was proposed by Fulop and Fitz [27], inspired from empirical observations. This method exploits the statistical behaviour that the 2^{nd} derivative of the spectral coefficients manifests. Moreover, this technique is only used for analysis, since the spectral components are arbitrarily placed, both in time and frequency.

2.3.4.4 Multitapers

Multitapers approach the STFT from a different angle. From a statistical point of view, the results of STFT lack validity, since the signal's spectrogram is the result of a single observation (estimation). The corresponding amplitude and phase measures are not always correct due to the deficiencies of DFT, which have been thoroughly examined in 2.3.1. Subsequently, the results are thought

to be biased and of great variance. This issue is tackled by multitapers, which introduces multiple estimates for every frame.

Multitapers, first introduced by Thomson [28], and also named as multi-window analysis in many papers [29, 30], is an approach that attempts to increase the validity of the results and achieve higher credibility by obtaining more than one measurement (transformation) for each frame. Every observation is calculated with a different window function that is applied to the data, and the final output is an average of the estimates obtained. The window functions are all orthogonal to each other, and optimally concentrated in frequency. This was judged to be necessary by Thomson in order to minimise the variance and the bias of the estimates.

Pitton's paper, named "Time-frequency spectrum estimation: An adaptive multitaper method" [31], should not be confused with the adaptive as it is used in the ASTFT. Pitton is following a different approach when he combines the estimates for the obtainment of the spectrum. Instead of simple averaging, he is intelligently weighting each observation with respect to a quality measure he devised about the amount of spectral leakage they manifest.

2.3.5 Summary

This section has elaborated on the fundamentals of spectral processing by explaining the functionality of the STFT/DFT and its underlying technicalities, and reviewed a number of modifications developed to compensate with the limitations of STFT.

The ultimate STFT algorithm is envisioned as a combination of the modifications that were covered in 2.3.4, since the internal deficiencies that come with the discrete implementation of the Fourier transform are inevitable. This version of STFT should be adaptable, with unfixed time-frequency representation, whose output will be credible due to the number of estimations obtained. Although this idealistic product is far from what is currently available and it would require the consideration of several factors (computational expensive), there are algorithms that attempt to marry multiple modifications of STFT, as described in 2.3.4. More specifically, Xiao et al. [32] have developed a hybrid modification of STFT

that combines multitapers with frequency reassignment. Although at very early stages, it seems that the evolution of STFT is heading this way.

Despite the fact that the available modifications of the STFT attempt to tackle most of its limitations, there is no modification that deals with the arbitrary selection of the starting and ending points of each frame. It was shown in 2.3.1 that this can incur considerable amounts of spectral leakage. Also, the lack of interest in the phase information obtained from the spectral analysis technically results in incomplete analysis of the data. To the best of the authors knowledge, there is no modification of the STFT that exploits phase information for the improvement of the credibility of the analysed data. It is understandable that phase might not be meaningful or coherent for signals in various fields, however, it can be for audio signals. The following chapter focuses on the research conducted in an attempt to address the aforementioned issues.

Chapter 3

Phase Stability Quality Measure

Fourier techniques are plagued with a variety of assumptions and user-specific design choices, which result in a number of compromises.

- The foremost inevitable assumption is the stationarity of every framed signal considered by Fourier approaches. This often results in incoherent data, since the varying frequency content of non-stationary signals is interpreted as separate frequency components.
- Moreover, the arbitrary partition of the signal into frames in the STFT, whose starting and ending points are determined by fixed offsets with respect to the data start point, often results in edge effects, which also deteriorate the credibility of the data (described in 2.3.1).

In addition, a set of user-specific design choices require determination in STFT, which result in further compromises. A detailed description of the user-specific design choices can be found in 2.3.3.3 but a summary is provided in the table 3.1, where each choice is linked to its subsequent compromise.

Numerous techniques have been developed that attempt to compensate the deficiencies of the STFT (see 2.3.4). They, however, focus on the issues that are described in table 3.1 (with the exception of the discard of phase information), leaving the list of issues as described by the bullet points unaddressed. A relatively simple concept is proposed of a different mindset to those described in 2.3.4 that attempts to address these issues. The aim of this novel modification

Frame length	-	Time vs. frequency resolution
Window function	-	Spectral leakage vs. peak bandwidth
Overlap	-	Temporal interpolation vs. computational expense
Points considered by FFT (> frame length, if zero padding is applied)	-	Frequency interpolation vs. computational expense
Discard of phase information		

Table 3.1: User-specific design choices of STFT and their implications

of STFT is to improve the quality and credibility of the estimated results for the analysis of stationary or near-stationary digital signals.

3.1 Motivation: PASS with EASE

This work is based on some unpublished initial studies carried out by the project supervisor [33]. These studies focus on the development of an ensemble of estimations in order to compensate some of the artefacts that arise due to discontinuities. This approach also indicated that the phase content of a signal could carry useful information. The earlier work, however, was neither fully tested nor applied to any specific signal processing application. This project extends this initial studies with the development of a function that utilises phase information to define a confidence level for the estimated data, and applies it in the framework of source separation to assess its suitability and effectiveness.

3.2 Research Hypothesis, Aims and Objectives

It is **hypothesised** that the phase information for a sampled frequency component arising from a partial observed at sufficiently small intervals manifests structure which distinguishes it from phase information due to noise or Fourier-related artefacts. This can then be exploited in order to obtain a confidence level that can be attached to every frequency bin of the estimated spectrum, and pro-

duce the enhanced spectra of the signal. The end result is anticipated to be more credible and of better quality, since it should be easier to discriminate between "structure" and "noise" or "artefacts".

The **novelty** of this work lies on the use of ensembles of STFT estimates obtained around the area of the original starting point of the frame instead of a single observation for every arbitrarily selected frame. In addition, the use of the phase information in a meaningful fashion for the improvement of the credibility of the data differentiates this approach from the available STFT modifications.

The **aim** of this research was the implementation, testing and validation of this novel approach, the definition of the measure that will act as a confidence level for every individual bin, and its employment in the framework of source separation in order to assess its effectiveness (chapter 5).

The development of this project was achieved with the attainment of the following **objectives**:

1. Investigation of the phase behaviour of simple synthetic signals and the initial phase angles obtained from an STFT approach.

2. Development of the analysis tool and the necessary underlying functions.

3. The testing of this method on a set of signals in order to validate its functionality.

4. Evaluation of the developed functionality with its incorporation in an example application (chapter 5) and consolidation of a list of aims for attainment in the future (chapter 7).

3.3 Principles

A set of simple synthetic signals, both stationary and non-stationary, are employed in this section to introduce the methodology proposed, illustrate the potential of the ensemble of closely-related estimates approach, and define the phase stability quality measure. The length of the signals and the number of additional estimates were kept small to allow the portrayal of all relevant information.

3.3.1 Stationary Signals

An idealised cosine signal is considered in this sub-section.

$$y(t) = \cos(\varphi(t)) \tag{3.1}$$

$$\varphi(t) = \omega t + \phi(0) \tag{3.2}$$

The cosine, which is comprised of 128 samples in total, with a single period containing 16 samples, is depicted in figure 3.1. In addition, the wrapped phase coefficients of the cosine that are plotted against time and the amplitude spectrum of the signal are provided and serve as a reference points. They allow comparisons to be made between the phase and amplitude spectrum behaviour of the original signal and the following framed signals.

Consider the application of an arbitrary frame on the cosine and 3 additional frames of high overlap with respect to the first frame to obtain the ensemble of closely-related estimates, with the application of rectangular window functions. The additional 3 frames are required in order to obtain the short-time evolution of the phase behaviour of the signal. The first frame is thought to be the original as applied by STFT, and the rest 3 are the additional estimates as suggested by this project's approach. Therefore, each frame is named after the number of the original frame and the number of estimate, i.e. for frame 1, the 6^{th} estimate is called Frame 1.6. Setting the frame length to 41 samples and a relatively short sample shift for every additional estimate, 2 samples (corresponds to $\frac{\pi}{8}$ shift in phase in the particular example), results into the scenario illustrated in figure 3.2. The figures 3.3 and 3.4 accompany figure 3.2, and depict the subsequent periodic wrapped phase behaviour of the framed signal as considered by FFT, and its actual logarithmic amplitude spectrum in order to showcase the spectral leakage levels.

Frame 1.1 of figure 3.2 is the frame that manifests the greatest degree of edge discontinuity. The selected portion of the signal starts at the maximum value and ends at the minimum. This discontinuity is expected to result in large

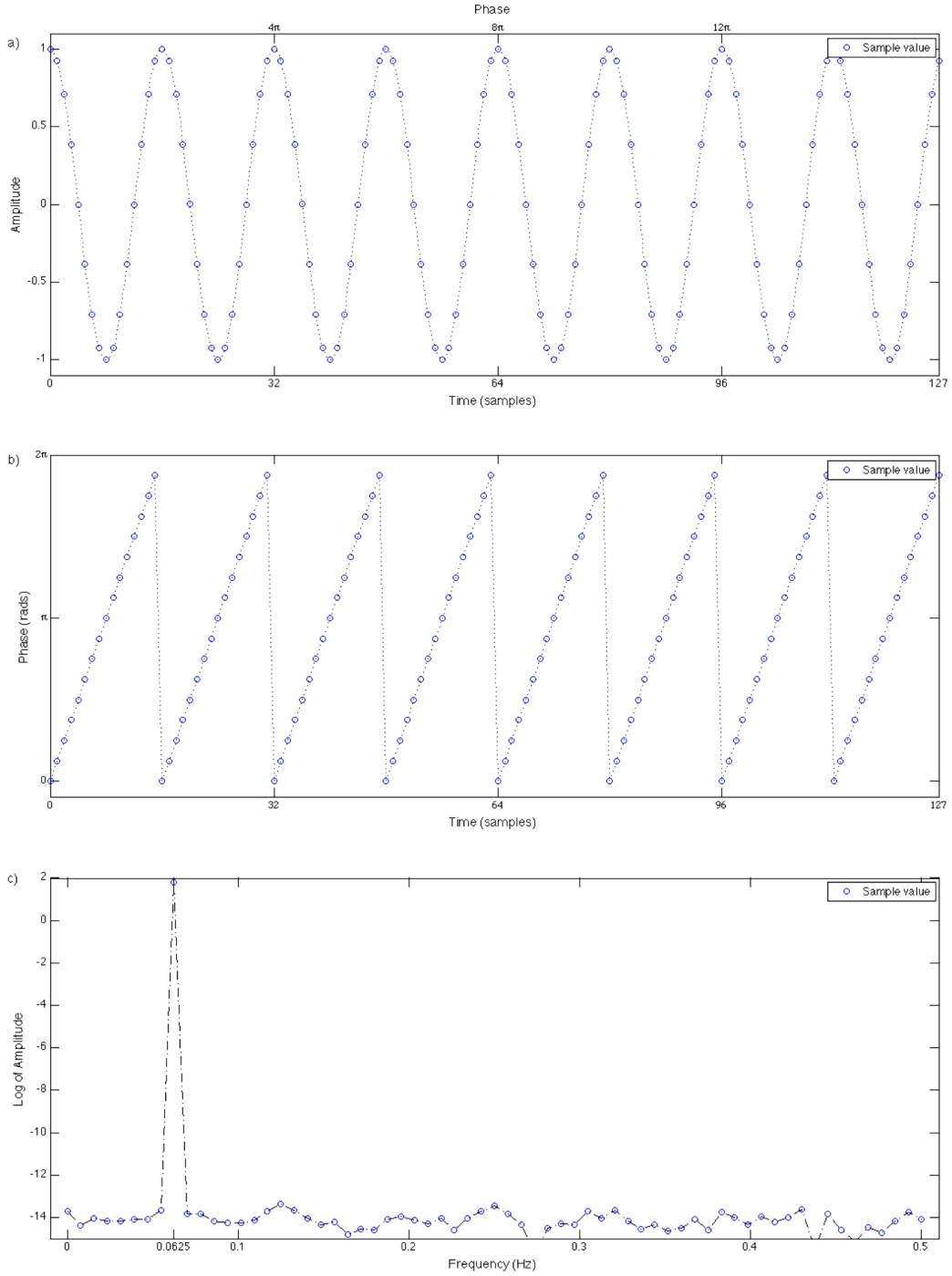

Figure 3.1: (a) Representation of an idealised cosine ($N = 128$, $T = 16$, $\varphi(0) = 0$). (b) The wrapped phase angle values of the signal depicted in a) as calculated during its generation. (c) The logarithmic amplitude spectrum of the signal depicted in a). A single peak is depicted as expected due to the lack of discontinuities, with all the rest of the sampled frequency components being virtually zero

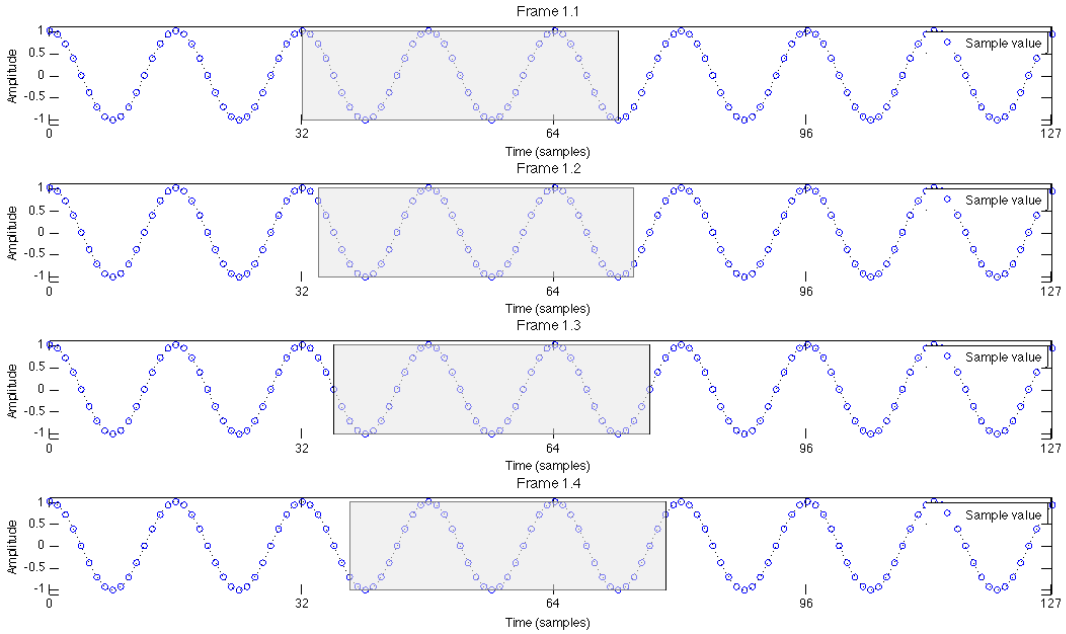

Figure 3.2: Hypothetical scenario of ensemble of closely-related estimates applied to the signal of 3.1-a)

spectral leakage, and the actual amount is portrayed in figure 3.4. **Frame 1.2** of figure 3.2 manifests a smaller degree of discontinuity with regards to Frame 1.1. It is therefore expected to exhibit smaller amounts of spectral leakage, and this is verified in the amplitude spectrum of Frame 1.2 in figure 3.4. **Frame 1.3** of figure 3.2 has zero discontinuities. However, the spectral leakage will not be zero due to the change in the gradient of the periodic signal. The reason of the existence of spectral leakage is better illustrated in the signal's periodic wrapped phase angle values, as depicted by figure 3.3. Despite the fact that there are no discontinuities in the representation of the signal's amplitude with respect to time, there are discontinuities in the signal's phase angle values with respect to time. Hence, spread in the frequency domain occurs as portrayed by figure 3.4. **Frame 1.4** of figure 3.2 manifests similar amounts of discontinuities as Frame 1.2. Thus, its amplitude spectrum resembles the amplitude spectrum of Frame 1.2, as illustrated in figure 3.4. It is important to stress that small amounts of discontinuities will occur even in the case where a window function that tapers

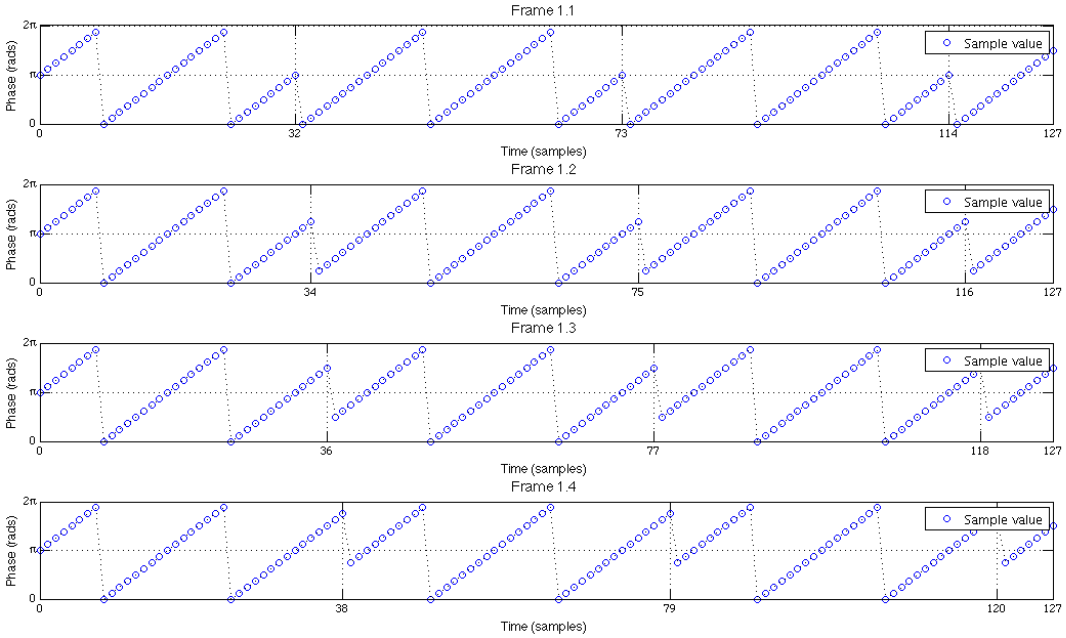

Figure 3.3: The periodic version of the wrapped phase angle values of the framed signals depicted in figure 3.2, as considered by FFT

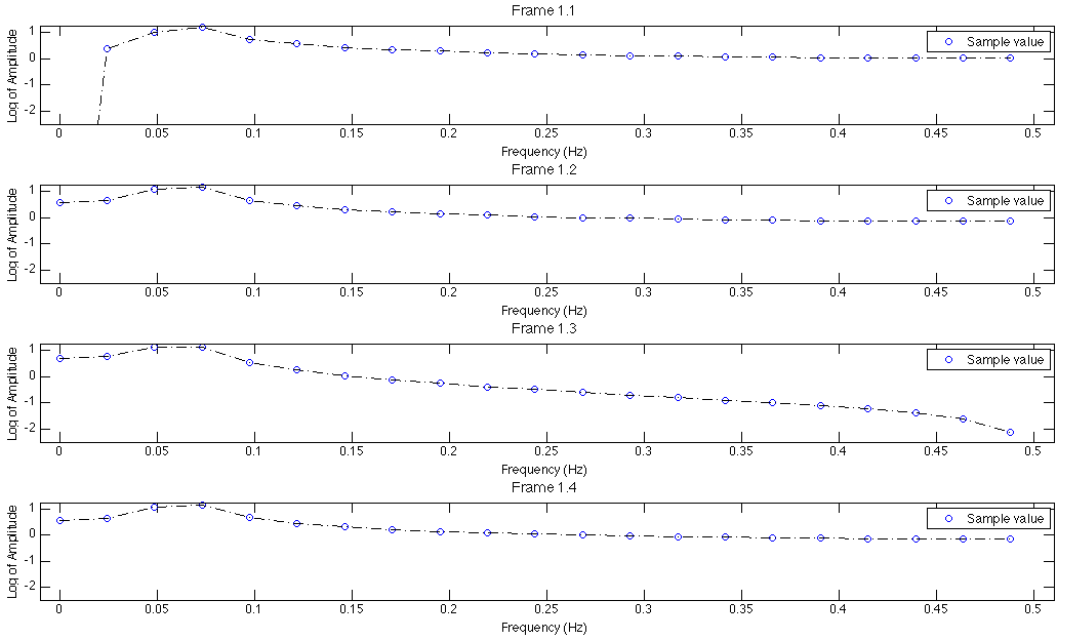

Figure 3.4: The logarithmic amplitude spectra of the framed signals of figure 3.2

to zero towards the edges is applied.

According to the amplitude spectra of the closely-related estimates as illustrated by figure 3.4, the bins that exhibit significant presence of a frequency component and preserve their amplitude approximately on the same levels are in the area of $(0.03 - 0.1$ Hz$)$. It is known from the specifications of the signal that its frequency lies within this area ($T = 16$, hence $f = \frac{1}{T} = 0.0625$). In contrary, the amplitude of the rest of the bins vary greatly with regards to every shifted estimate. Respectively, these are the bins that they do not relate to the frequency of the signal component, and can be thought as the bins that arise from algorithmic artefacts, specifically spectral leakage in this case.

Having examined the amplitude behaviour, attention is now focused on phase and its variance with respect to frame position. Specifically, the sets of initial phase angle values of two bins is investigated, one from the neighbourhood of the frequency component and one from the spectral leakage neighbourhood. The complete set of initial phase angle values obtained by FFT is included in Appendix A on page 93, but the values of the two representative bins are copied in table 3.2. Moreover, a graph is plotted (figure 3.5) holding the values of each frame sequentially in order to make their observation easier.

	Frame 1.1 Initial phase (rads)	**Frame 1.2 Initial phase (rads)**	**Frame 1.3 Initial phase (rads)**	**Frame 1.4 Initial phase (rads)**
Bin 4	-1.341	-0.636	0.230	1.096
Bin 18	-0.268	-0.214	1.303	2.819

Table 3.2: Initial phase for every frame estimate for bin 4 and 18

Figure 3.5 reveals interesting results. The phase values of the bin that holds significant part of the frequency component's energy are a linear function of the shift number. On the other hand, the coefficients of the bin that occurs due to spectral leakage exhibit some degree of randomness. This information is then exploited in order to produce a quality measure for each bin.

A 1^{st} order curve is fitted to the data, which represents the behaviour of the phase of a stable frequency component (equation 3.2). Figure 3.6 portrays the modelled phase values of the idealistic frequency component against the actual

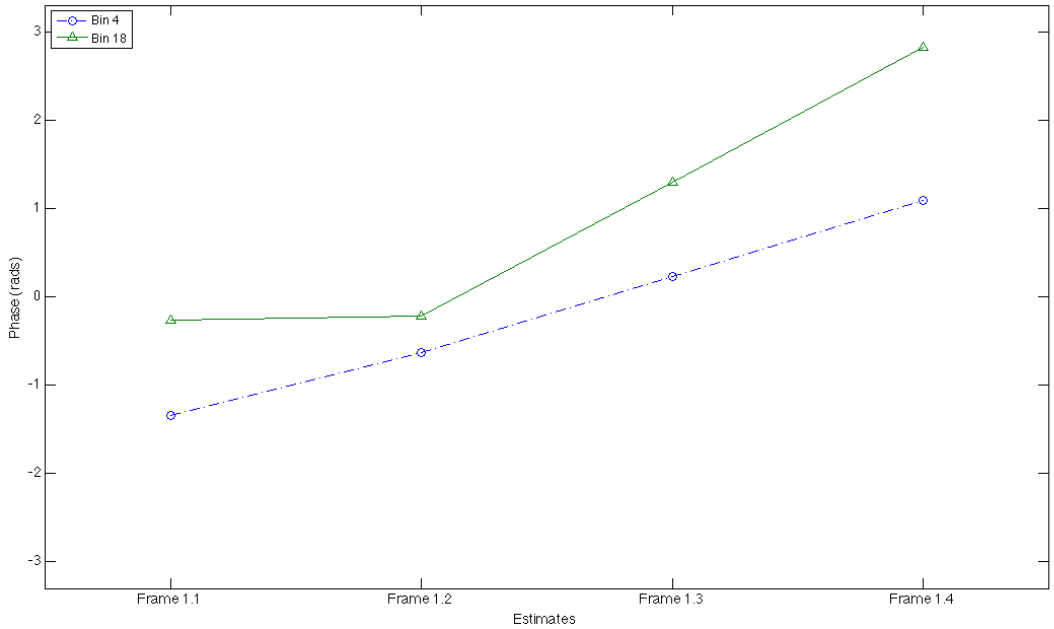

Figure 3.5: Initial phase angle value variation for each estimate, as obtained from FFT, for bins 4 and 18

values obtained by FFT in order to illustrate their difference. Then, the deviation of the initial phase values obtained by FFT from the modelled data is calculated in order to find the deviation of the actual measurement from the behaviour of an idealistic frequency component (portrayed in figure 3.7-a & b). Finally, calculating the least squares of the deviation of the phase values from the 1^{st} order curve results in the measure that indicates the variance of the actual frequency component as perceived by FFT from an idealistic frequency component. This measure is here defined as the **phase stability**.

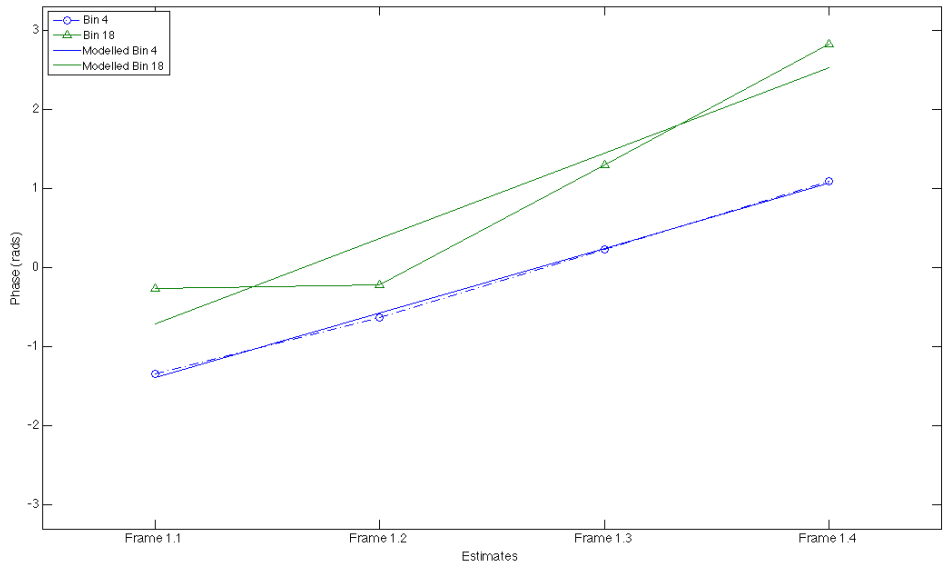

Figure 3.6: Initial phase angle value variation for each estimate as obtained from FFT against the modelled phase angle values of an idealistic frequency component for two representative bins

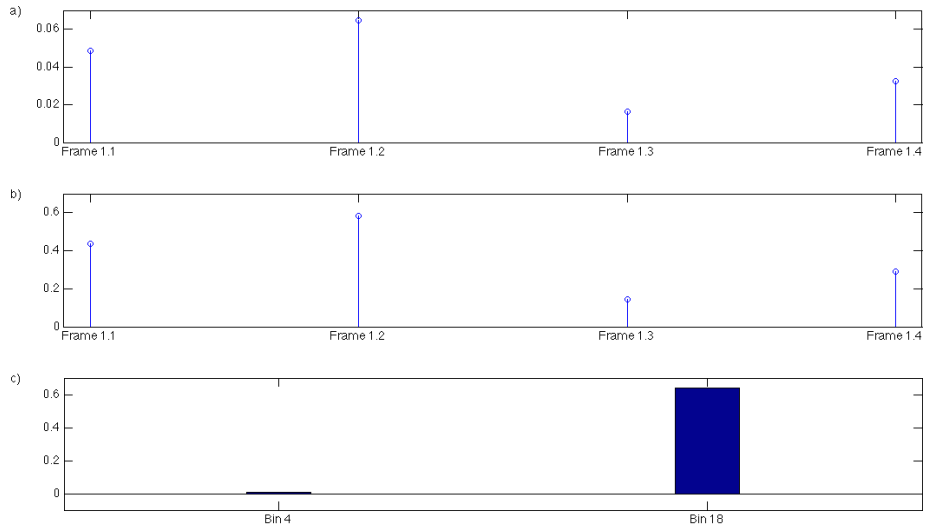

Figure 3.7: (a) Deviation of the phase values calculated by FFT from the modelled phase values of an idealistic frequency component for bin 4. (b) Deviation of the phase values calculated by FFT from the modelled phase values of an idealistic frequency component for bin 18. (c) Phase Stability: The sum of the least squares of the deviation for each bin

3.3.2 Non-Stationary Signals

The behaviour of a near-stationary signal and a non-stationary signal is examined in this section. These signals have been tailored to represent common realistic musical effects that are often incorporated in musical performances. The aim is to investigate the performance of the ensemble of closely-related estimates approach and the phase behaviour with regards to the frame shift on these cases of greater complexity where conventional Fourier techniques are inadequate.

1. The first signal contains the same cosine examined in the previous section but with vibrato applied on it.

$$y(t) = cos(\varphi(t)) \tag{3.3}$$

$$\varphi(t) = Asin(\omega_v t) + \omega_c t + \phi(0) \tag{3.4}$$

   The signal is 128 samples long, with centre frequency of $f_c = 0.0625$ Hz. A typical vibrato effect may vary the centre frequency by two semitones. Thus, in order to find the interval of a semitone, an octave was devised with starting note at 0.0625 Hz and ending at 0.125 Hz. It was then divided into 12 equal intervals, which unveiled the value of a semitone, $A_v = 0.0057$ (Hz deviation from f_c). Thus, the end result varied between 0.0568 Hz and 0.0682 Hz four times in the span of these 128 samples ($f_v = 32$ Hz) (figure 3.8-a). The particular vibrato frequency was found appropriate for illustrative purposes, although it differs largely with respect to realistic vibrato rates.

2. The second signal represents a frequency sweep (chirp), which corresponds to the glissando effect.

$$y(t) = cos(\varphi(t)) \tag{3.5}$$

$$\varphi(t) = g\pi t^2 + \omega t + \phi(0) \tag{3.6}$$

$$g = \frac{f_1 - f_0}{t_1} \tag{3.7}$$

where g is the chirp rate.

Glissandos may start at a note and terminate at the same note an octave above. Therefore, the frequency of the subject signal starts at $f_0 = 0.0625$ Hz and progresses linearly to $f_1 = 0.125$ Hz in the span of the 128 samples (figure 3.9-a)

The wrapped phase angle values as calculated during the generation of the signals, and the amplitude spectra of the signals are provided in addition to their temporal representations (figure 3.8-b & c, figure 3.9-b & c). Moreover, the unwrapped phase angle values as calculated during the generation of the signals are provided to demonstrate that these cases also exhibit trends (figure 3.10 & 3.11).

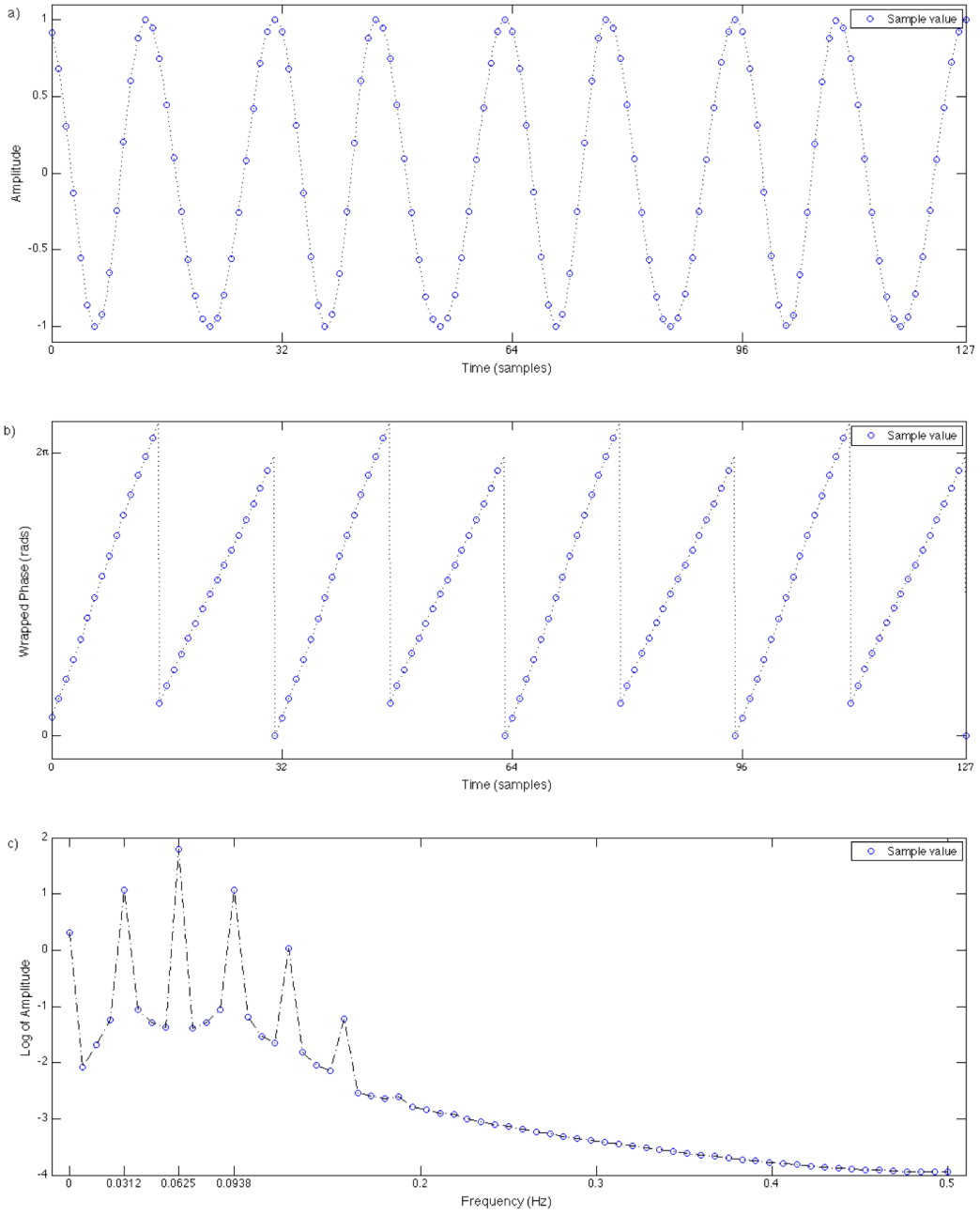

Figure 3.8: (a) Representation of the idealised cosine with vibrato. (b) The wrapped phase angle values of the signal depicted in a) as calculated during its generation. (c) The logarithmic amplitude spectrum of the signal depicted in a)

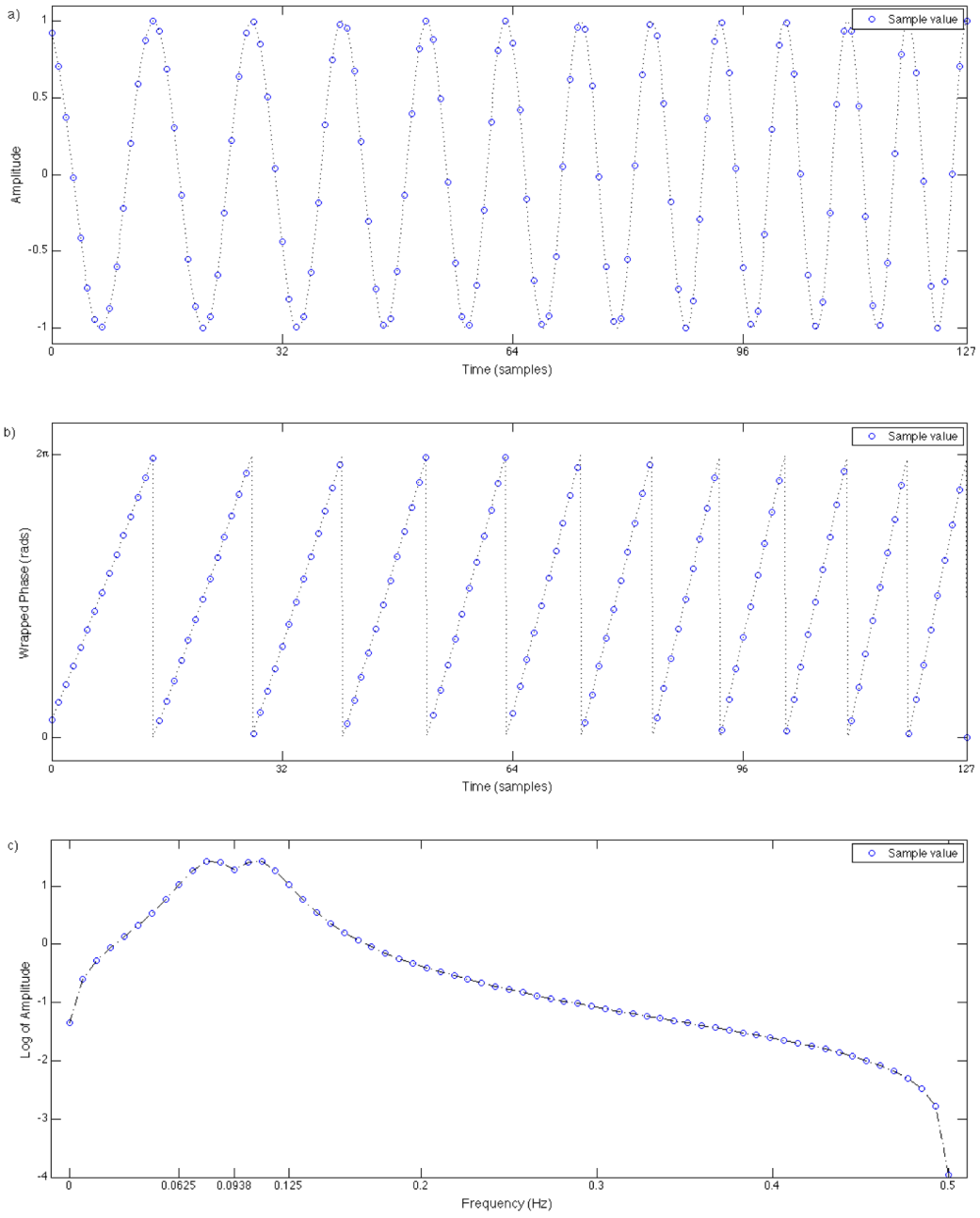

Figure 3.9: (a) Representation of the idealised chirp. (b) The wrapped phase angle values of the signal depicted in a) as calculated during its generation. (c) The logarithmic amplitude spectrum of the signal depicted in a)

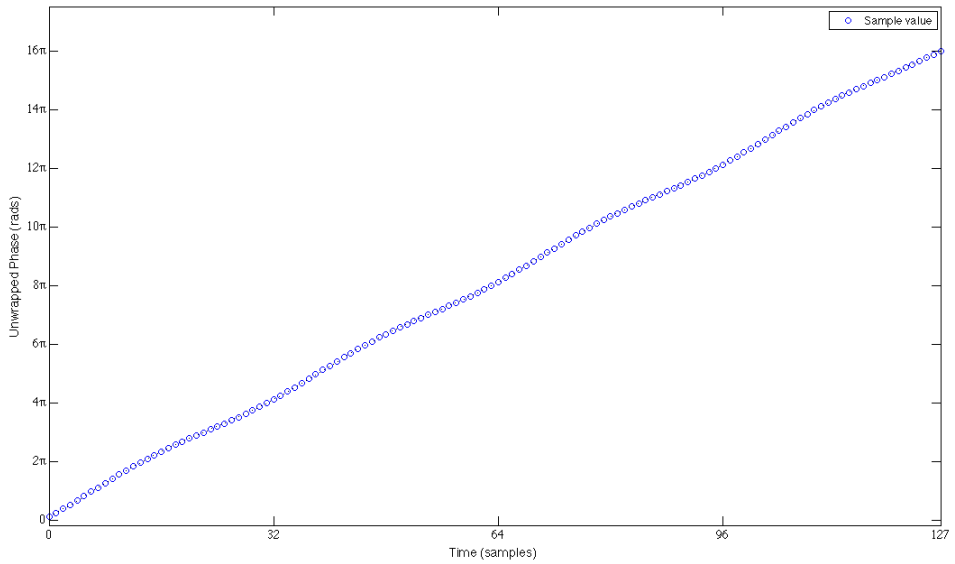

Figure 3.10: The unwrapped phase angle values of the cosine with vibrato depicted in fig. 3.8-a) as calculated during the signal's generation.

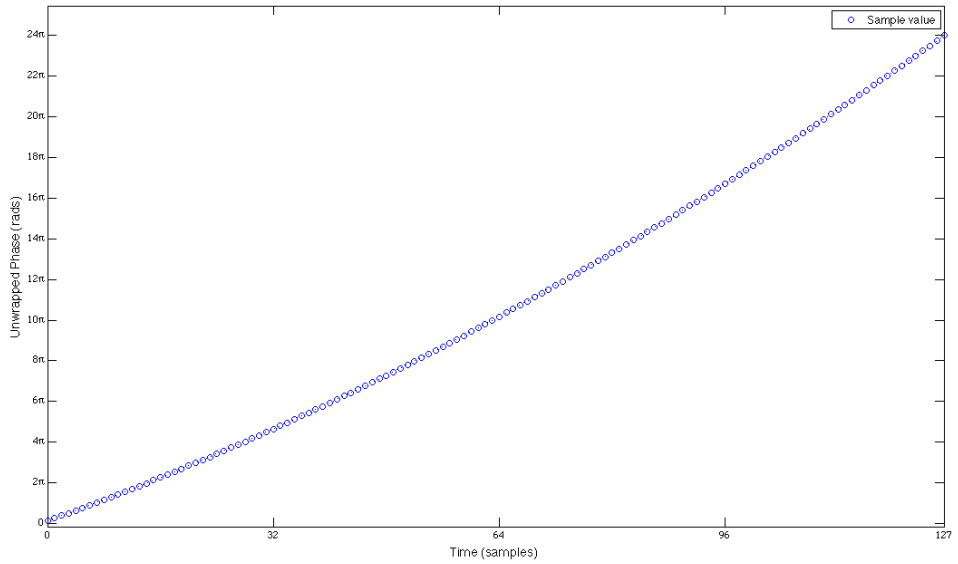

Figure 3.11: The unwrapped phase angle values of the chirp depicted in fig. 3.9-a) as calculated during the signal's generation

The signals were subjected to four frames, as it was illustrated in figure 3.2 in sub-section 3.3.1, and the amplitude spectrum of each frame was calculated with FFT. The initial phase angle values of each analysis are included in Appendix B & C, pages 94 and 95. Attention is focused on the same bins that were examined in the previous example for the signal with vibrato, bin 4 and 18, whereas bin 8 and 18 are examined for the example with glissando due to the fact that bin 4 does not hold a significant component for the frequency sweep example (figure 3.9-c). Table 3.3 contains the phase values of the aforementioned bins for each analysed frame of the signal with vibrato, whereas table 3.4 contains the phase values of the signal with glissando.

	Frame 1.1 Initial phase (rads)	**Frame 1.2 Initial phase (rads)**	**Frame 1.3 Initial phase (rads)**	**Frame 1.4 Initial phase (rads)**
Bin 4	-0.657	0.195	1.063	1.759
Bin 18	-0.221	0.567	2.816	2.878

Table 3.3: Initial phase angle values for bin 4 and 18 for the cosine with vibrato

	Frame 1.1 Initial phase (rads)	**Frame 1.2 Initial phase (rads)**	**Frame 1.3 Initial phase (rads)**	**Frame 1.4 Initial phase (rads)**
Bin 8	1.517	2.220	-3.077	-1.368
Bin 18	2.761	2.890	3.135	2.819[1]

Table 3.4: Initial phase angle values for bin 8 and 18 for the chirp

Plotting the initial phase angle values sequentially for each bin reveals similar results to the results obtained for the stationary signal (figure 3.12 represents the vibrato signal, and figure 3.14 represents the chirp). The initial phase angle values of the bins that contain a significant part of the subject signal are a function of the shift number. Unlike with the stationary signal, the values are not linearly related. Non-stationary signals that represent realistic musical performance styles are best described with a second order curve.

[1] One π added to the original value for continuation purposes.

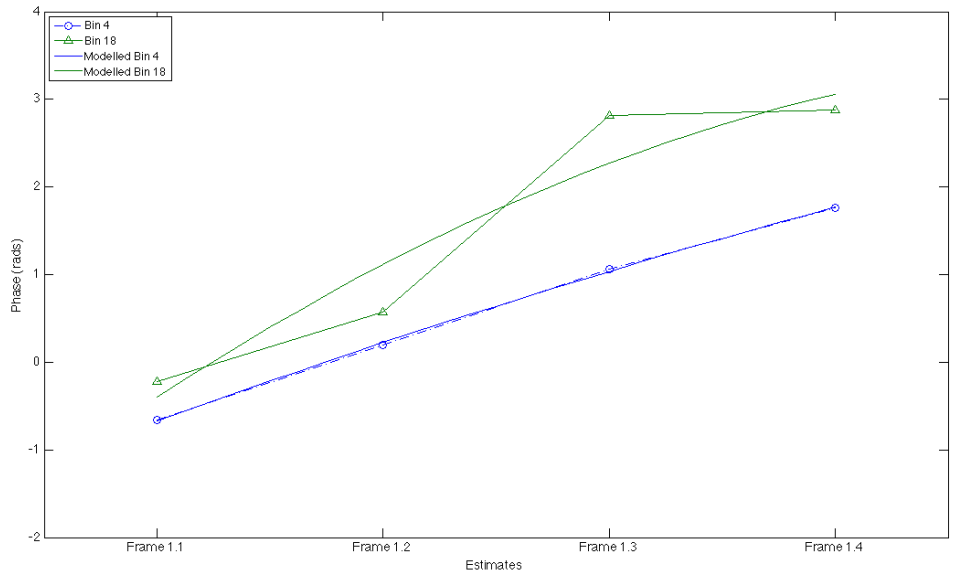

Figure 3.12: Phase coefficients as obtained from FFT for the cosine with vibrato against the modelled phase values of an idealistic frequency component

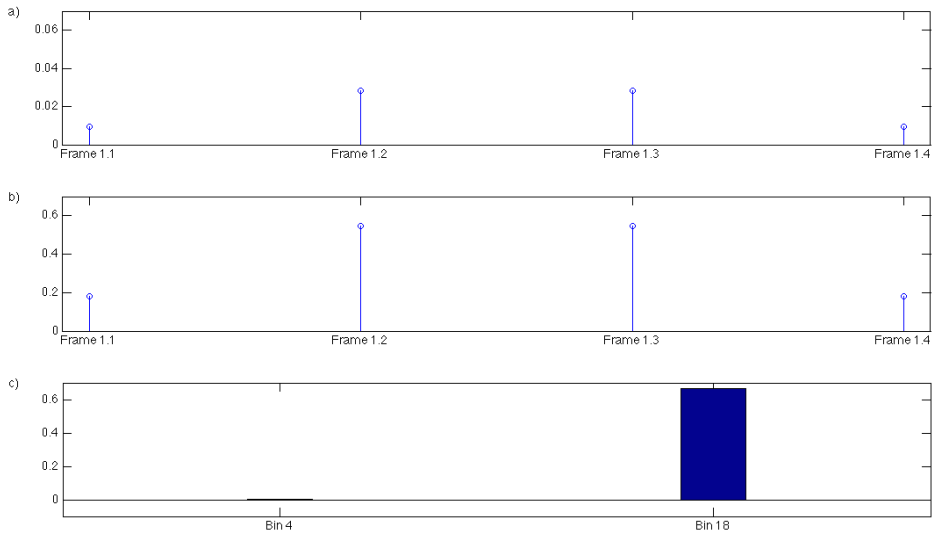

Figure 3.13: (a) Deviation of the actual phase values calculated by FFT from the modelled phase values of an idealistic frequency component with vibrato for bin 4. (b) Deviation of the actual phase values calculated by FFT from the modelled phase values of an idealistic frequency component with vibrato for bin 18. (c) Phase Stability: The sum of the least squares of the deviation for each bin

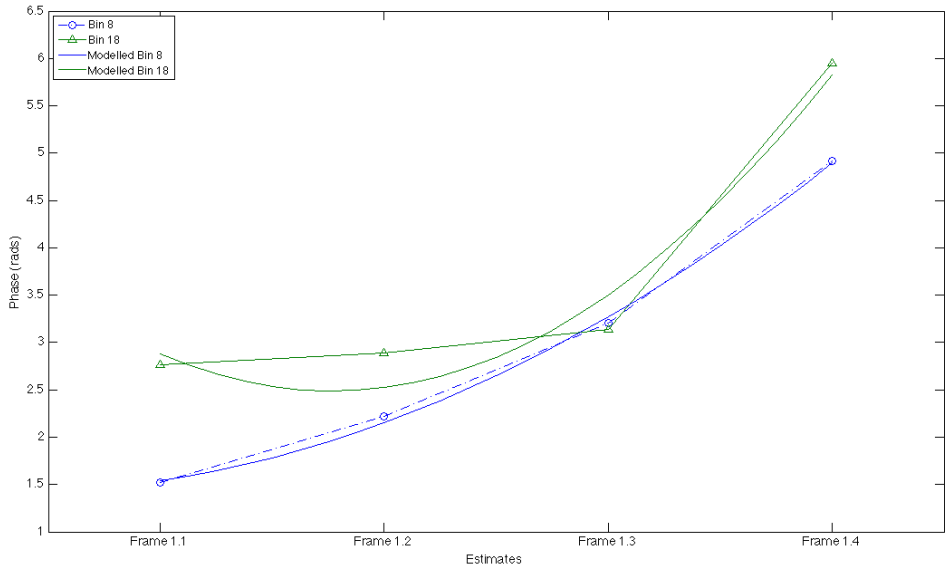

Figure 3.14: Phase coefficients as obtained from FFT for the chirp against the modelled phase values of an idealistic frequency component

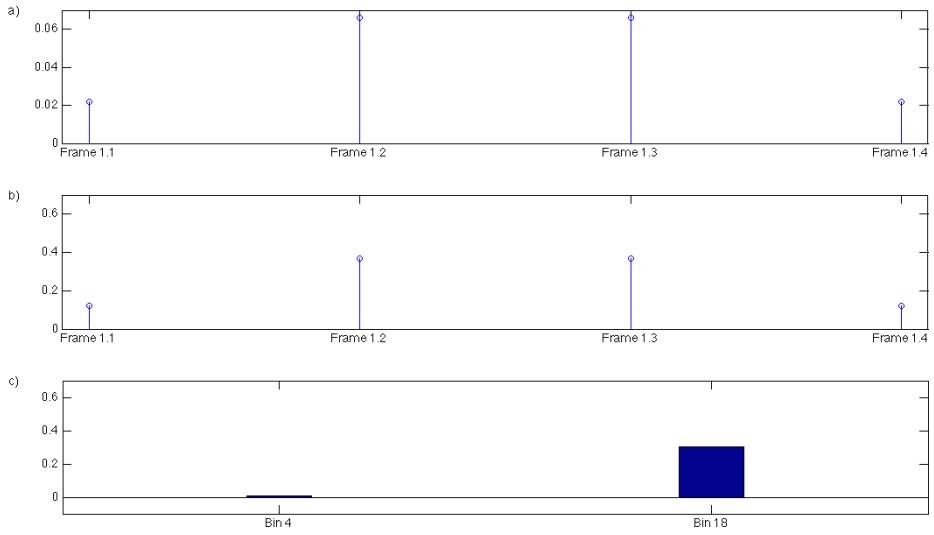

Figure 3.15: (a) Deviation of the actual phase values calculated by FFT from the modelled phase values of an idealistic frequency sweep for bin 8. (b) Deviation of the actual phase values calculated by FFT from the modelled phase values of an idealistic frequency sweep for bin 18. (c) Phase Stability: The sum of the least squares of the deviation for each bin.

3.4 Examples

The previous section introduced the phase stability quality measure with the aid of a set of simple synthetic signals. The length of these signals was intentionally kept short in order to allow the inclusion of all sample points for illustrative purposes. The proportion of the sample shift with the frame length was deliberately chosen to be relatively big in order to have more dramatic changes in the phase information of the signals. Thorough investigation was conducted on the analysed data, and particular attention was paid to the phase evolution of two representative bins with respect to frame shift.

This section calculates the phase stability of a set of synthetic and real signals (instrument recordings), which are of greater complexity and more realistic duration. The focus is now shifted to the phase stability behaviour of all bins of a particular frame. The amplitude spectra of the signals are also provided for comparison.

The following paragraphs describe the nature of the signals under investigation and include the graphs displaying their analysed data. These graphs illustrate the relation between the phase stability and the amplitude spectra. Moreover, an additional representation is included, the inverse phase stability[1] to enhance the illustration of the structures found in the information represented by phase stability. The parameters used for the analysis of these signals were kept the same for every analysis for consistency reasons (see table 3.5). These parameters were chosen as a representative example, although any set of analysis parameters can be used (see further work in chapter 7). The number of estimates and sample shift were set to 10 and 24 respectively in order to estimate the short-term phase evolution of the signal and avoid the association of this particular analysis with the analysis of very high temporal interpolation[2].

There were 6 signals analysed in total, forming two groups; synthetic (3 signals) and real signals (3 signals), of which the sustain part is considered. Each

[1] Inverse phase stability is merely the inverted phase stability value plus eps, where eps is the smallest possible number considered by MATLAB.

[2] Setting the number of estimates to 10 and the sample shift to 24 results in 216 samples offset of the starting point of the final estimate from the starting point of the first estimate (or beginning of frame). The aim is to keep this product relatively small with regards to the frame length.

Parameter Name	Value
Frame length	4096
Overlap	50%
Zero padding Factor	0
Window function	Hamming
Number of estimates	10
Sample shift	24

Table 3.5: Phase stability analysis parameters for the analysis of the signals

group contained a stationary, a near-stationary (vibrato), and a non-stationary (glissando) signal. All signals were comprised of multiple partials. Their length was 1 second long and the sampling frequency was 44100 Hz. The graphs that portray the analysed data of the synthetic signals display the second frame of their analysis, which was arbitrarily selected. For the representation of the real signals, however, the tenth frame is illustrated, which corresponds to the analysis of the sustain part of the note.

The specification of the synthetic signals are described in the following list.

1. The first synthetic signal was comprised of four stationary frequency components of [200 450 800 1300] Hz and amplitudes [0.2 0.1 0.03 0.08], respectively.

2. The second synthetic signal was comprised of three partials of centre frequency [300 800 1800] that each one deviates from the centre frequency by 20 Hz at a rate of 4 Hz. Their corresponding amplitudes are [0.2 0.1 0.5].

3. The synthetic signal with glissando consisted of three partials, starting at [100 450 1100] Hz and terminating at [200 900 2200] Hz within the 1 second, with amplitudes [0.2 0.1 0.5].

The real instrument recording was an A4 violin note obtained from the Music Instrument Samples library of the University of Iowa [34]. The vibrato and glissando effects were applied to the note artificially in Cubase 7.5 in order to know the exact parameters of the signals. For the signal with vibrato, the pitch deviates by 1 semitone from the original pitch at a rate of 5 Hz, and the processing with

which this was achieved is depicted in Appendix D, page 96. For the signal with glissando, the pitch progresses linearly to 3 semitones higher from A4, within the length of the sample recording. The processing with which this was achieved is depicted in Appendix E, page 97. The analysis of the signals are displayed in the following figures.

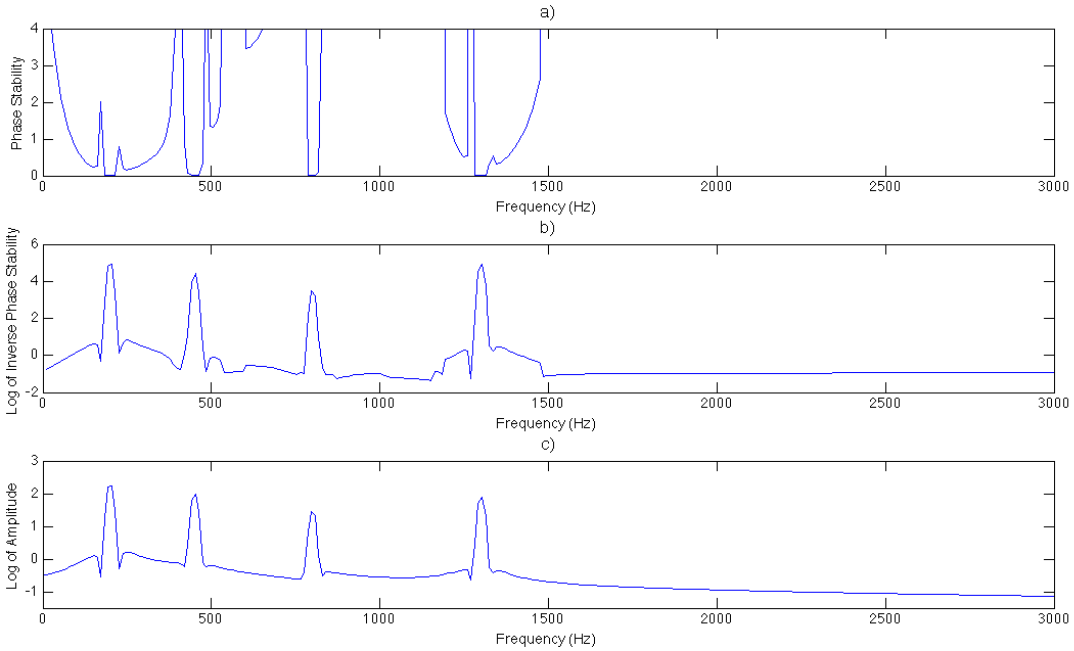

Figure 3.16: Analysed data of the 2^{nd} frame of the synthetic signal with 4 stationary components (a) Phase stability. (b) Inverse phase stability. (c) Amplitude spectra

Figure 3.16 illustrates very interesting results. These are particularly evident in graph b), where the inverted phase stability is depicted. The inverted phase stability exhibits similar trends with the amplitude spectra of the frame. Specifically, the peaks are located at the same position on the frequency axis, and the lobes occupy approximately the same amount of bins. Moreover, the dynamic range of the inverse phase stability graph is greater than the dynamic range of the amplitude spectrum. Nevertheless, the relative height of the peaks remains the same in this example, which is particularly interesting given that the phase stability plot makes absolutely no use of amplitude information. Moreover, the

amplitude spectrum appears slightly smoother than the inverse phase stability graph.

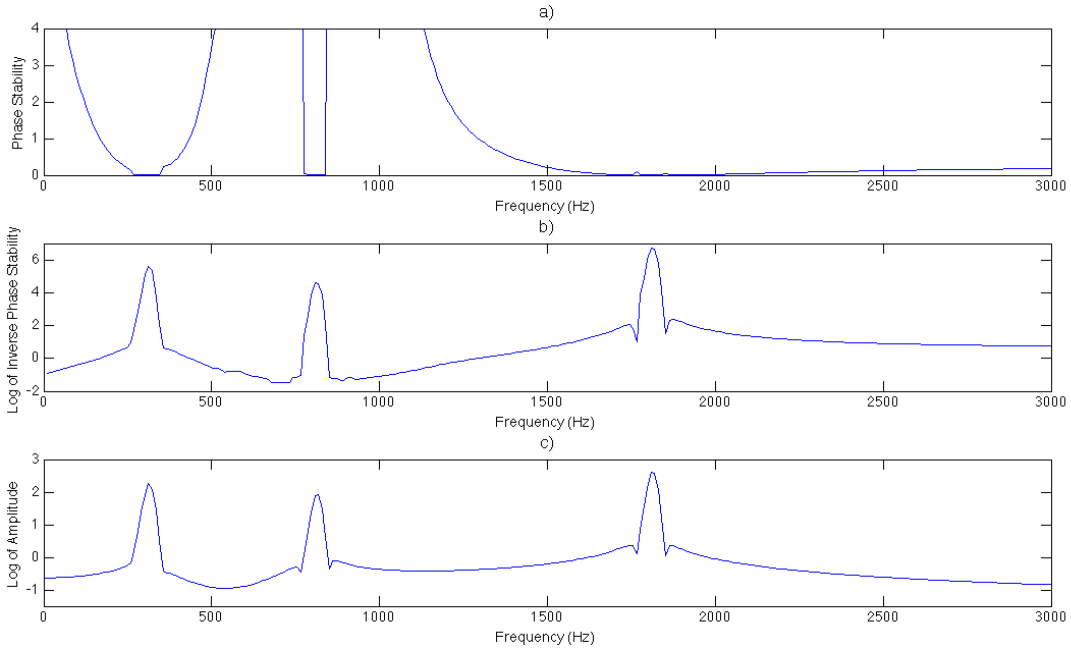

Figure 3.17: Analysed data of the 2^{nd} frame of the synthetic signal with 3 near-stationary components (signal with vibrato). (a) Phase stability. (b) Inverse phase stability. (c) Amplitude spectra

Similar results were obtained for the analysis of the stationary component with vibrato, which can be seen in figure 3.17. The behaviour of the inverse phase stability resembles the behaviour of the amplitude spectrum, with the peaks located at the same place, occupying the same amount of bins. In this example, however, the second lobe is much better defined by the inverse phase stability. Again, the dynamic range is greater in the inverse phase stability than the amplitude spectrum. Graph b) differs from graph c), however, towards the high-end of the frequency axis where there seems to be a rise on the curve, which does not exist in the amplitude spectrum.

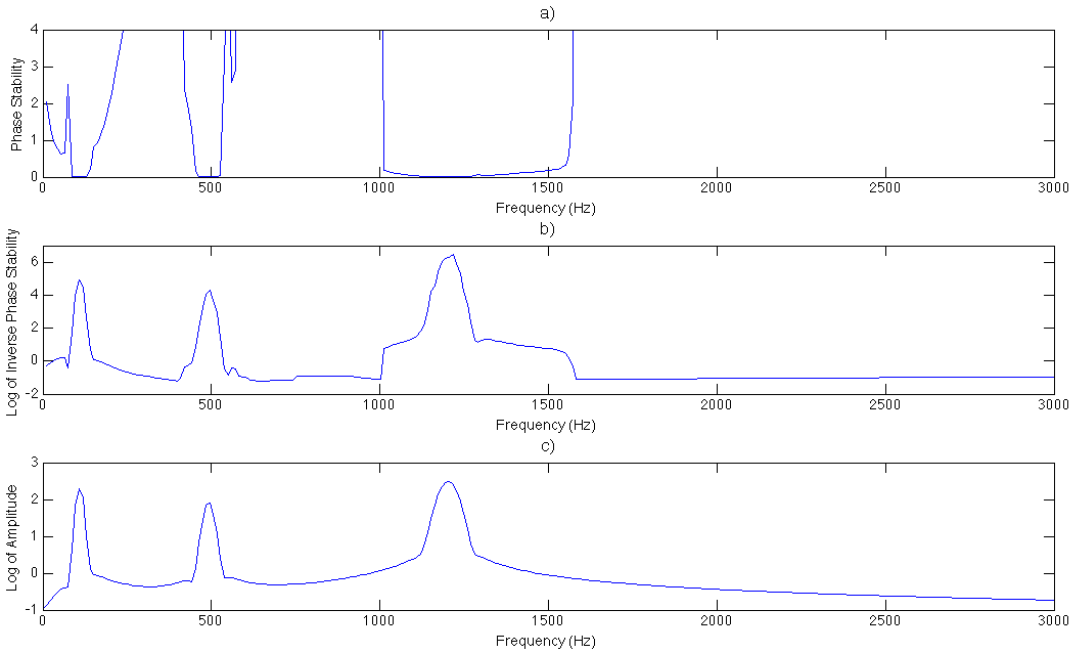

Figure 3.18: Analysed data of the 2^{nd} frame of the synthetic signal with 3 non-stationary components (signal with glissando). (a) Phase stability. (b) Inverse phase stability. (c) Amplitude spectra

More noticable are the differences between the inverse phase stability and the amplitude spectrum for the analysis of the synthetic example with glissando effect. As with the previous examples, the inverse phase stability manifests similar trends to the amplitude spectrum of the signal, and the lobes are approximately of the same width. Also, the dynamic range of the graph that holds the inverse phase stability is greater than the amplitude spectrum. However, the third lobe exhibits interesting trends. The main peak is of the same width with respect to the amplitude spectrum but there is an unexplainable increased activity around it, which appears to be flat, that ends abruptly.

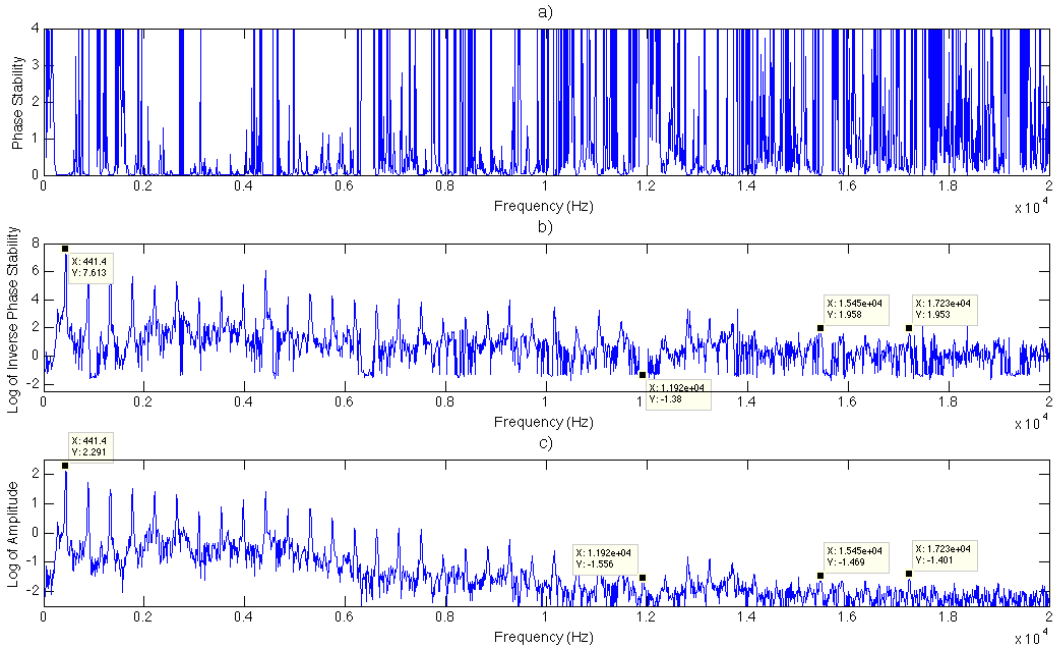

Figure 3.19: Analysed data of the 2^{nd} frame of the signal of an A4 violin note. (a) Phase stability. (b) Inverse phase stability. (c) Amplitude spectra

	Graph B		Graph C	
Point	**Frequency**	**Sample value**	**Frequency**	**Sample Value**
1	441.4	7.613	441.4	2.291
2	11920	-1.38	11920	-1.556
3	15450	1.958	15450	-1.469
4	17230	1.953	17230	-1.401

Table 3.6: Point values marked in graph b) and c) of figure 3.19.

Figure 3.19 is the first illustration of the behaviour of the phase stability (and inverse phase stability) of real signals. The inverse phase stability graph appears to manifest similar trends to the amplitude spectrum of the signal, where almost all peaks can be spotted in both representations with the exception of the peak at 11920 Hz. The dynamic range of the inverse phase stability appears to be three times greater than the dynamic range of the amplitude spectrum. The roll off of the high frequencies of the inverse phase stability graph is considerably smaller than the roll off of the amplitude spectrum. Having located the fundamental, a few points were highlighted in the graphs that are thought to be harmonics, whose values can be found in table 3.6.

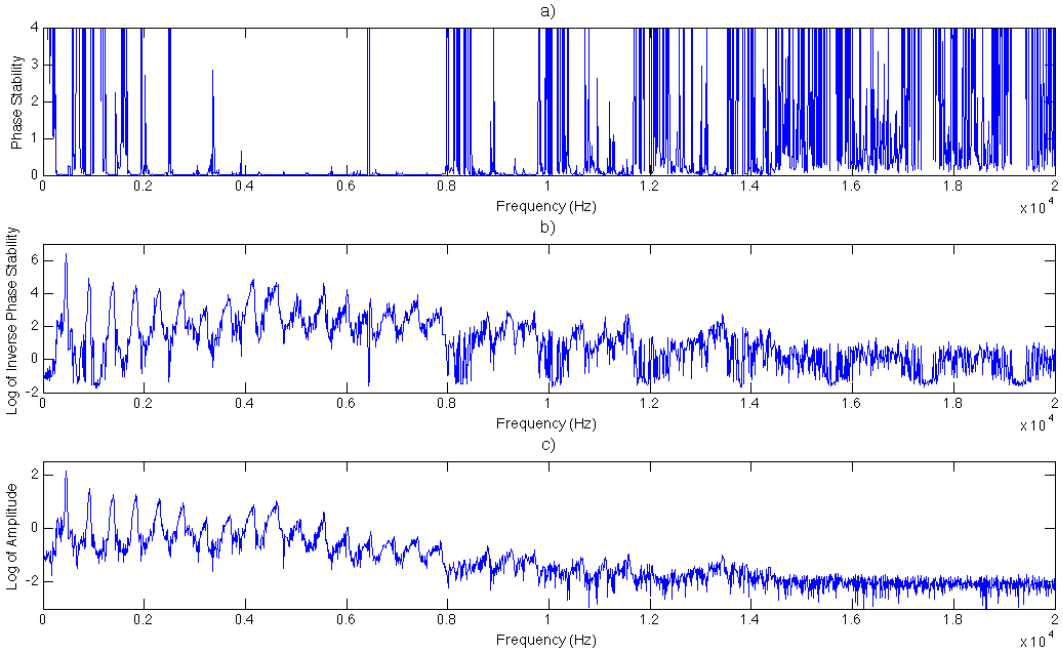

Figure 3.20: Analysed data of the 2^{nd} frame of the signal of an A4 violin note with vibrato. (a) Phase stability. (b) Inverse phase stability. (c) Amplitude spectra

Similar features were observed in the analysis of the violin signal with vibrato in figure 3.20. Many peaks are common in both the inverse phase stability graph and the amplitude spectrum of the signal. The frequency response of the low-end of the inverse phase stability appears to be flatter than the amplitude spectrum, although there is a sudden level decrease of the values at the high-end of the frequency axis (above 8000 Hz) in both representations. The dynamic range of the inverse phase stability graph is three times bigger than the dynamic range of the amplitude spectrum. The fundamental frequency is well represented in both the inverse phase stability graph and the amplitude spectrum, which is located at 453 Hz, although the rest of the peaks are not very well defined, which is the case for both representations.

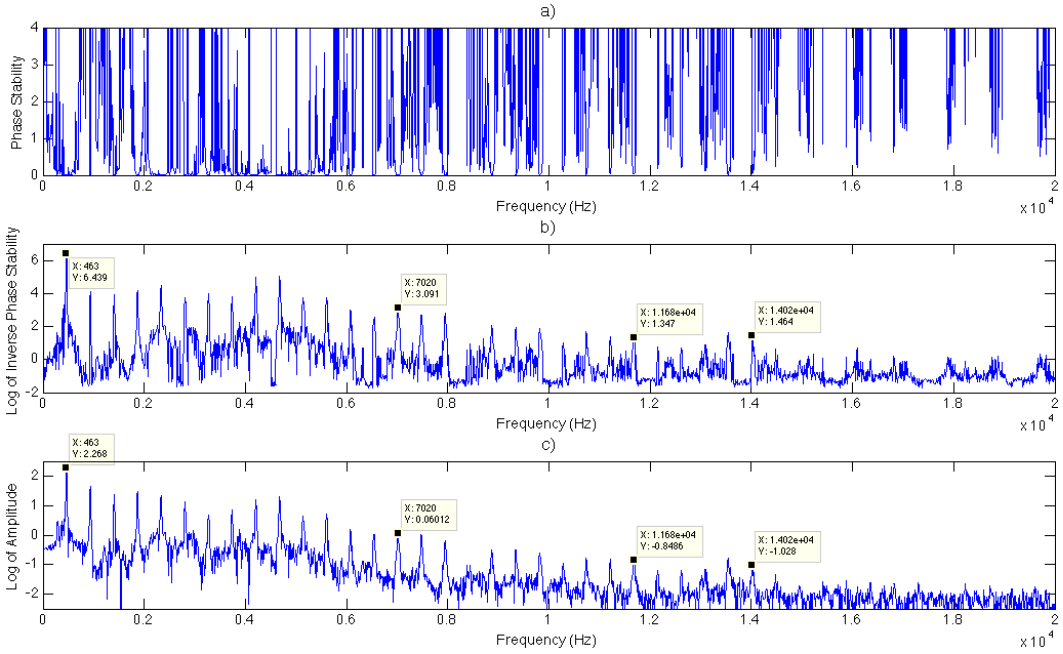

Figure 3.21: Analysed data of the 2^{nd} frame of the signal of an A4 violin note with glissando. (a) Phase stability. (b) Inverse phase stability. (c) Amplitude spectra

	Graph B		Graph C	
Point	**Frequency**	**Sample value**	**Frequency**	**Sample Value**
1	463	6.439	463	2.268
2	7020	-3.091	7020	0.06
3	11680	1.347	11680	-0.8486
4	14020	1.464	14020	-1.028

Table 3.7: Point values marked in graph b) and c) of figure 3.21

Finally, the results of the analysis for the violin signal with glissando are depicted in figure 3.21. The inverse phase stability and amplitude spectrum manifest similar trends, where it appears they have many peaks in common. The frequency response of the inverse phase stability graph is not much flatter in comparison to the frequency response of the amplitude spectrum. However its dynamic range is greater than the dynamic range of the amplitude spectrum. Having located the fundamental, 463 Hz, which is clearly depicted in both the inverse phase stability and the amplitude spectrum, a few other peaks were highlighted that are considered to be harmonics. These peaks manifest a significant degree of prominence in their neighbourhood.

3.5 Summary

The potential of the ensemble of closely-related estimates and the phase stability quality measure have been investigated in this chapter. This approach circumvents a number of deficiencies that plague the conventional STFT approaches, and provides more credible results. Specifically, it provides an additional insight to the data, which also allows the incorporation of non-stationarity. A few analysis examples were provided, both synthetic and real signals, where interesting results were obtained. Specifically, with the aid of the inverse phase stability, it was found that the phase stability generally exhibits smaller roll off of the sample values towards the high end of the frequency axis and has greater dynamic range than the amplitude spectrum.

The two following chapters focus on the development of the function that implements this approach and the application of the phase stability quality measure in the framework of source separation.

Chapter 4

PhiStab Function

The development of the function that calculates the phase stability quality measure was achieved in two steps:

1. Modification of the conventional STFT algorithm in order to enable it to construct the ensemble of estimates.

2. Processing of the data acquired from the modified STFT function to determine the phase stability quality measure for every bin of the spectra.

This chapter provides a thorough description of the steps carried out for the implementation of the two objectives described in the previous bullet points. At first, the development of the STFT modification is documented, followed by the implementation of the method that calculates the phase stability quality measure. Finally, the testing conducted on the newly developed functions is described.

4.1 STFT Modification: Construction of the ensemble of estimates

The implementation of the methodology that produces the ensemble of closely-related estimates in 3.3.1 and 3.3.2 requires the introduction of two additional variables. These variables are (1) the number of estimates calculated for each original frame (including the estimate of the conventional STFT), Q, and (2) the corresponding sample shift of the frame for every estimate, C. These were

then incorporated into the conventional STFT algorithm in order to successfully extend its functionality and enable it to construct the ensemble of estimates.

The first thing that required modification was the formula that determines the number of frames in which the signal is segmented (see eq. 2.23). The discard of the last incomplete frame for the conventional implementation of the STFT was considered. This feature is also embodied in the modified version of the STFT, which requires $(Q-1)\cdot C$ additional samples for the construction of the ensemble of estimates for the last frame. The modified formula that incorporates the two new variables and calculates the number of frames is:

$$M = rounddown(\frac{N-(Q-1)\cdot C-(L-H)}{L-H}), \quad 1 < H \leq L \tag{4.1}$$

The pseudo code of the practical implementation of the conventional STFT algorithm is introduced in order to highlight the turn with which events occur. Then, the additional steps that are required for the implementation of the ensemble of estimates approach are defined and incorporated in the pseudo code of the conventional STFT algorithm, which results in the desired modification of the STFT.

The practical implementation of the STFT algorithm is described by eq. 2.28. This equation is copied here (eq. 4.2) to allow comparisons to be made with the modified version.

$$X_m[k] \triangleq \sum_{n=0}^{L-1} x[n+(m-1)H]w[n]e^{-j\varphi_k[n]}, \qquad \begin{matrix} k=0,1,\ldots,L-1 \\ m=1,2,\ldots,M \end{matrix} \tag{4.2}$$

This equation can be translated into the following:

·	Set m equal to 1.
1.	Calculate the starting and ending points of frame m, $(m-1)H+1$ & $(m-1)H+L$.
2.	Segment the portion of the signal, x, in accordance with the starting and ending points.
3.	Apply the normalised window function, w, on the segmented signal.
4.	Project the windowed frame on the basis, $e^{-j\varphi_k[n]}$, to obtain the spectral coefficients.
5.	As long as $m \leq M$, increment m by 1 and go to step 1, else finish.

Table 4.1: Pseudo code of the conventional STFT algorithm

The window function is determined by the user, who can choose between three functions; rectangular, Hamming and Hann. The rectangular window function is generated manually by generating a string of '1' of length equal to the frame length, L, whereas the Hamming and the Hann are obtained with the aid of the *hamming* and *hann* functions that come with the Signal Processing toolbox, in MATLAB. The analysis of the windowed framed signal is then achieved with the use of the *fft* function, which is also available in MATLAB's Signal Processing toolbox.

The modification requires the STFT to obtain additional estimates of spectra with a time increment applied to each frame. Therefore, an additional loop is required in order to sequentially increase the sample offset from the initial starting point of the frame determined by the conventional STFT algorithm and obtain the additional estimates (see table 4.2).

Again, the same window functions are available for the user to choose, and the analysis of the framed signal is achieved with the use of the *fft* function. The mathematical equation that describes the modified algorithm is:

$$X_m[k] \triangleq \sum_{n=0}^{L-1} \sum_{Q=0}^{Q-1} x[n + (Q \cdot C) + (m-1) \cdot H] w[n] e^{-j\varphi_k[n]} \qquad (4.3)$$

$$k = 0, 1, \ldots, L-1 \quad m = 1, 2, \ldots, M$$

·	Set m equal to 1 and Q equal to 0.
1.	Calculate the starting and ending points of the frame $m.(Q+1)$, $(m-1)H+(Q\cdot C)+1$ & $(m-1)H+(Q\cdot C)+L$
2.	Segment the portion of the signal, x, in accordance with the starting and ending points.
3.	Apply the normalised window function, w, on the segmented signal.
4.	Project the windowed frame on the basis $e^{-j\varphi_k[n]}$ to obtain the spectral coefficients.
5.	As long as $Q \leq Q-1$, increment Q by 1 and go to step 1, else break out of loop.
6.	As long as $m \leq M$, increment m by 1, set Q equal to 0, and go to step 1, else finish.

Table 4.2: Pseudo code of the modified STFT algorithm that implements the ensemble of estimates approach

A new function was created in MATLAB that implements both the conventional and the modified STFT algorithm, despite the fact that the Signal Processing Toolbox contains a function that implements the conventional STFT algorithm (*spectrogram*). Although it could be called repeatedly for the construction of the ensemble of estimates, the generation of a new function was necessary for the following two reasons:

1. To provide additional options in terms of window functions, since *spectrogram* is restricted to use Hamming.

2. To have a standalone STFT function that implements both the conventional and the modified algorithm.

The function was named *stft*, and the documented source code can be found in Appendix F, on page 98.

4.2 PhiStab Function

The function that calculates the phase stability depends on the *stft* function. It calls *stft* internally to obtain the analysed data, and applies further processing

in order to determine the quality measure. A pseudo code of the methodology described in 3.3 is included in the following table.

1.	Acquisition of the analysed data from the *stft* function.
2.	Discard of the mirrored coefficients to optimise the processing speed.
3.	Calculation of the unwrapped initial phase angle values for all bins.
4.	Calculation of the coefficients of the best fitting quadratic curve for the ensemble of phase angle values for each bin.
5.	Calculation of the modelled phase angle values.
6.	Determination of the phase variance, which is the residual between the subtraction of the modelled phase angles and the actual initial phase angle values obtained from *stft*.
7.	Calculation of the sum of the least squares of the phase variance for every bin.

Table 4.3: Pseudo code of the function that calculates the phase stability quality measure

The unwrapped angle values of the spectral coefficients are calculated with the aid of the *angle* and *unwrap* functions that are available in MATLAB. The fitting of the quadratic curve is achieved with the use of the *polyfit* and *polyval* functions, which are also available in MATLAB. These two functions work in combination in order to calculate the modelled initial phase angle values. The *polyfit* receives the ensemble of unwrapped angle values of each bin and the order of the curve as arguments, and calculates the coefficients of the curve that fits the data best. Then, the modelled coefficients are fed in the *polyval* function, along with a set of indices (depending on the number of the data required), in order to generate the values of the modelled phase angles. The aforementioned algorithm was programmed as a function and named *phistab*. The source code of *phistab* can be found in Appendix G, on page 102.

4.3 Testing

Thorough testing was conducted on both *stft* and *phistab* functions in order to ensure their proper functionality. The numerical performance of both functions was examined in order to eliminate potential errors due to incorrect indexing. The following sub-sections describe the routines carried out, and includes their conclusions.

4.3.1 STFT Testing

A number of elements required attention to ensure the proper functionality of the *stft* function. These are listed in the following bullet points, and further elaboration is included in the following paragraphs:

- Argument check.
- Correct calculation of the number of frames.
- Correct calculation of the starting and ending points of each frame.
- Appropriate windowing.

Argument check is the test routine carried out every time the function is called. It is the first procedure that takes place prior to the conduction of any processing, and prevents the user from feeding arguments of the wrong type to the function. The following table (4.4) lists the arguments of the *stft* function, their type and a brief description.

In the event where the user provides only the first five arguments, the function automatically sets nEnsemble to '1′ and sampleshift to '0′. This allows the *stft* function to be used in the conventional way without having to provide values for the last two arguments.

The expression that calculates the number of frames (eq. 4.1) was tested for numerous scenarios in debugging mode. Similar routines were applied for the testing of the expressions that calculate the starting and ending points of each frame (both for the conventional and the ensemble mode).

Argument name	Type	Description
x	vector or 2D matrix	The subject data. The function accepts both monophonic and stereophonic signals. If a stereophonic signal is fed as an argument, the function converts it to monophonic.
frame	scalar	Frame length.
overlap	scalar	Overlap.
zpf	scalar	Zero padding factor.
window	string	Window function. Options: rectwin, hamming and hann.
nEnsemble	scalar	Number of estimates including the original STFT estimate.
sampleshift	scalar	Number of samples offset for every additional estimate from the original starting point.

Table 4.4: List of arguments, along with their type and description, for the *stft* function

In terms of windowing, two factors required attention; the behaviour of the window and its energy. It is important to normalise the window in order to preserve the energy of the signal. This was achieved by introducing a section in the *stft* function that calculates the energy of the windowing function as generated by the *hamming* and *hann* functions, and normalises it by dividing each sample value with it. Moreover, the *hamming* and *hann* functions were set to produce periodic window functions to conserve the continuity of the signal. The two aforementioned points were tested by analysing a simple synthetic signal with the *stft* function and resynthesising it with the *istft* function (introduced in 2.3.3.5 and used in chapter 5).

4.3.2 PhiStab Testing

The only testing procedure that the *phistab* function required was the argument check. The rest of the processing utilises built-in MATLAB functions. The *phistab* function has many arguments in common with the *stft* because it calls the function internally. Nevertheless, there are two additional arguments that

are solely used in the *phistab* function. The following table illustrates the list of arguments of *phistab*, their type and description:

Argument name	**Type**	**Description**
x	vector or 2D matrix	The subject data. The function accepts both monophonic and stereophonic signals. If a stereophonic signal is fed as an argument, the function converts it to monophonic.
frame	scalar	Frame length.
overlap	scalar	Overlap.
zpf	scalar	Zero padding factor.
window	string	Window function. Options: rectwin, hamming and hann.
nEnsemble	scalar	Number of estimations including the original STFT estimate.
sampleshift	scalar	Number of sample offset from the original frame points for every additional estimate.
det	scalar	First order curve fitting. Enable (set to 1) or disable (set to 0) detrend functionality. This functionality was included for research purposes but it is not part of the *phistab* algorithm.
order	scalar	Order of the curve calculated by polyfit/polyval. It can either be '1' - for 1^{st} order - or '2' - for 2^{nd} order.

Table 4.5: List of arguments, along with their type and description, for the *phistab* function

4.4 Summary

This chapter documented the development of the *stft* and *phistab* functions, which implement the concept of phase stability. It described the modification of the conventional STFT algorithm in order to be able to obtain the additional estimates required, and its incorporation in *phistab* for the calculation of the phase stability quality measure for every bin of the spectra. These tools were then applied in

the framework of source separation (chapter 5) in order to test the potential of the phase stability quality measure on a more complex and realistic scenario.

Chapter 5

Phase Stability with Source Separation

The phase stability quality measure is incorporated within a source separation algorithm in order to investigate whether it can improve the algorithm's performance. Its ability to distinguish between "structure" and "noise" or "artefacts" qualifies it as a measure that can potentially aid in distinguishing of the "important" frequency components lying in the spectra and result in separated sources of better quality.

This chapter details the work carried out on the development of the algorithm and the manner in which phase stability is utilised. Specifically, it provides a brief historical background and definition of the problem of source separation, followed by the motivational reasons that prompted this experiment, the documentation of the algorithm, and the assessment of the results.

5.1 Source Separation: Definition and history of the problem

Source separation is the field of Digital Signal Processing (DSP) that focuses on the retrieval of the original component signals that are mixed in a combined signal(s). The algorithms that tackle this problem usually receive the mixed signal(s) as their input and they exploit different levels and types of information, depending on the application, for the achievement of the separation. Some examples of the type of information exploited are (1) the statistical independence of the

sources from Blind Source Separation (BSS) approaches [35, 36, 37, 38], (2) the utilisation of multiple related signals of foreign language mixes in addition to an English copy for film soundtrack separation [39], and (3) the harmonic structure of the sources to overcome the spectral overlap problem [40, 41, 42, 43, 44]. The following figure portrays an idealised structure of the source separation procedure, as considered in this project.

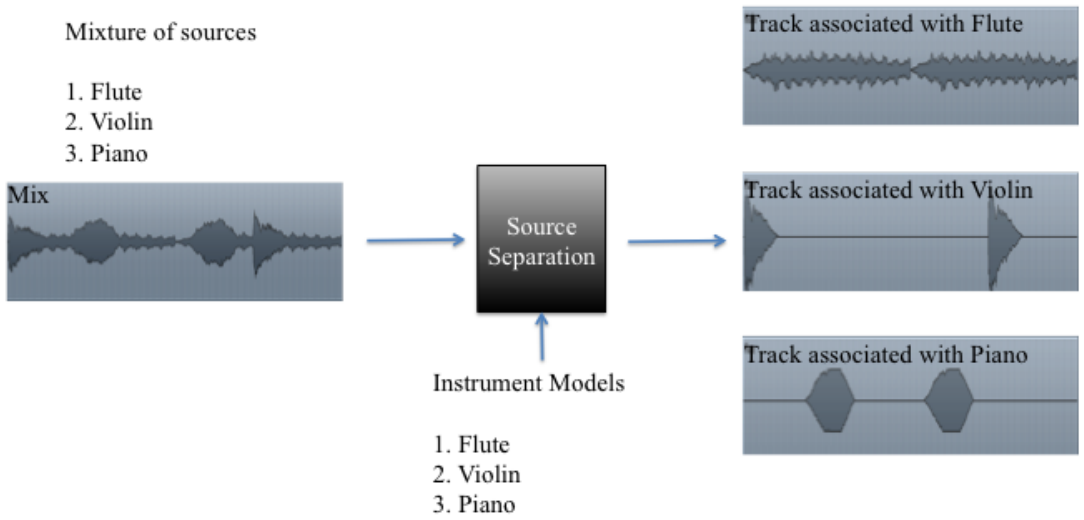

Figure 5.1: Generic structure of an idealised model-based source separation algorithm applied to a single-track audio signal

The concept of source separation was first noted by Cherry in 1956 and recorded in his book 'On Human Communications' [45], although it was not explicitly formulated. Cherry examined the ability of our hearing system to focus and comprehend the talk of a particular speaker in a noisy environment. He named it 'the cocktail party problem' and used it as an example to illustrate the powers of our perception and recognition. He investigated this problem mainly from a structural point of view, as he focused only on the syntax of speech and completely neglected binaural cues in his experiments. His observation was very accurate and there are certainly a lot we could learn from our hearing system's operation that could lead towards the improvement of the efficiency of the current source separation algorithms.

Source separation, as it is known nowadays, was introduced in the 1980s

with the introduction of the first adaptive equalisers that were used in digital communications [46, 47, 48, 49]. According to Comon et al. [50], the term 'source separation' was established only after 1987. A few other names were used prior to it, such as source discrimination and source segmentation. The first separation systems were dealing with instantaneous signals, which means that the algorithms were memoryless. The objective was to cancel the effects of a single-input, single-output (SISO) transmitting system to retrieve the original signal at the terminal [50].

The technological advancement of the processing capabilities in combination with the increase of the temporary and permanent storage space of today's electronic equipment has enabled the processing of multiple-input, multiple-output (MIMO) type of signals. Furthermore, it allows the development of sophisticated source separation systems that can computationally afford the consideration of several factors in order to achieve the separation of more complicated signals. Today's state of the art source separation algorithms manage the separation of signals that contain more sources than the available mixtures that undergo processing. Some examples are (1) Fitzgerald's system that upmixes monophonic recordings to stereophonic [51], (2) Audionamix's algorithm that attempts to separate the music and effects channels found in a soundtrack with the utilisation of additional copies of the soundtrack in different languages [39], and (3) a commercial product that reduces/eliminates the spill of the adjacent drums in the recording of the percussion of interest of a drum-kit [52].

5.2 Motivation, Aims and Objectives

Source separation algorithms are multi-dimensional systems that vary greatly with respect to the methodology they follow and the nature of the data they tackle. However, a generic model that can describe the vast majority is the following:

- Transformation of the data to a representation where the structures of the signal's contents are well defined.
- Processing of the transformed data in order to distinguish and separate the

underlying sources.

- Transformation of the separated sources to the time domain to complete the separation.

This project considers algorithms that apply processing in the frequency domain, and, more specifically, utilise the STFT for the transformation of the data. Such algorithms attempt to distinguish and isolate the mixed sources by applying processing to the spectral content of the signal. It is often, however, required to further decrease the degree of complexity of the spectra of the signal prior to the main processing in order to aid the algorithm distinguish between the "important" and the "unimportant" frequency components. This processing routine is called spectral peak picking (see figure 5.2). The differentiation of the "important" from the "unimportant" frequency components is achieved with the definition of a threshold. This technique is found in most of the projects that focus on source separation in the University of York [53, 54, 55, 56, 57, 58, 59, 60]. It is, therefore, essential to investigate its performance and seek for optimisations, where applicable.

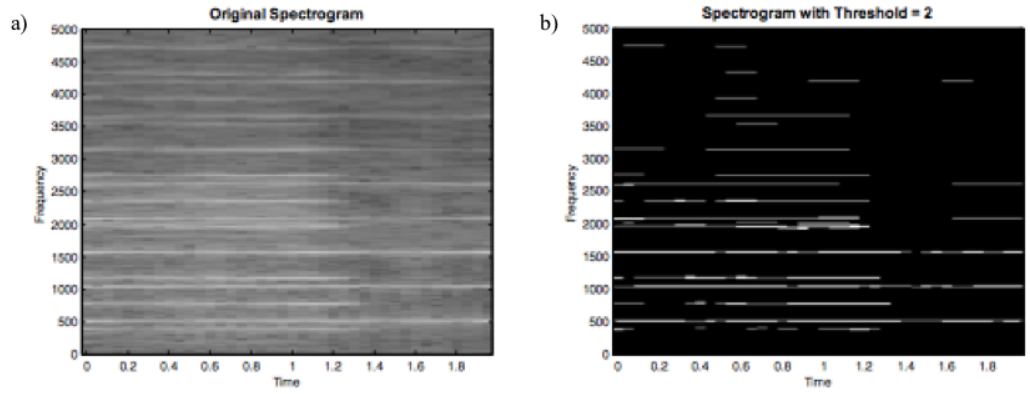

Figure 5.2: An example of a thresholded spectrum from Benson's work [53] (a) Original spectrum of mixture of cello and flute notes of different pitches. (b) Processed (data-reduced) spectrum of a) with the aid of a threshold. The units of the x and y axis are seconds and hertz, respectively

The estimation of this threshold may be achieved in numerous ways, some of them being unintelligent and computationally inexpensive (static), and others being sophisticated and computationally expensive (adaptive). The definition of a static threshold is usually achieved through empirical observation of the data by the developer and the utilisation of a simple model, such as linear or exponential. This threshold is then assumed to be valid for every frame. Adaptive thresholds are defined with regards to the contents of the subject frame, which is achieved with the calculation of the spectral envelope and adjustment of its parameters. An example of the function that achieves this is the moving average filtering technique. Figure 5.3 portrays a set of static and adaptive examples of thresholding.

The spectral peak picking technique has a number of weaknesses. Firstly, setting a static threshold (1) results in the discard of the biggest part of the amplitude spectrum, and hence the spectral coefficients, which can reduce the credibility of processing techniques such as fundamental estimation (described in 5.3.2.4), and (2) may be particularly inefficient if the energy of the signal vary with respect to time. Adaptive thresholding is not ideal either. The estimation of the thresholding curve merely depends on the amplitude information of the spectra, whose credibility and consistency varies greatly, as has been thoroughly discussed in sub-section 2.3.1 on DFT and summarised in the introductory paragraph of chapter 3. Moreover, there are many parameters that are user-specific (window size, scaling etc.), which lead to yet another layer of complexity, whose determination is made empirically.

These thresholding techniques are generic statistical tools that can be applied to any data. On the other hand, phase stability, by definition, attempts to differentiate the "structured" data from "noise" or edge effect/"artefacts". Hence, it is anticipated that the phase stability quality measure is more appropriate for the reduction of the degree of complexity of the data, and thus can lead to improved separation results.

The investigation of this hypothesis involves the development of a source separation algorithm that utilises the phase stability quality measure in the spectral peak picking processing step. The aim here is to examine whether the phase stability quality measure is effective. The idea is, instead of using any preset,

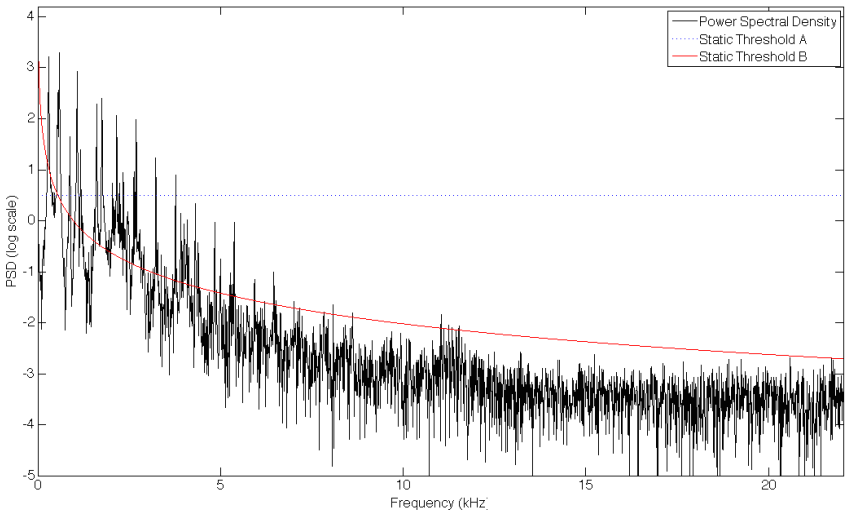

(a) Static Thresholding

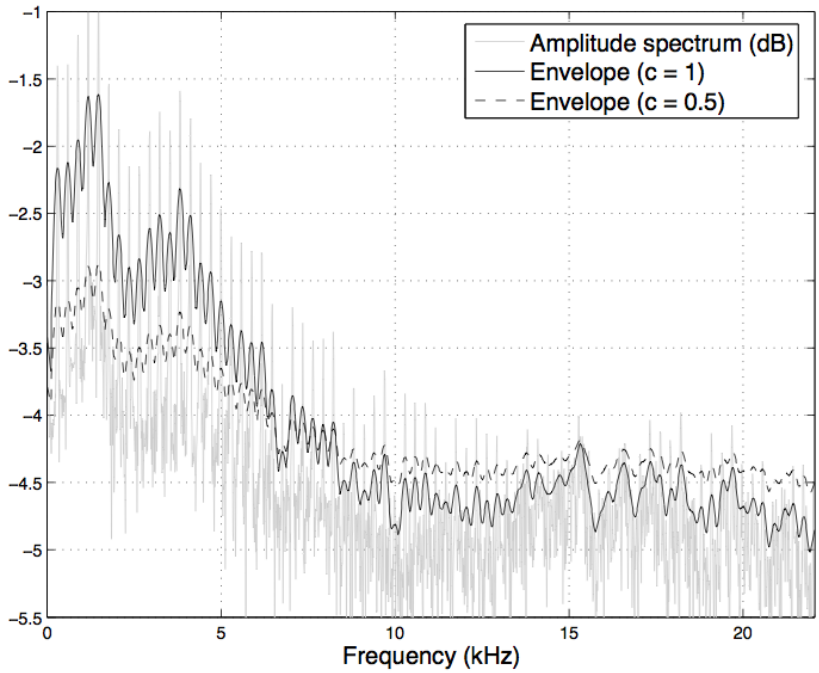

(b) Adaptive Thresholding

Figure 5.3: Example of various thresholding functions. Spectrum of mixture of violin and flute notes with a static threshold (Flute $f_0 = 293$ Hz, Violin $f_0 = 510$ Hz) (b) Every's adaptive thresholding technique on the spectrum of an oboe note ($f_0 = 293$ Hz) [54]

averaged or model threshold curve, to use a content-adaptive measure, which is based entirely on phase information and consequently not dependent on the amplitude spectra and frame to frame variations in the amplitudes. The assessment of the performance of the algorithm that incorporates the phase stability quality measure will be achieved with its comparison to the performance of the same algorithm that considers the unprocessed, conventional spectra.

5.3 The Algorithm

A numerical model-based source separation algorithm was programmed to test the performance of the phase stability quality measure used as a threshold for the reduction of the data of the conventional spectra. The algorithm, which is instantiated twice, distinguishes the individual sources with the application of a series of harmonic models on the (1) conventional amplitude spectra, and (2) the data-reduced (with regards to phase stability) amplitude spectra. Then, the fundamentals of the sources are estimated by processing the harmonic partials of the selected models. Finally, the separation of the sources is achieved with the application of spectral filters (binary masking), which are defined by the selected harmonic models, on the original spectra obtained by the STFT algorithm and transformation of the separated spectra in time domain.

The following sections describe the specification of the algorithm, document its design, and examine the results for the assessment of the suitability of the phase stability as a threshold measure in the data reduction step.

5.3.1 Specification

The specification of the source separation algorithm is directly related to the nature of the signals that it attempts to separate. A set of restrictions were imposed on the subject signals in order to make the goal attainable within the time allocated for a masters programme.

Musical signals were considered with the following restrictions applied:

- Real instrument signals, excluding percussions and voice.
- Monophonic signals.

- A high Signal-to-Noise (SNR) ratio.

  This is an important prerequisite due to the discrimination of the sources with the aid of spectral models. It is therefore necessary for the partials that exist due to the sources to be relatively greater in amplitude.

- Absence of artistic effects, such as reverb, distortion, delay etc.

  Similarly, artistic effects are undesired because they introduce additional partials that are not part of the instrument models or increase the noise floor.

- Two instruments, approximately of the same amplitude with different fundamentals and not related in octave intervals, playing simultaneously.

- Consideration of the sustain part of the note.

- Stationarity.

- Harmonicity.

- A constrained range of possible note frequencies.

Further elaboration on the points with no comments of the previous bullet list is included in the chapter regarding to further work 7.

5.3.2 Design

The algorithm is comprised of five main steps, which are included in the following list. The description of each step is included in the following sub-sub sections.

1. Declaration of the parameters.

2. Import of the subject signals.

3. Analysis.

4. Voting system (fundamental estimation and generation of the spectral filters).

5. Separation and resynthesis.

Each of the above steps is a section of the main script, which serves as the test-bench for the algorithm.

5.3.2.1 Declaration of the parameters

The declaration of the global settings of the entire algorithm is the first step carried. The algorithm is completely parameterised, and every user-specific parameter is included in this section in order to make the testing of numerous cases easier.

The parameters can be categorised in three main groups:

1. The STFT analysis parameters (frame size, overlap, zero padding factor, windowing function, number of estimates for the ensemble approach (phase stability mode), sample shift (phase stability mode)).

2. The mode of the algorithm (conventional or phase stability enhanced).

3. The parameters for the calculation of the harmonic models that are used for the fundamental estimation and spectral filter generation in the voting stage (the interval of frequencies where the fundamentals may lie, the number of partials for each harmonic model, and the width of every partial).

5.3.2.2 Import of the subject signals

The sustain part of a violin and a flute note were selected in Cubase 7.5 from the available recordings and mixed in a monophonic file, which is then imported in the workspace of the algorithm. The subject signals used in this project are courtesy of the Music Instrument Samples library produced by the University of Iowa [34].

5.3.2.3 Analysis

Two analysis routines were programmed in order to obtain the necessary material to assess the performance of the phase stability quality measure. Both routines

output two sets of data; (1) the complete set of spectra obtained from the conventional STFT algorithm that is used in the separation and resynthesis stage, and (2) an additional set of spectra, which differs for each routine, that is used for the estimation of the fundamentals in the voting system.

The second set of data outputted from the first routine is the spectra obtained from the conventional STFT algorithm with discarded mirrored coefficients. This was necessary in order to reduce the computational expense of the algorithm. The second set of data outputted from the second routine, which is also mirrored coefficients-free, is the data-reduced (binary masked) spectra with regards to the phase stability quality measure. The data reduction is a processing step prior to the source separation that eliminates spectral components that are not "structured", according to the phase stability measure. Hence, they are assumed to not be part of the sources. A threshold value was determined empirically and kept the same for all frames. The flowcharts of the analysis routines are depicted in figures 5.4 and 5.5. An example that illustrates the difference between the unprocessed and processed amplitude spectra used in the voting system is portrayed in figure 5.7, section 5.4. Additional comments on the differences are provided.

5.3.2.4 Voting system

This step involves the generation of a set of harmonic models and their application to the second set of data outputted by the analysis step in order to estimate the fundamentals of the instruments and produce the appropriate spectral filters for each source. This is achieved by correlating every individual model with the data and, with some additional processing applied on the results, picking the two models with the highest correlation degree for every frame. The partials of the selected harmonic models are then processed for the determination of the fundamentals for each frame, and the spectral filters are defined by allocating the selected harmonic models in the corresponding variable.

The voting system section in the main script is comprised of three functions that implement the aforementioned method; *modelgen*, *modelpicker* and *specfilt*. Each function receives a combination of user-specific parameters and algorithm-processed data. Their functionality is described in the following paragraphs.

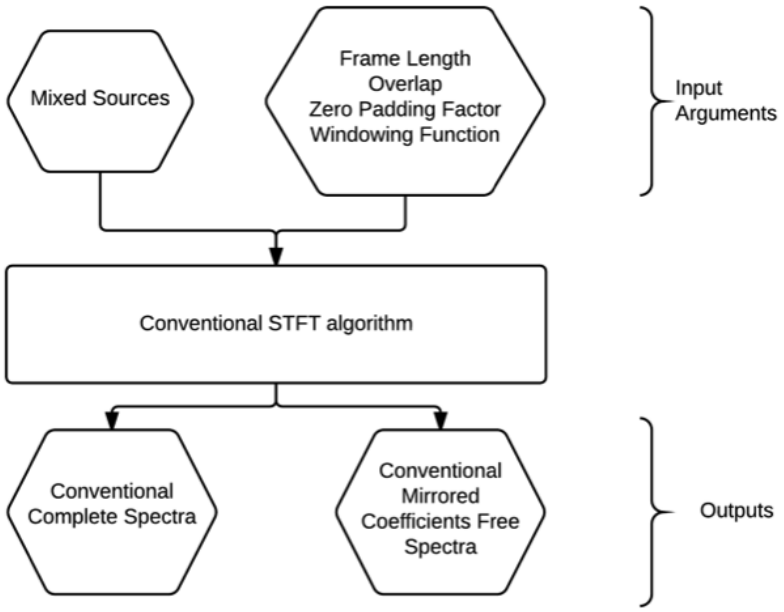

Figure 5.4: Analysis routine 1 of the source separation algorithm: Conventional STFT Mode

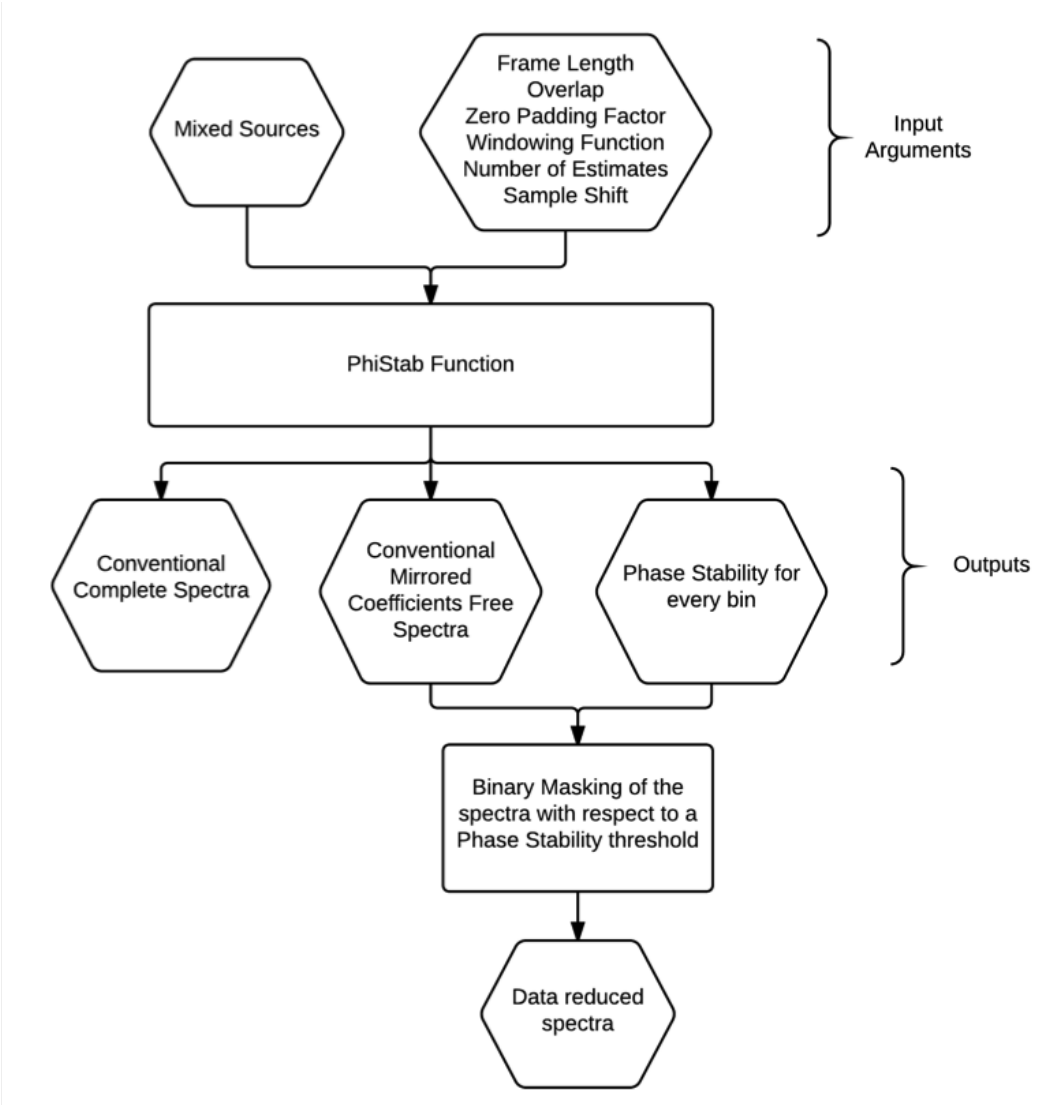

Figure 5.5: Analysis routine 2 of the source separation algorithm: Phase Stability Enhanced Spectrum Mode

The *modelgen* function generates all possible harmonic models according to the specification set by the user. The main arguments that determine the models are the lowest possible fundamental (in Hz), the highest possible fundamental (in Hz), the number of harmonics, and the width of every partial (in bins). Firstly, the input arguments that describe the lowest and highest possible fundamental frequencies in hertz are converted to the corresponding bins. Once this step has been calculated, testing is applied in order to ensure that the highest partial, which is comprised of the highest centre bin plus the additional bins specified by the peakwidth argument, is within the limits of the analysed data (calculated by the analysis step). The number of harmonic partials is adjusted accordingly, if the highest harmonic partial exceeds the number of available bins. Then, the harmonic partials of each model are calculated by dividing the highest possible partial with the factor that describes the number of every lower partial. This way the models describe all possible fundamental frequencies, even if it is undistinguishable due to the fixed grid. The rest of the models are generated by sequentially decreasing the centre bin of the highest harmonic partial by 1 bin, until the centre bin of the lowest partial of the models reaches the limit set by the user. Different weighting was applied for the first two harmonics, because of their greater importance in the discrimination of the underlying sources. The first harmonic peak contributes 3 times more and the second harmonic peak contributes 2 times more than the rest of the harmonic partials (see figure 5.6).

The *modelpick* function receives either the mirrored coefficient-free spectra or the data reduced spectra and the generated models in order to determine the two best fitting models for each frame, and calculate the fundamentals of the sources. It calculates the correlation coefficient of each model with the subject frame by multiplying the models with the amplitude spectrum element-wise and storing the sum of the values of each product in a variable. Then, it selects the two models with the highest correlation coefficient that meet the following criteria:

1. The model picked for the first instrument must not have a zero valued first peak or great amplitude difference[1] between the first and second peak.

2. The model picked for the second instrument must not (1) be an octave

[1]Empirically determined and set equal to 10.

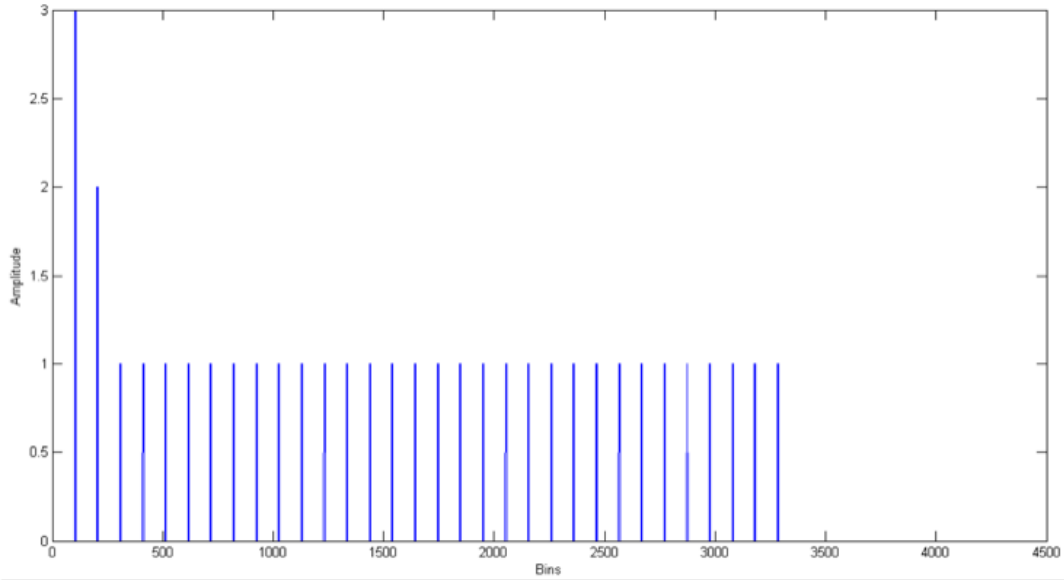

Figure 5.6: Example of a harmonic model with 32 partials

above or below the model selected for instrument 1, and (2) have a zero valued first peak or great amplitude difference[1] between the first and second peak.

Once these criteria are met, the index of the selected models for every frame is stored in a variable and the fundamentals are calculated. This is achieved by dividing every centre bin of each harmonic partial with the corresponding partial number, and averaging the values. For instance, if bin 248 is the centre bin of the 17^{th} partial, the fundamental in hertz according to this estimate is $\frac{248}{17} \times binresolution$. The general expression for the estimation of the fundamental is:

$$f_{0,v}(m) = \frac{\frac{\sum_{p=1}^{P} centrebin(p)}{p}}{P} \times binresolution \tag{5.1}$$

Finally, the spectral filters for the separation of the sources for each frame are compiled in *specfilt*. This function receives the indices of the selected models for

each instrument and frame, and the variable that holds the entire set of models. It then creates two spectral filters, assigns the corresponding models, and calculates the mirrored coefficients because they are applied to the original spectra obtained by STFT. An additional spectral filter is generated for the residual components that contains the bins that are not included either in the spectral filter of source 1 or 2. In the event of overlapping partials, the amplitude and the phase of the frequency component are left intact. This may result in some augmented frequency components in the instrument spectra, but it can be easily fixed with simple filtering.

5.3.2.5 Separation and resynthesis

This step merely applies binary masking on the original spectra of the signal with regards to the spectral filters obtained from the voting system. Finally, the processed spectra (source 1, source 2 and residual) are transferred in time domain with the utilisation of the *istft* function.

5.4 Result Review

The performance of the algorithm was judged successful by listening to the separated sources (available on the CD). The criteria for success was the lack of sudden changes in pitch during the span of the note of the separated sources, which could result from the incorrect selection of harmonic model for a particular frame. Therefore, the separated sources had to resemble the pitch behaviour of the original signals.

As was discussed in 5.3, the algorithm was instantiated twice, the only difference being the mode in which it ran and the number of partials comprising the harmonic models. The number of the partials is of interest here because each partial contributes an estimation of the fundamental for each source, in each frame (see equation 5.1). Therefore, for a credible estimate of low variance, many fundamental estimates are desired, and thus many partials. The rest of the parameters, which are included in table 5.1, remained the same for both instances of the algorithm. Reasoning for the particular settings used is provided in the following paragraphs.

The parameter of the analysis stage that required the most careful consideration was the frame length. A window of 8192 samples long was found to be appropriate, given the relative stationarity of the sources comprising the subject signals used in this work. The application of a Hamming windowing function was judged suitable for its accuracy in peak estimation (see table 2.1), which also required the use of 50% overlap in order to achieve the resynthesis of the separated sources without loss of energy. There was no need for frequency interpolation, since the length of the frame provided adequate frequency resolution. The number of total estimates was set to 10, with a sample shift of 24, in the case of phase stability mode.

Parameter Name	**Value**
Frame length	8192
Overlap	4096
Zero padding factor	0
Windowing function	Hamming
Number of estimates	10
Sample shift	24

Table 5.1: Analysis parameters for both conventional and phase stability enhanced modes

As was discussed in 5.3.2.3, the empirical definition of a threshold value with regards to phase stability was required for the generation of the phase stability enhanced spectra. The value of 0.009 was found appropriate, and kept constant for all frames. Figure 5.7 illustrates the difference between the (1) conventional amplitude spectrum and (2) the phase stability enhanced spectrum of the first frame of the analysis for the aforementioned analysis parameters of the mixture of signals as specified in 5.3.1. Moreover, an additional phase stability enhanced spectrum is provided, which is produced with a different threshold value. This graph is generated with a phase stability threshold value of 0.09 and is included to showcase the difference in which it results.

Regarding to the voting system parameters, the interval of potential fundamental frequencies specified by the user was 130 - 670 Hz, which covers two western musical octaves. This was found to be a satisfactory starting point, since big part of the mainstream lead melodies lie within the aforementioned limits.

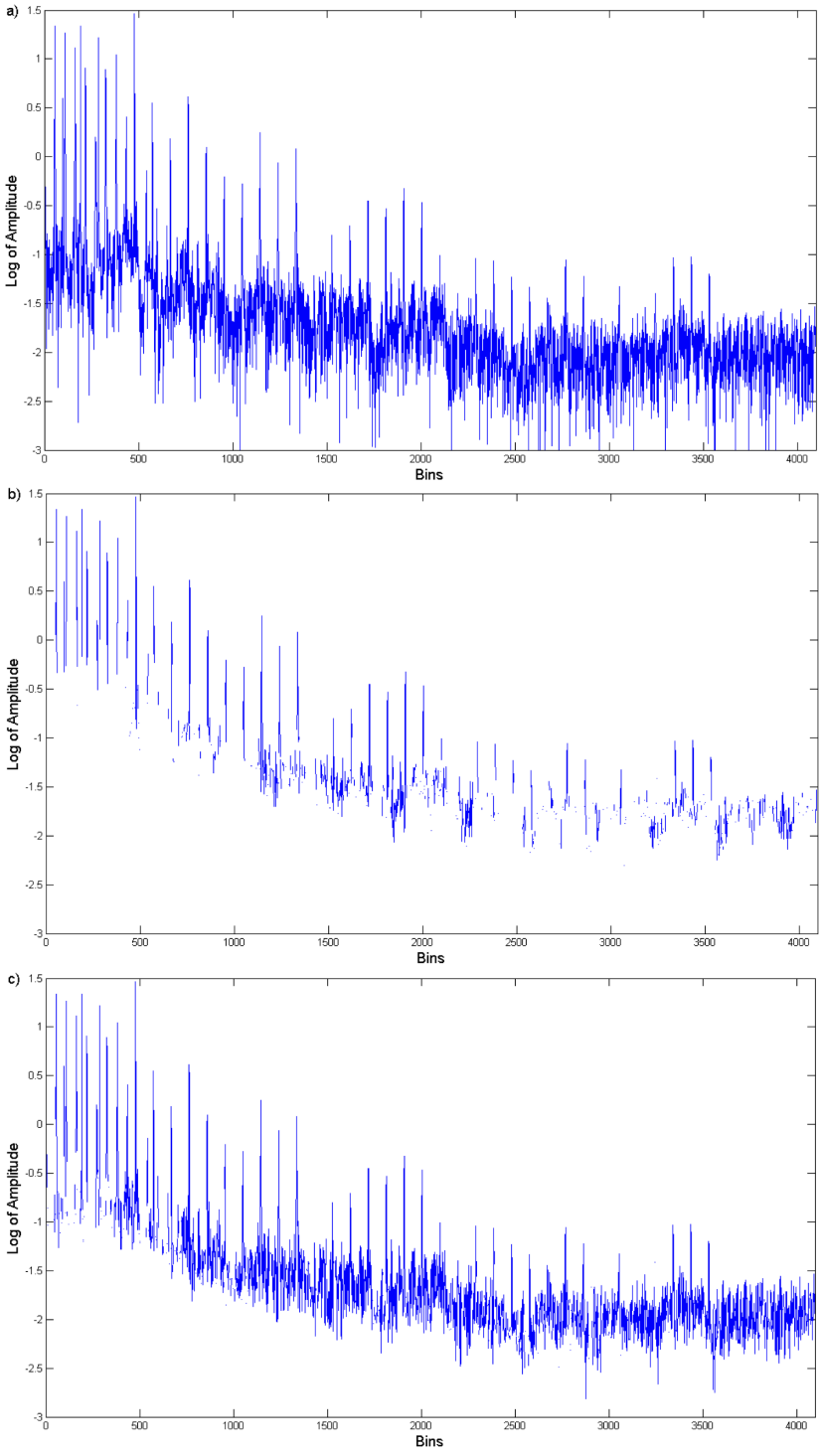

Figure 5.7: Analysis of a mixture of violin and flute notes. (a) Conventional amplitude spectrum (b) Phase Stability Enhanced Spectrum (PSES) with threshold value 0.009 (c) Phase Stability Enhanced Spectrum (PSES) with threshold value 0.09

The width of every partial peak was set to 5 bins in order to abide by the properties of the main lobe of the Hamming window function (see table 2.1). Finally, the number of harmonic partials varied for each mode. It was found that the algorithm in conventional mode meets the performance criteria only with models that contain up to 23 harmonic partials, whereas in phase stability enhanced mode can use 32 harmonic partials (maximum number that the models can fit due to the available number of bins and the interval of potential fundamentals).

To conclude, the capability of the phase stability enhanced algorithm to separate sources with the application of harmonic models of a larger number of partials than the conventional instance proves that the phase stability quality measure is appropriate for the efficient reduction of the complexity of the data. Having eliminated the "unstable" frequency components (bins) results into an amplitude spectrum that theoretically contains only the "important" components and no baseline "noise". This improves the performance of the step that correlates the harmonic models with the analysed data, as there are less "unstable" bins to contribute into the calculation of the correlation coefficient. Finally, it also improves the performance of the algorithm in two ways:

1. the estimation of the fundamentals is more accurate, credible and of smaller variations, since more partials contribute in the estimation of the fundamental frequency for every source, in every frame,

2. and the separated sources contain a higher number of harmonics, which results in separated results of higher quality.

Chapter 6

Conclusions

One of the most important, yet least considered, assumptions of the STFT was investigated in this work, stationarity. This principle that forms the foundation of the STFT and also happens to be one of its greatest deficiencies often results in potentially misleading data. A novel method was proposed and examined that attempts to circumvent this limitation of STFT. This method attempts to achieve comprehensible results of greater credibility with the allowance of a certain degree of deviation from stationarity incorporated into the analysis. This was achieved by constructing an ensemble of closely-related spectral estimates instead of a single estimation in order to acquire the short-time phase evolution of each frequency bin. The phase information is then compared to that of a model of an idealised but not necessarily stationary partial of an acoustic source in order to define a quality measure that discriminates the "structured" from the "unstructured" frequency bins. This quality measure, named phase stability, describes the degree of deviation of the phase behaviour of a subject frequency bin from the behaviour of its corresponding idealistic frequency component. The incorporation of a certain degree of deviation from stationarity is achieved with the consideration of non-stationary idealistic frequency components. The results of the phase stability of the sustain portion of real signals exhibited a flatter frequency response in contrary to the common high-frequency roll off that is found in the amplitude spectra and had greater dynamic range than the amplitude spectra.

The potential of this quality measure was then investigated with its incor-

poration in the framework of source separation, as a single application example. Used in the spectral peak picking step of a numerical model-based algorithm, it was found that it effectively reduces the complexity of the spectra of a mixture of signals without the discard of the "important" frequency components. The assessment of the effectiveness of the processed spectra was achieved with their consideration in the separation step, where numerous harmonic models were applied to them in order to distinguish the underlying sources. The algorithm successfully separated the mixture of the sustain parts of the two notes, flute and violin, with the utilisation of harmonic models that contain a larger number of partials than the instance of the algorithm that considered the conventional amplitude spectra (in this simple exemplar case, success was judged entirely by ear as opposed to using quantitative measures). This resulted in better informed estimates of fundamental frequency, since more harmonic peak position estimates are available.

The results obtained from the application of the phase stability in the framework of source separation are promising. It is anticipated that this quality measure has great potential, in particular where there can be assumed relative phase continuity. The aim of this project was to set the fundamental principles and groundwork, which was successfully accomplished. However, there are multiple aspects that were not examined due to the lack of time. A set of aims is defined in the following chapter regarding further work in order to prompt further investigation and development of the proposed method.

Chapter 7

Further Work

The complete and thorough investigation of the subject topics of this project was impossible within the limited amount of time allocated for an one-year research project. Careful consideration was given to select the vital aspects that required investigation in order to obtain an essential insight to the problem, establish the foundation and prompt further work, accordingly.

This chapter consolidates a framework that includes the additional aspects that require investigation and further exploration. The two main topics on which this project elaborates are phase stability and source separation. Hence, the suggested further work is documented as such.

7.1 Phase Stability

The investigation of the behaviour of the phase stability quality measure of additional signals of greater variety is required. This project focused on the analysis of musical signals, initially synthetic and then real, and, in particular, it considered the sustain part of harmonic instrument signals. This type of signals was considered in order to introduce the notion of 'stability' in phase information. However, phase stability is anticipated to yield interesting insights in all types of musical signals (and not only!). Specifically, it is speculated that it can provide interesting results in the analysis of transients (i.e. percussive sounds), where there are "structured" components (i.e. the pitch in which the drum is tuned, which results to a fundamental frequency component), as well as "unstructured" (i.e. the attack phase of the percussive sound). It is likely that this measure can

be used as an indicator for the beginning and ending points of attack and sustain phases. Moreover, this concept is expected to be applicable to any type of signals that exhibit phase continuity.

The implementation of the proposed method that obtains the phase stability quality measure resulted in two additional user-specific parameters; number of additional estimates (Q) and sample shift (C). These variables have an important impact on the analysed results. Large number of estimates, Q, may result into more accurate phase behaviour modelling, but that might not be an option depending on the frame length and hop size set in the STFT. Ideally, the relatively short-term phase behaviour is of interest, and the total amount of sample shift due to the additional estimates is desired to be relatively small with regards to the predifined frame lenght of the analysis, because otherwise the analysis could be associated with an analysis of very high temporal interpolation.

The aforementioned concerns have important impacts in speech and thus formant analysis. Despite the fact that phase stability is expected to be appropriate for the analysis of speech signals due to their structured spectral behaviour, it might not be possible due to the very short frame lengths with which speech is usually analysed (i.e. frames of 256 samples). The construction of an ensemble of 10 estimates with a shift of 4 samples in between, results in a total of 40 samples, which corresponds to 15% of a frame length of 256 samples. Nevertheless, it is definitely worthy of investigation, since even a sample shift of 2 could potentially yield interesting results.

This method may also have uses of a different fashion. The allowance of a certain degree of deviation from stationarity within the analysis, which is achieved with the comparision of the analysed data with the modelled short-time phase behaviour of non-stationary frequency components, is implemented with the fitting of a quadratic curve to the data of the form:

$$at^2 + bt + c \tag{7.1}$$

where a, b, and c are the calculated coefficients.
For stationary signals, a is approximately zero. However, for non-stationary

signals, a corresponds to the degree of linear change in phase, and hence frequency. Therefore, it could be exploited for chirp rate estimation purposes.

Finally, the incorporation of the phase stability in additional areas and applications requires careful consideration. An example is provided in this project with the incorporation of the phase stability in a numerical model-based source separation algorithm, and it is shown that its potential is great.

7.2 Source Separation

The specification of the source separation algorithm have been introduced in 5.3.1 with the definition of the type of signals that it is able to separate. This restricted sub-group of musical signals was selected as a starting point in order to obtain a better insight into the problem of separation and establish the necessary groundwork. The envisioned improved version of the project's algorithm is expected to be more versatile and capable. The aim is to develop it further in order to enable it to process the standard type of musical signals that are common nowadays. The restrictions, as stated by the bullet points, that can be overcome are included in the following paragraphs, along with the proposed work.

- *Real instrument signals, excluding percussions and voice.*

  Expanding the algorithm's capabilities to enable it to consider voice should be relatively simple, since modelling formants in the frequency domain is achievable. However, the consideration of percussions would be more challenging due to the unstructured behaviour of their spectral information. Nevertheless, an interesting approach has been suggested for the separation of percussive sounds from the rest of the mixture of instrumental signals in the frequency domain by Fitzgerald [51], which is anticipated to be appropriate for incorporation in the current algorithm.

- *Monophonic signals.*

  The consideration of stereophonic signals is anticipated not only to be possible but also to provide additional exploitable information (directionality) that will help in the separation of the sources. Moreover, the phase stability

quality measure might be another measure for consideration in addition to amplitude. Similar phase stability values with a certain delay between the two channels is expected to aid in the discrimination of the sources.

- *Two instruments, approximately of the same amplitude with different fundamentals and not related in octave intervals, playing simultaneously.*

  There has been done work on the discrimination of instrument notes that are related in octave intervals in [57], and the incorporation of the proposed method in the current algorithm is expected to be feasible. However, the consideration of instrument notes of the same pitch is expected to be much more challenging, since there is a great amount of overlap in pitch between different instruments in today's western music. Nevertheless, it is definitely an area that requires attention.

- *Consideration of the sustain part of the note.*

  The attack phase of a note is not considered because its modelling in frequency domain is rather complicated. Nonetheless, preliminary work of a different fashion that attempts to identify the non-allocated attack parts found in the residual component source and assign them to the corresponding source has been done in [60]. This is achieved by obtaining the 'fingerprint' of the attack phases identified in the residual source and trying to match it with the separated source to which it belongs. This approach can be further investigated and developed in order to incorporate it in the current algorithm and enable it consider whole notes.

- *Stationarity.*

  The assumption of stationarity is implied in general in the use of Fourier approaches and, of course, is in general not true. Part of the purpose of this work is the development of a method that allows a certain degree of deviation from stationarity to be incorporated into the analysis process, as represented by the curvature of the phase evolution curve.

- *Harmonicity.*

Likewise, harmonicity is a widely used assumption and although exploited here, for simplicity, more realistic spectral models can be used, as implemented in [56].

- *A constrained range of possible note frequencies.*

  This step requires additional investigation, since it has been noticed that for the current settings of this project, the performance of the algorithm varies (in terms of the number of harmonic partials with which successful separation is achieved) with respect to the subject signals.

Finally, the energy allocation of overlapping partials is an issue that requires attention. The current algorithm merely allocates the full amount of energy to both sources. However, this results in the introduction of additional energy. It is therefore required to implement a method that measures the relative energy of each source for every frame in order to allocate the respective amount of energy of the overlapping partial to each source accordingly. This way the preservation of energy can be achieved. Moreover, the coherent reconstruction of the phase of each modified bin is required. The modification of the amplitude information of a bin during the energy allocation of overlapping partials may result in the reconstruction of perceptually bad sounding sources. This issue is discussed in Le Roux's et al. [61] and Fitzgerald's paper on masking filters [62] where methods for tackling it are suggested.

Appendix A: Initial phase angles obtained from the analysis of the cosine in chapter 3

	Frame 1.1 Initial phase (rads)	Frame 1.1 Initial phase (rads)	Frame 1.1 Initial phase (rads)	Frame 1.1 Initial phase (rads)
Bin 1	3.142	3.142	3.142	3.142
Bin 2	1.647	2.85	-3.065	-2.697
Bin 3	1.724	2.635	-2.988	-2.328
Bin 4	-1.341	-0.636	0.23	1.096
Bin 5	-1.264	-0.703	0.306	1.316
Bin 6	-1.188	-0.729	0.383	1.495
Bin 7	-1.111	-0.729	0.46	1.649
Bin 8	-1.034	-0.712	0.536	1.784
Bin 9	-0.958	-0.682	0.613	1.908
Bin 10	-0.881	-0.645	0.69	2.024
Bin 11	-0.805	-0.601	0.766	2.133
Bin 12	-0.728	-0.552	0.843	2.238
Bin 13	-0.651	-0.501	0.919	2.34
Bin 14	-0.575	-0.447	0.996	2.439
Bin 15	-0.498	-0.39	1.073	2.536
Bin 16	-0.421	-0.332	1.149	2.631
Bin 17	-0.345	-0.273	1.226	2.725
Bin 18	-0.268	-0.214	1.303	2.819
Bin 19	-0.192	-0.153	1.379	2.911
Bin 20	-0.115	-0.092	1.456	3.004
Bin 21	-0.038	-0.031	1.532	3.096

Appendix B: Initial phase angles obtained from the analysis of the cosine with vibrato in chapter 3

	Frame 1.1 Initial phase (rads)	Frame 1.2 Initial phase (rads)	Frame 1.3 Initial phase (rads)	Frame 1.4 Initial phase (rads)
Bin 1	3.142	3.142	3.142	0
Bin 2	2.235	3.088	-2.814	0.032
Bin 3	2.62	-3.001	-2.35	-1.488
Bin 4	-0.657	0.195	1.063	1.759
Bin 5	-0.874	0.198	1.321	2.142
Bin 6	-0.864	0.257	1.501	2.115
Bin 7	-0.783	0.337	1.632	2.072
Bin 8	-0.75	0.395	1.765	2.134
Bin 9	-0.717	0.443	1.892	2.208
Bin 10	-0.676	0.49	2.01	2.282
Bin 11	-0.628	0.533	2.122	2.355
Bin 12	-0.576	0.572	2.228	2.429
Bin 13	-0.521	0.605	2.331	2.504
Bin 14	-0.464	0.63	2.431	2.578
Bin 15	-0.405	0.645	2.53	2.653
Bin 16	-0.345	0.643	2.626	2.728
Bin 17	-0.283	0.621	2.721	2.803
Bin 18	-0.221	0.567	2.816	2.878
Bin 19	-0.158	0.471	2.909	2.953
Bin 20	-0.095	0.32	3.002	3.029
Bin 21	-0.032	0.115	3.095	3.104

Appendix C: Initial phase angles obtained from the analysis of the cosine with glissando in chapter 3

	Frame 1.1 Initial phase (rads)	Frame 1.2 Initial phase (rads)	Frame 1.3 Initial phase (rads)	Frame 1.4 Initial phase (rads)
Bin 1	3.142	0	0	0
Bin 2	-2.926	-1.316	-0.07	0.267
Bin 3	-2.763	-1.464	-0.193	0.449
Bin 4	-2.974	-1.895	-0.668	0.232
Bin 5	0.451	1.553	2.643	-2.42
Bin 6	1.147	2.11	-3.041	-1.638
Bin 7	1.355	2.171	-3.047	-1.487
Bin 8	1.517	2.22	-3.077	-1.368
Bin 9	1.666	2.276	-3.098	-1.253
Bin 10	1.806	2.337	-3.114	-1.14
Bin 11	1.939	2.402	-3.126	-1.031
Bin 12	2.067	2.469	-3.134	-0.925
Bin 13	2.19	2.537	-3.14	-0.822
Bin 14	2.309	2.606	3.139	-0.721
Bin 15	2.425	2.676	3.136	-0.622
Bin 16	2.539	2.747	3.135	-0.524
Bin 17	2.651	2.818	3.135	-0.427
Bin 18	2.761	2.89	3.135	-0.331
Bin 19	2.871	2.962	3.137	-0.236
Bin 20	2.979	3.034	3.139	-0.142
Bin 21	3.088	3.106	3.141	-0.047

Appendix D: Application of artificial vibrato on the violin sample in Cubase 7.5

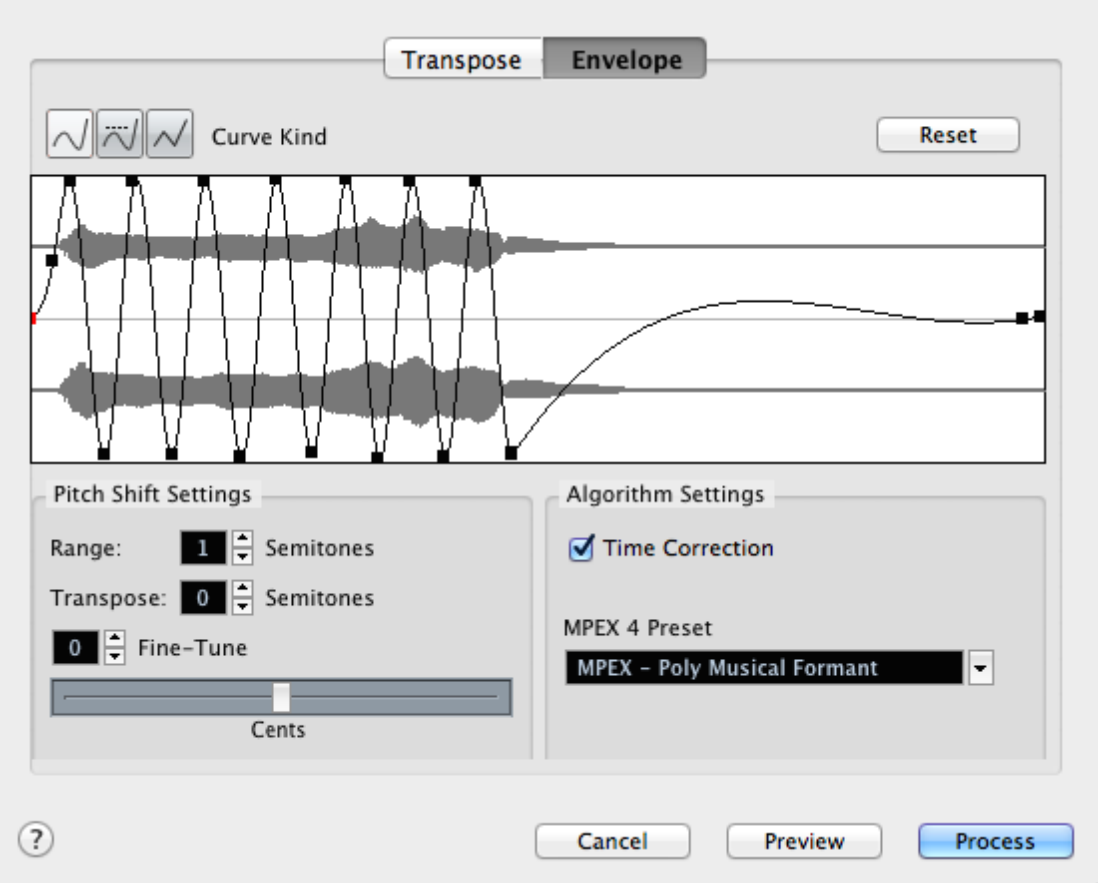

Appendix E: Application of artificial glissando on the violin sample in Cubase 7.5

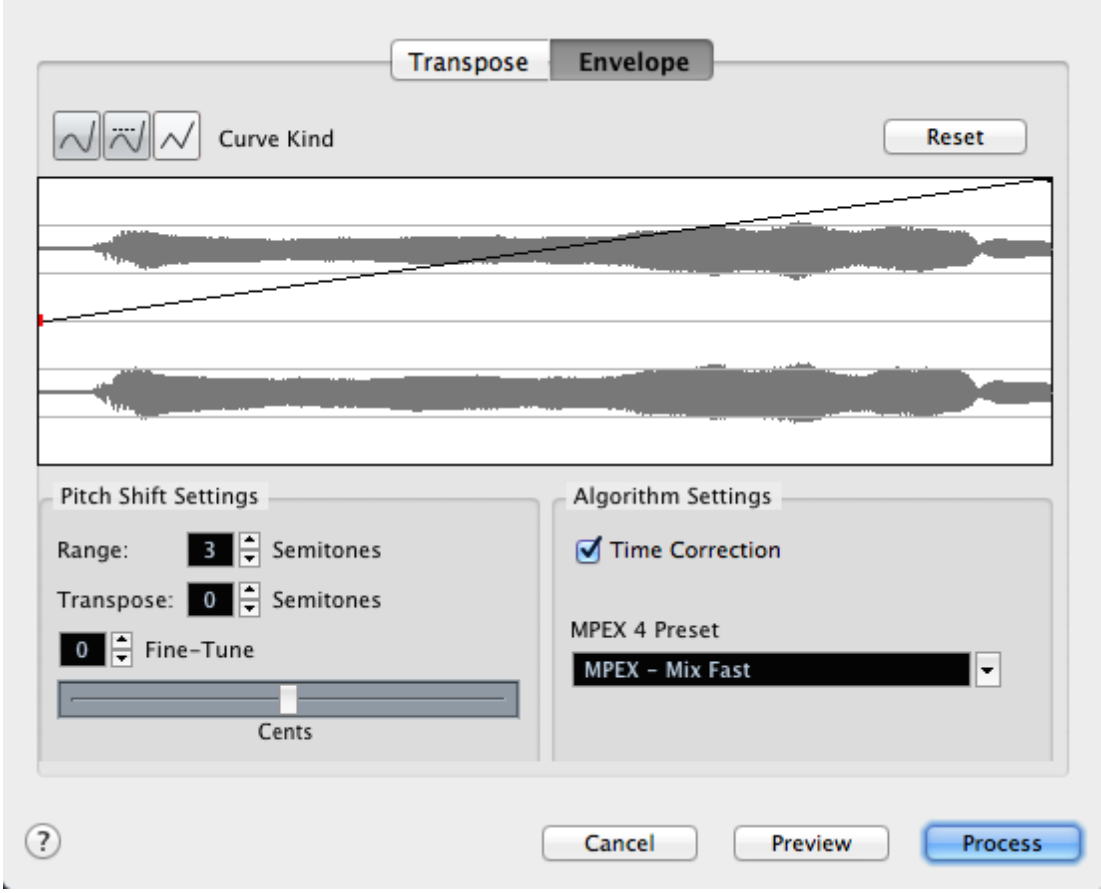

Appendix F: The *stft* function

```
function [ X ] = stft( ...
    x,frame,overlap,zpf,window,nEnsemble,sampleshift )
%STFT Short-Time Fourier Transform
%   [X]=STFT(X,FRAME,OVERLAP,ZPF,WINDOW) returns the ...
    Short-Time Fourier
%   Transform of the vector x in the matrix X. Three window ...
    functions are
%   available; rectangular, Hamming and Hanning. ...
    [X<NFRAMES:NFFT>]
%
%   ...
    [X]=STFT(X,FRAME,OVERLAP,ZPF,WINDOW,NENSEMBLE,SAMPLESHIFT) ...
    implements
%   the ensemble of closely-related estimates approach. It ...
    calculates
%   (NENSEMBLE-1) additional spectra for each frame ...
    determined by the
%   conventional STFT algorithm. An offset equal to ...
    SAMPLESHIFT is
%   introduced to each additional estimate. ...
    [X<NENSEMBLE:NFFT:NFRAMES>]
%
%   This function can receive either monophonic or ...
    stereophonic signals. If
%   the input signal is sterephonic, it converts it to ...
    monophonic.
%
%Example:
%   x = sin(2*pi*(800/44100)*(0:44099));
%   X1 = stft(x,4096,0,0,'rectwin');        % Conventional STFT.
%   X2 = stft(x,4096,0,0,'rectwin',10,24);  % Ensemble STFT ...
    for PSES.
%
%Author:
%   Thomas Arvanitidis, thomasarvanitidis AT gmail DOT com
%
```

```
24 %History:
25 %   05/01/2014: Programmed and Documented.
26 %   03/03/2014: Implemented ensemble of estimations approach ...
       (PASS w EASE).
27 %   30/06/2014: Thorough testing, bug fix and optimisation.
28 %   08/07/2014: Corrected the zero-padding logic for the PASS ...
       with EASE
29 %               functionality.
30 %   10/07/2014: Modified to store the ensemble FT into a 3 ...
       dimensional
31 %               matrix instead of a cell array.
32 %   01/10/2014: Produced the generic formula for the ...
       calculation of
33 %               nframes, which works for both conventional ...
       and ensemble
34 %               approach.
35 %   02/10/2014: Corrected the expression for the calculation ...
       of the number
36 %               of frames. From ...
       (L-(nEnsemble-1)*sampleshift-hop)/(hop)
37 %               to (L-(nEnsemble-1)*sampleshift-overlap)/(hop).
38
39 % Argument check.
40 if nargin < 6, nEnsemble = 1; end
41 if nargin < 7, sampleshift = 0; end
42 assert(all(isscalar(frame)==1&&isscalar(overlap)==1&&...
43     isscalar(zpf)==1&&isscalar(nEnsemble)==1&&...
44     isscalar(sampleshift)==1), ...
45     'Ensure frame,overlap,zpf,nEnsemble and sampleshift are ...
          scalars.')
46 assert(all(ischar(window)),'Window should be char variable')
47 assert(all(isvector(x)==1)||(size(x,1)==2||size(x,2)==2),...
48     'Subject signal must be either monophonic or stereo')   % ...
          Assert x is either monophonic or stereo.
49 if size(x,1)==2 || size(x,2)==2
50     if size(x,2)==2, x = x'; end                            % ...
          If x is stereo
51     x = 0.5.*(x(1,:) + x(2,:));                             % ...
          convert x to monophonic.
52 end
53 if iscolumn(x) == 1, x = x'; end                           % ...
       Represent x as row-vector if it is not.
54
55 % Generate window function.
56 switch window  % Window functions are (all =0 outside the ...
       interval 0≤n≤wl)
57     case 'rectwin'
58         win=ones(1,frame); % Rectangular Window
59     case 'hann'
```

```
60          win=hann(frame,'periodic')'; % Hann window ...
               w[n]=0.5-0.5*cos(2*pi*n/M), for 0≤n≤M
61          %                win=hann2(frame)'; % Hann window ...
               w[n]=0.5-0.5*cos(2*pi*n/M), for 0≤n≤M
62      case 'hamming'
63          win=hamming(frame,'periodic')';  % Hamming window ...
               w[n]=0.54-.46*cos(2*pi*n/M) for 0≤n≤M
64          %                win=hamming2(frame)';  % Hamming ...
               window w[n]=0.54-.46*cos(2*pi*n/M) for 0≤n≤M
65      otherwise
66          win=ones(1,frame);
67          disp('Invalid window type, defaulting to rectangular ...
               window.');
68  end
69
70  % General parameters.
71  L = length(x);
72  hop = frame - overlap;
73  if zpf ≠ 0, nfft = (zpf+1)*frame; else nfft = frame; end
74  nframes = floor((L-(nEnsemble-1)*sampleshift-overlap)/(hop));
75
76  % Instantiate FT variable.
77  if nEnsemble == 1   % Conventional STFT variables.
78      X = zeros(nframes,nfft);
79  else                % PASS with EASE variables.
80      X = zeros(nEnsemble,nfft,nframes);
81  end
82
83  % Calculate window normalisation factor.
84  if strcmp(window,'rectwin') && overlap == 0
85      wnorm = sum(win)/frame;
86  elseif (strcmp(window,'hann') || strcmp(window,'hamming')) && ...
       overlap == frame/2
87      wnorm = 2.*sum(win)/frame;
88  % else
89  %     error('myApp:argChk', 'Wrong combination of input ...
       arguments, window and overlap.')
90  end
91  wnorm = 2.*sum(win)/frame;
92  % Main function.
93  str = 1; len = frame;
94  if nEnsemble == 1
95      % Conventional STFT.
96      for i = 1:nframes
97          temp = x(str:len).*win/wnorm;       % Frame picking ...
               and normalised windowing. This (sum(win)/nfft) ...
               used to be (4.*sum(win)/nfft) but gave wrong ...
               results during the resynthesis stage.
98          X(i,:) = fft(temp,nfft);            % Analysis.
```

```
99          str=str+hop; len=str+frame-1;       % Index variables ...
               update.
100     end
101 else
102     % PASS with EASE.
103     for i = 1:nframes
104         for obs = 1:nEnsemble               % Each ...
               observation is a FT analysis.
105             % Frame picking and normalised windowing.
106             temp = x((obs-1)*sampleshift+str:...
107                 (obs-1)*sampleshift+len).*win/wnorm;
108             X(obs,:,i) = fft(temp,nfft);    % Analysis.
109         end
110         str=str+hop; len=str+frame-1;       % Index variables ...
               update.
111     end
112 end
```

Appendix G: The *phistab* function

```
function [ output,mode ] = ...
    phistab(data,frame,overlap,zpf,window,nEnsemble,...
     sampleshift,det,order)
%PHISTAB Phase Stability
%    ...
    [OUTPUT]=PHISTAB(X,FRAMELENGTH,OVERLAP,ZPF,WINDOW,NENSEMBLE,...
%    SAMPLESHIFT,DET,ORDER) calculates the phase stability ...
    quality ...
%    measure for the analysed data.
%
%Notes:
%    This function is dependent on the modified STFT function ...
    developed by
%    Thomas Arvanitidis.
%
%Example:
%    x = sin(2*pi*(80/44100)*(0:44099));
%    [data,¬] = phistab(x,4096,0,0,'rectwin',10,24);
%
%Author:
%    Thomas Arvanitidis, thomasarvanitidis AT gmail DOT com
%
%History:
%    26/04/2014: Programmed and documented.
%    09/07/2014: Substituted detrend with polyfit/polyval.
%    29/07/2014: Added progress feedback.
%    29/09/2014: Renamed the function from IPV to PSES.
%    16/10/2014: Renamed the function from PSES to PHISTAB.

% Argument check.
if nargin < 8, det = 0; end     % Preset det to 0 to disable ...
    functionality.
```

```
28 if nargin < 9, order = 2; end   % Order of polynomial fit by ...
      polyfit.
29 assert(all(isscalar(frame)==1&&isscalar(overlap)==1&&...
30     isscalar(zpf)==1&&isscalar(nEnsemble)==1&&...
31     isscalar(sampleshift)==1&&isscalar(det)==1&&...
32     isscalar(order)==1),'Ensure frame,overlap,zpf,nEnsemble ...
          and sampleshift are scalars.')
33 assert(all(ischar(window)),'Window should be char variable')
34 assert(all((nEnsemble>1)),'nEnsemble must be bigger than 1')
35 assert(all((sampleshift>0)),'sampleShift must be bigger than 0')
36 assert(all((det==1||det==0)),'Det can either be on (1) or off ...
      (0)')
37 assert(all((order>0&&order<3)),'Polynomial can either be of ...
      1st or 2nd order')
38
39
40 % Data calculation.
41 DATA = stft(data,frame,overlap,zpf,window,nEnsemble,sampleshift);
42 DATA = DATA(:,1:size(DATA,2)/2+1,:);    % Discard mirrored ...
      coefficients.
43
44 % Parameter setting.
45 nObs = size(DATA,1);      % # of ensemble.
46 nBins = size(DATA,2);     % # of bins.
47 nFrames = size(DATA,3);   % # of frames.
48
49 % Variable declaration: Polyfit/Polyval.
50 idx = (1:nObs)';                          % Polyval input indices.
51 r = zeros(nObs,nBins,nFrames);            % Phase variance.
52 r2 = zeros(nFrames,nBins);                % Sum of least ...
      squares (Phase Stability).
53 r2i = zeros(nFrames,nBins);               % Inverse Phase Variance.
54 angles = zeros(nObs,nBins,nFrames);       % STFT unwrapped angles.
55 coef = zeros(order+1,nBins,nFrames);      % Polyfit coefficients.
56 modelang = zeros(nObs,nBins,nFrames);     % Polyval output ...
      values (modelled angles).
57
58 % The followings are available for comparison purposes (det ...
      vs. polyfit/val).
59 % This comparison can only be made if the order of the ...
      polyfit is set to 1.
60 % Variable declaration: Detrend.
61 if det == 1                               % Instantiate only if ...
      requested.
62     rdet = zeros(nObs,nBins,nFrames);     % Phase variance.
63     r2det = zeros(nFrames,nBins);         % Sum of least ...
          squares (Phase Stability).
64     r2idet = zeros(nFrames,nBins);        % Inverse Phase Variance.
65 end
```

```
66
67  % Monitoring the progress of the function.
68  ur = 0.2;                               % Update rate 20%.
69  step = nFrames*ur;                      % Step interval.
70  nsteps = 1:(1/ur);                      % Number of steps.
71  updatesteps = step.*nsteps;             % Feedback display indeces.
72  updatesteps = ceil(updatesteps);        % Rounded-up indeces.
73  countPrint = 1;                         % Feedback algorithm flag.
74
75  % Main: Phase stability algorithm.
76  for i = 1:nFrames
77      angles(:,:,i) = unwrap(angle(DATA(:,:,i)));     % Unwrap ...
            the angles.
78      for ii = 1:nBins
79          coef(:,ii,i) = polyfit(idx,angles(:,ii,i),order);   % ...
                Calculate the curve coefficients for each bin.
80          modelang(:,ii,i) = polyval(coef(:,ii,i),idx);       % ...
                Calculate the modelled angles.
81          r(:,ii,i) = angles(:,ii,i)' - modelang(:,ii,i)';    % ...
                Phase variance.
82      end
83      r2(i,:) = sum(r(:,:,i).*r(:,:,i));          % Sum of ...
            least squares of phase variance (Phase Stability).
84      r2i(i,:) = 1./(r2(i,:)+eps);                % Inverse ...
            Phase Variance <nFrames x nBins>
85
86      % The followings are available for comparison purposes ...
            (det vs. polyfit/val).
87      % Curve fitting with DETREND.
88      if det == 1
89          rdet(:,:,i) = detrend(angles(:,:,i));           % ...
                Phase variance.
90          r2det(i,:) = sum(rdet(:,:,i).*rdet(:,:,i));     % Sum ...
                of least squares of phase variance (Phase Stability).
91          r2idet(i,:) = 1./(r2det(i,:)+eps);              % ...
                Inverse Phase Variance <nFrames x nBins>
92      end
93
94      % Progress feedback.
95      if any(i==updatesteps)      % Display percentage on ...
            specific steps.
96          done = (i*100)/nFrames; % Calculate percentage completed.
97          if countPrint == 1, fprintf('PS analysis percentage: ...
                %.1f\n',done);
98          else fprintf('\b\b\b\b\b%.1f\n',done); end
99          countPrint = countPrint +1;
100     end
101 end
102
```

```
103 % Select return variables.
104 switch nargout
105     case 1
106         output = r2i;                    % Inverse Phase ...
                Variance <nFrames x nBins>
107     otherwise
108         output.IPV = r2i;                % Inverse Phase ...
                Variance <nFrames x nBins>
109         output.r = r;                    % Phase variance.
110         output.PS = r2;                  % Least squares of ...
                phase variance (Phase Stability).
111         output.angles = angles;          % Unwrapped angles ...
                {nFrames,1}(nObs x nBins)
112         output.modelang = modelang;      % Modelled angles ...
                {nFrames,1}(nObs x nBins)
113         output.coef = coef;              % Polynomial ...
                coefficients {nFrames,1}(3 x nBins). 3 due to 2nd ...
                order polyfit.
114         mode = 'monitoring';             % Dummy variable.
115         if det == 1
116             output.IPVdet = r2idet;      % DETREND Inverse ...
                    Phase Variance <nFrames x nBins>
117             output.rdet = rdet;          % DETREND Phase variance.
118             output.PS = r2det;           % DETREND Least ...
                    squares of phase variance (Phase Stability).
119         end
120 end
```

Nomenclature

Roman Symbols

A	Amplitude
C	Sample shift
E	Energy
f	Frequency
f_s	Sampling Frequency
H	Step size
I	Imaginary
L	Frame Length
M	Number of Frames
N	Signal length
n	Time (discrete)
P	Number of Partials
Q	Number of spectral estimates
R	Real
s	Fourier basis
t	Time (continuous)

X Fourier transform of signal x

x Signal

Greek Symbols

ω Angular frequency

$\phi(0)$ Initial phase angle

π $\simeq 3.14\ldots$

φ Phase angle

Superscripts

j unit imaginary number $\sqrt{-1}$

Subscripts

d Harmonic partial index

k Frequency counter

m Frame counter

p Partial index

v Source index

Acronyms

$ADSR$ Attack-Decay-Sustain-Release

$ASTFT$ Adaptive Short-Time Fourier Transform

BSS Blind Source Separation

CIF Channelised Instantaneous Frequency

DFT Discrete Fourier Transform

DSP Digital Signal Processing

FFT Fast Fourier Transform

$IDFT$ Inverse Discrete Fourier Transform

$IFFT$ Inverse Fast Fourier Transform

$ISTFT$ Inverse Short-Time Fourier Transform

LGD Local Group Delay

$MIMO$ Multiple-input, multiple-output

$nfft$ Number of points considered by FFT

PSD Power Spectral Density

$PSES$ Phase Stability Enhanced Spectra

$SISO$ Single-input, single-output

SNR Signal-to-Noise ratio

$STFT$ Short-Time Fourier Transform

$TCIF$ Time-Corrected Instantaneous Frequency

zpf Zero padding factor

References

[1] G. Pokol, L. Horvath, N. Lazanyi, G. Papp, G. Por, and V. Igochine, "Continuous linear time-frequency transforms in the analysis of fusion plasma transients," in *40th EPS Conf. on Plasma Physics*, Espoo, Jul. 1-5, 2013, pp. 1306–1309.

[2] R. Thirumalainambi and D. E. Thompson, "Gravitational Wave Signal identification and transformations in time-frequency domain," NASA, Tech. Rep.

[3] K. Darowicki and W. Felisiak, "On the joint time-frequency characteristics of chemical oscillations," *J. of Computational Chemistry*, vol. 27, no. 8, pp. 961–965, 2006.

[4] D. Tuncel, A. Dizibuyuk, and M. Kiymik, "Time Frequency Based Coherence Analysis Between EEG and EMG Activities in Fatigue Duration," *J. of Medical Syst.*, vol. 34, no. 2, pp. 131–138, 2010.

[5] Z. N. E. and H. R. Siahkoohi, "Single Frequency Seismic Attribute Based on Short Time Fourier Transform, Continuous Wavelet Transform, and S Transform," in *6th Conf. & Exposition on Petroleum Geophysics*, Kolkata, Jan. 2006.

[6] T. Pinch and F. Trocco, *Analog days : the invention and impact of the Moog synthesizer*. Cambridge, MA: Harvard University Press, 2002.

[7] Wikipedia. Arp odyssey. Accessed: 2014-12-17. [Online]. Available: http://en.wikipedia.org/wiki/ARP_Odyssey

[8] J. Moorer, "Signal processing aspects of computer music: A survey," in *Proc. of the IEEE*, vol. 65, no. 8, Aug. 1977, pp. 1108–1137.

[9] D. M. Howard and J. S. Angus, *Acoustics and psychoacoustics*, 4th ed. Oxford: Focal, 2009.

[10] L. V. Barbosa, "Fourier Transform Time and Frequency domains," accessed: 2014-12-17. [Online]. Available: http://en.wikipedia.org/wiki/Fourier_transform#mediaviewer/File:Fourier_transform_time_and_frequency_domains_(small).gif

[11] J. O. Smith. Spectral Audio Signal Processing. Accessed: 2014-12-17. [Online]. Available: http://www.dsprelated.com/dspbooks/sasp/

[12] J. W. Cooley and J. W. Tukey, "An Algorithm for the Machine Calculation of Complex Fourier Series," *Math. of Computation*, vol. 19, no. 90, pp. 297–301, Apr. 1965.

[13] F. J. Harris, "On the use of windows for harmonic analysis with the discrete Fourier transform," *Proc. of the IEEE*, vol. 66, no. 1, pp. 51–83, Jan. 1978.

[14] A. H. Nuttall, "Some windows with very good sidelobe behavior," *IEEE Trans. Acoust., Speech, Signal Process.*, vol. 29, no. 1, pp. 84–91, Feb. 1981.

[15] J. B. Allen, "Short term spectral analysis, synthesis, and modification by discrete fourier transform," *IEEE Trans. Acoust., Speech, Signal Process.*, vol. 25, no. 3, pp. 235–238, Jun. 1977.

[16] M. S. Bartlett, "Smoothing Periodograms from Time-Series with Continuous Spectra," *Nature*, vol. 161, pp. 686–687, May 1948.

[17] ——, "Periodogram Analysis and Continuous Spectra," *Biometrika*, vol. 37, no. 1/2, pp. 1–16, Jun. 1950.

[18] P. D. Welch, "The use of fast Fourier transform for the estimation of power spectra: A method based on time averaging over short, modified periodograms," *IEEE Trans. Audio Electroacoust.*, vol. 15, no. 2, pp. 70–73, Jun. 1967.

[19] P. Depalle and T. Helie, "Extraction of spectral peak parameters using a short-time Fourier transform modeling and no sidelobe windows," in *IEEE ASSP Workshop on Applications of Signal Processing to Audio and Acoustics*, Oct. 1997, p. 4.

[20] A. Oppenheim, D. Johnson, and K. Steiglitz, "Computation of spectra with unequal resolution using the fast Fourier transform," in *Proc. of the IEEE*, vol. 59, no. 2, Feb. 1971, pp. 299–301.

[21] J. C. Brown, "Calculation of a constant Q spectral transform," *The J. of the Acoustical Soc. of America*, vol. 89, no. 1, pp. 425–434, 1991.

[22] A. Lukin, "Multiresolution STFT for Analysis and Processing of Audio," Talk at B.U., September 2010. [Online]. Available: audio.rightmark.org/lukin/temp/exchange/LukinTalk.ppt

[23] D. L. Jones and T. W. Parks, "A high resolution data-adaptive time-frequency representation," in *IEEE Trans. Acoust., Speech, Signal Process.*, vol. 38, no. 12, pp. 2127–2135, Dec. 1990.

[24] D. Rudoy, P. Basu, T. Quatieri, B. Dunn, and P. Wolfe, "Adaptive short-time analysis-synthesis for speech enhancement," in *IEEE Int. Conf. on Acoustics, Speech, and Signal Processing (ICASSP 2008)*, Mar. 2008, pp. 4905–4908.

[25] S. A. Fulop and K. Fitz, "Algorithms for computing the time-corrected instantaneous frequency (reassigned) spectrogram, with applications," *The J. of the Acoustical Soc. of America*, vol. 119, no. 1, pp. 360–371, 2006.

[26] K. Kodera, C. De Villedary, and R. Gendrin, "A new method for the numerical analysis of non-stationary signals," *Physics of the Earth and Planetary Interiors*, vol. 12, no. 2-3, pp. 142–150, 1976.

[27] S. A. Fulop and K. Fitz, "Separation of components from impulses in reassigned spectrograms," *The J. of the Acoustical Soc. of America*, vol. 121, no. 3, pp. 1510–1518, 2007.

[28] D. J. Thomson, "Spectrum estimation and harmonic analysis," in *Proc. IEEE*, vol. 70, no. 9, Sep. 1982, pp. 1055–1096.

[29] M. Bayram and R. Baraniuk, "Multiple window time-frequency analysis," in *Proc. of the IEEE-SP Int. Symp. on Time-Frequency and Time-Scale Analysis*, Jun. 1996, pp. 173–176.

[30] F. Cakrak and P. J. Loughlin, "Multiwindow time-varying spectrum with instantaneous bandwidth and frequency constraints," *IEEE Trans. Signal Process.*, vol. 49, no. 8, pp. 1656–1666, Aug. 2001.

[31] J. W. Pitton, "Time-frequency spectrum estimation: an adaptive multitaper method," in *Proc. of the IEEE-SP Int. Symp. on Time-Frequency and Time-Scale Analysis*, Oct. 1998, pp. 665–668.

[32] J. Xiao and P. Flandrin, "Multitaper time-frequency reassignment," in *14th European Signal Processing Conf. (EUSIPCO 2006)*, Florence, Sep. 4-8, 2006.

[33] J. E. Szymanski, "PASS with EASE - Phase Amplitude Shift Stability via Ensemble Averaged Spectral Estimation," unpublished.

[34] University of Iowa. Music Instrument Samples. Accessed: 2014-12-17. [Online]. Available: http://theremin.music.uiowa.edu/MIS.html

[35] K. J. Pope and R. E. Bogner, "Blind Signal Separation I. Linear, Instantaneous Combinations: I. Linear, Instantaneous Combinations," *Digital Signal Process.*, vol. 6, no. 1, pp. 5–16, 1996.

[36] ——, "Blind Signal Separation II. Linear, Convolutive Combinations: II. Linear, Convolutive Combinations," *Digital Signal Process.*, vol. 6, no. 1, pp. 17–28, 1996.

[37] O. Yilmaz and S. Rickard, "Blind separation of speech mixtures via time-frequency masking," *IEEE Trans. Signal Process.*, vol. 52, no. 7, pp. 1830–1847, Jul. 2004.

[38] H. Shim, J. S. Abel, and K.-M. Sung, "Stereo Music Source Separation for 3-D Upmixing," in *127th AES Conv.*, New York, NY, Oct. 9-12, 2009, p. 7938.

[39] J. Burred and P. Leveau, "Geometric multichannel common signal separation with application to music and effects extraction from film soundtracks," in *IEEE Int. Conf. on Acoustics, Speech, and Signal Processing (ICASSP 2011)*, May 2011, pp. 201–204.

[40] A. Klapuri, T. Virtanen, and T. Heittola, "Sound source separation in monaural music signals using excitation-filter model and em algorithm," in *IEEE Int. Conf. on Acoustics, Speech, and Signal Processing (ICASSP 2010)*, Mar. 2010, pp. 5510–5513.

[41] T. Virtanen, "Sound source separation in monaural music signals," Ph.D. dissertation, Tampere Univ. of Technology, 2006.

[42] T. Virtanen and A. Klapuri, "Separation of harmonic sounds using linear models for the overtone series," in *IEEE Int. Conf. on Acoustics, Speech, and Signal Processing (ICASSP 2002)*, vol. 2, May 2002, pp. II–1757–II–1760.

[43] ——, "Separation of harmonic sounds using multipitch analysis and iterative parameter estimation," *IEEE Workshop on the Applications of Signal Processing to Audio and Acoustics*, pp. 83–86, 2001.

[44] ——, "Separation of harmonic sound sources using sinusoidal modeling," in *Proc. in 2000 IEEE Int. Conf. on Acoustics, Speech, and Signal Processing (ICASSP '00)*, vol. 2, 2000, pp. II765–II768.

[45] C. Cherry, *On human communication : a review, a survey, and a criticism.* Cambridge, MA: MIT Press, 1957.

[46] A. Benveniste, M. Goursat, and G. Ruget, "Robust identification of a nonminimum phase system: Blind adjustment of a linear equalizer in data communications," *IEEE Trans. Autom. Control*, vol. 25, no. 3, pp. 385–399, Jun. 1980.

[47] D. L. Donoho, "On minimum entropy deconvolution," *in Applied Time Series Analysis II*, pp. 565–608, 1981.

[48] D. Godard, "Self-Recovering Equalization and Carrier Tracking in Two-Dimensional Data Communication Systems," *IEEE Trans. Commun.*, vol. 28, no. 11, pp. 1867–1875, Nov. 1980.

[49] Y. Sato, "A Method of Self-Recovering Equalization for Multilevel Amplitude-Modulation Systems," *IEEE Trans. Commun.*, vol. 23, no. 6, pp. 679–682, Jun. 1975.

[50] P. Comon and C. Jutten, *Handbook of blind source separation: Independent component analysis and blind deconvolution.* Amsterdam & London ; Oxford: Elsevier ; Academic Press, 2010.

[51] D. FitzGerald, "Upmixing from mono - A source separation approach," in *17th Int. Conf. on Digital Signal Processing (DSP)*, Jul. 2011, pp. 1–7.

[52] Accusonus. Drumatom. Accessed: 2014-12-17. [Online]. Available: http://drumatom.com

[53] G. Benson, "Musical signal separation: Separation of harmonic sounds using a model-based numeric approach," M.S. thesis, Dept. Elec. Eng., Univ. of York, York, 2003.

[54] M. R. Every, "Separation of musical sources and structure from single-channel polyphonic recordings," Ph.D. dissertation, Dept. Elec. Eng., Univ. of York, York, 2006.

[55] T. Vandecasteele, "Source separation and possibilities in music genre recognition," M.Eng. thesis, Dept. Elec. Eng., Univ. of York, York, 2012.

[56] T. W. Stokes, "Mono-To-Stereo & Beyond," M.Eng. thesis, Dept. Elec. Eng., Univ. of York, York, 2011.

[57] R. J. G. Graham, "Mono-To-Stereo & Beyond: Audio Signal Separation," M.Eng. thesis, Dept. Elec. Eng., Univ. of York, York, 2005.

[58] R. Mani, "Signal Source Separation: The Analysis and Separation of Audio Signals with Intersecting Pitch Trajectories," M.S. thesis, Dept. Elec. Eng., Univ. of York, York, 2005.

[59] J. E. McMillan, "Mono-To-Stereo & Beyond: An adaptable approach to monophonic audio signal segmentation for use in audio applications," M.S. thesis, Dept. Elec. Eng., Univ. of York, York, 2004.

[60] J. Dickin, "Audio Signal Separation," B.Eng. thesis, Dept. Elec. Eng., Univ. of York, York, 2004.

[61] J. Le Roux, N. Ono, and S. Sagayama, "Explicit consistency constraints for stft spectrograms and their application to phase reconstruction," in *Proc. SAPA 2008 Workshop on Statistical and Perceptual Audition (SAPA 2008)*, 2008.

[62] D. FitzGerald and R. Jaiswal, "On the use of masking filters in sound source separation," in *Proc. 15th Int. Conf. on Digital Audio Effects (DAFx-12)*, York, Sep. 17-21, 2012.